



Università degli Studi di Palermo



DIPARTIMENTO DI SCIENZE DELLA TERRA E DEL MARE
(Di.S.Te.M)

Ph.D. in Geochemistry

PhD course in Geochemistry - XXIV Cycle (GEO/08)

GASEOUS EMISSIONS FROM GEOTHERMAL AND
VOLCANIC AREAS: FOCUS ON METHANE AND
METHANOTROPHS

Ph.D. thesis by

Antonina Lisa Gagliano

Ph.D. Coordinator:

Prof. F. Parello (University of Palermo)

Supervisors:

Prof. F. Parello (University of Palermo)

Dr. W. D'Alessandro (INGV sez. Palermo)

Dr. P. Quatrini (University of Palermo)

Reviewers:

Dr. Richard L. Smith (USGS – United States Geological Survey)

Dr. Martin Krüger (Bundesanstalt fuer Geowissenschaften und Rohstoffe - BGR)

Jan 2011 – Dec 2013

"Gli ostacoli non mi fermano. Ogni ostacolo si sottomette alla rigida determinazione..."

*"Obstacles cannot crush me. Every obstacle yields
to stern resolve..."*

- Leonardo da Vinci -

ACKNOWLEDGMENTS

First and foremost I want to thank my supervisor Prof. Francesco Parello, who believed in my scientific skills and in this project; he supported and advised me during this PhD course. But above all, he shared with me his knowledge in geochemistry resulting in my formation as a scientist.

I want to thank my co-tutors Walter D'Alessandro and Paola Quatrini, who were and are my masters of science and life; they teach me what research is and who a researcher has to be. All my supervisors and I worked in a pleasant group, full of enthusiasm and with innovative ideas, which is the best I could expect.

I want to thank all the kind people who helped me in the laboratory at the INGV and during the field campaigns: Lorenzo Brusca, Sergio Bellomo, Mauro Martelli, Guendalina Pecoraino, Francesco Salerno. They helped me with my work and patiently taught me new techniques, completing my scientific background.

I thank Marcello Taglivia; he helped me in molecular analyses and we have had constructive conversations during the very long laboratory waiting times.

I thank Dr. Franco Tassi and his team for field activities and collaboration.

I want to thank Dr. A. Pol, who kindly supplied me a sample of *Methilacidiphilum fumarolicum SolV*, that was a key element for my research.

A special thanks to my dissertation referees Dr. Robert Smith and Dr. Martin Krüger. Their fundamental, professional and punctual advises helped me to improve my dissertation.

I appreciate my colleagues, with whom I have shared this PhD adventures, that become very fun with them.

Finally, I want to thank my family and friends for all their encouragements.

My special thanks go to my fiancé Vincenzo, who lovingly helped me, supported me and shared with me all the best and worst moments of this journey. Thank you all.

*Antonina Lisa Gagliano,
University of Palermo,
January 2014.*

LIST OF FIGURES

Fig. 1.1- Variation of methane abundance in the atmosphere (IPCC, 2001).....	2
Fig. 1.2 - ¹³ C and deuterium concentrations in naturally occurring methane. Fields BR and BF are the areas which encompass bacterial methanes that form by CO ₂ reduction and fermentation, respectively. The heavy outlined area encompasses methane of thermogenic origin, wherein the shaded part depicts methane associated with oils and the unshaded part the non-associated methane. I = Sacramento Basin, California (Jenden and Kaplan, 1988); 2 = Cooper Basin, Western Australia (Rigby and Smith, 1981); 3 = Canadian Shield gases (Sherwood et al., 1988); 4 = geothermal methane (Des Marais et al., 1981; Lyon and Hulston, 1984; Welhan, 1988 in this special issue); EPR=East Pacific Rise (Welhan, 1981); ZOM= Zambales Ophiolite methane Philippines (Abrajano et al., (1988 in this special issue); Migr. = migrated Rotliegendes gases, G.D.R. (Runge, 1980); LC and HC and LD and HD are highest and lowest concentrations for ¹³ C and deuterium, respectively, found so far in natural methane, Atmospheric methane (Wahlen et al., 1987; Schoell, 1988).....	5
Fig. 1.3 - Methane emission from different sources (Kvenvolden et al., 2005).	6
Fig. 1.4 - Geological sources of methane	7
Fig. 1.5 - Main European geothermal.....	7
Fig. 1.6 - Methane sinks in soil and in atmosphere.	9
Fig. 1.7 - Pathways for the oxidation of methane and assimilation of formaldehyde. Abbreviations: CytC, cytochrome c; FADH, formaldehyde dehydrogenase; FDH formate dehydrogenase (Hansen and Hansen, 1996).	12
Fig. 1.8 – a) pMMO and b) sMMO encoding genes and subunits; c) pMMO: methane conversion in methanol.....	13
Fig. 1.9 - a) RuMP pathway for formaldehyde fixation. The reaction is catalyzed by the unique enzymes of this pathway, hexulose – 6- phosphate synthase and hexulose-phosphate isomerase, are indicated. b) Serine pathway for formaldehyde fixation. Unique reactions catalyzed by serine hydroxymethyl transferase (STHM), hydroxypyruvate reductase (HPR), malate thiokinase (MTK), and malyl coenzyme A lyase (MCL) are identified (modify by Hansennand Hansen, 1996).....	15
Fig. 1.10- CO ₂ /CH ₄ flux ratio measures at a) Nisyros island, b) Pantelleria Island and c) Sousaki. Line indicates the ratio measured in fumaroles, symbols ratio measures in degassing areas close to the fumaroles.....	22
Fig. 1.11 - Sampled areas, a) Pantelleria Island, Italy b) Vulcano Island, Italy, c) Sousaki, Greece, d) Nea Kameni - Santorini, Greece, and e) Nisyros, Greece island; table indicates chemical-physical conditions of the selected areas.	23
Fig. 2.1– Geological structure of Pantelleria island.	26
Fig. 2.2 - Geological map of Pantelleria Island.....	27
Fig. 2.3.– Conceptual model of the geothermal system of Pantelleria ; 1. Recent pyroclastic rocks; 2. Trachyte; 3. Faults; 4. Isotherms; 5. Boundaries between zone characterized by fluids of diverse origin; 6. Direction of meteoric recharge; 7. Direction of marine recharge (Modify by Giannelli et al., 2001).	28
Fig. 2.4 - Sampling site at the geothermal area (FAV1 –FAV5) and at the agricultural area (FAV6 – FAV10), Favara Grande, Pantelleria island	30
Fig. 2.5 – Distribution map of the temperature.	31
Fig. 2.6 - Variation of Chemical –physical characteristics in FAV2 vertical profile.	32
Fig. 2.7 - Fumarolic and air gas distribution in sampled soil gases.....	36
Fig. 2.8 - Variation in a) CO ₂ amount, b) in CH ₄ amount and c) in N ₂ amount in soil gases.....	37
Fig. 2.9 - Variation in CO ₂ /CH ₄ ratio with depth.	38
Fig. 2.10 - a) variation of methane in laboratory incubation experiments using FAV1, FAV2 and FAV3 soil samples; b) variation of methane in laboratory incubation experiments using soils from FAV2 vertical profile.	39
Fig. 2.11 - methane consumption of the soils sampled at FAV2 vertical profile, incubated at different temperatures.	40
Fig. 2.12 - FAV2A methane consumption at different methane initial concentration after 24h incubation at controlled room temperature.....	41

Fig. 2.13 - Variation on CH ₄ – C composition; the arrows indicate the positivization of δ ¹³ C(CH ₄) due to microbial methane oxidation.....	42
Fig. 2. 14 - a) PCR – TTGE analysys of 16S V3; b) position of excided bands in the gel.....	45
Fig. 2.15 - Gel electrophoresis of PCR products obtained a) using primers 189F/682R targeting proteobacterial <i>pmoA</i> gene and b) using primer 156F/743R targeting verrucomicrobial <i>pmoA</i> gene. .	46
Fig. 2.16 - Steps of a gene cloning; 1. Selected gene fragement is amplified and inserted in a vector; 2. The vector is introduced in a bacterial cell (e.g. E. Coli).3. Vector is amplified in bacteria 4. Recombimated bacteria are selected and 5. Clone with selected gene are identified. (see Box 1).....	49
Fig. 2.17 - a) observation at optic microscope of the GRAM test on FAV2B isolate; b) growth on methanol of FAV2B isolate.....	50
Fig. 2.18- Growth (blu line) and corresponding methane consumption (red line) of Methylocistis sp strain after 3 days of incubation. Average of the optical density (OD600)± standard error are shown in five duplicate 150 serum bottles at 37°C. The pH was 5.	52
Fig. 2.19 - SEM micrographs of FAV2A isolate.....	53
Fig. 3.1 - Geological map of Nisyros island.....	60
Fig. 3.2 - Conceptual model of the geothermal system of Nisyros; blue arrows represent meteoric contribution of reservoir recharge, red arrow the marine contribution and green arrow the andesitic water contribution.	61
Fig. 3.3 – a) Nisyros Island, Greece; b) Micro polyvotes, crater; c) holes in the Stephanos crater; d) Lakki plain and distribution of creters and degassing areas.	63
Fig. 3.4 – Distribution of gas sampling areas in the Lakki Plain.....	64
Fig. 3.5 - Soil sampling area in Lakki plain.	65
Fig. 3.6 - Temperature maps at 20 and 50 cm of depth , Lakki Plain. Maps were created by the geostatistical tool of ArcMap 9.3.	66
Fig. 3.7 - QQ plot of CO ₂ content in soil gases sampled at Nisyros.....	68
Fig. 3.8 - QQ plot of H ₂ S content in soil gases sampled at Nisyros.	69
Fig. 3.9– QQ plot of CH ₄ content in soil gases sampled at Nisyros.....	69
Fig. 3.10 - Fumarolic and air gas distribution in sampled soil gases.....	70
Fig. 3.11 - Triangular plot of the distribution of fumarolic gases of soil gases at the Lakki plain craters.....	71
Fig. 3.12 - CH ₄ distribution in soil gases at sampled areas.	72
Fig. 3.13 - H ₂ S distribution in soil gases at sampled areas.	73
Fig. 3.14 - Air gases distribution in soil gases at sampled areas.	74
Fig. 3.15 - Hydrogen sulfide vs carbon dioxide in Nisyros soil gases.	75
Fig. 3.16 - Methane flux measured by accumulation chamber in the three sampling campaign.....	76
Fig. 3.17 - Frequency of the methane flux; sampling made in 2010 were integrated with the sampling campaing in 2013.	77
Fig. 3.18 - Methanotrophs culture in M3 mineral medium.	79
Fig. 4.1 - Geology of Vulcano island.	84
Fig. 4.2 - Sampling site at Vulcano island.....	85
Fig. 4.3 - Sampling site at Sousaki area.	88
Fig. 4.4 – Sousaki Fumaroles.	89
Fig. 4. 5 - Geological map of Santorini island.	90
Fig. 4.6 - sampling site at Nea Kameni, Santorini island.	92
Fig. 5.1 - Principal Component Analysis to associate methane consumption recorded in incubation experiment using soils from study areas with multiple factors.	98
Fig. 7. 1- Soil gases sampling from the underground.....	106
Fig. 7. 2 - Accumulation chamber.....	107
Fig. 7. 3- Micro GC.....	111

Fig. 7. 4 - Total DNA extracted from soil samples by using FastDNA Spin Kit for soil; 1. FAV1; 2. FAV2; 3. FAV1; 4. FAV2; 5. FAV3; 6. FAV3; 7. FAV4; 8. FAV5; 9. FAV6; 10. FAV7; 11. FAV8; 12. FAV9; 13. FAV9; 14. FAV10.....	112
Fig. 7. 5 - Total DNA extracted from soil samples by using phenol-chloroform method; 1. FAV1; 2. FAV1; 3. FAV1; 4. FAV2; 5. FAV2; 6. FAV2; 7. FAV3; 8. FAV3; 9. FAV3.....	113
Fig. 7. 6- Isolation of methanotrophic bacteria. a. enrichment in methane. b and c. Enrichment cultures in M3 broth with CH ₄ (25%) as sole C sources. c. isolate FAV2B1 in M3 agar with 25% of CH ₄ (right) and negative control (left).....	117

LIST OF TABLES

Table 1. 1 - Methane output from European	7
Table 1. 2- Comparison of all described families of methanotrophic bacteria. + = presence; - =absence.....	11
Table 1. 3 - Classifications of geothermal systems on the basis of temperature, enthalpy and physical state (Bodvarsson, 1964; Axelsson and Gunnlaugsson, 2000).....	17
Table 2. 1- Chemical –physical characterization of soils and gases sampled at 0-3 cm of depth at the geothermal (FAV1-FAV5) and the agricultural field (FAV6 – FAV10)	34
Table 2. 2 - Chemical Index of Alteration, Oxides and L.O.I. (loss on ignition) in %	35
Table 2. 3 - Methane consumption value after soil incubation at different temperatures; n.r. = not recorded.....	41
Table 2. 4 - Detection of the functional gene <i>pmoA</i> : a. amplification products with specific primer (see Table 7.2); b = absence of amplicon of the expected size; c = presence of an amplicon of the expected size.	47
Table 2. 5 - Methane monooxygenase gene diversity retrieved from FAV2 soil sample.	48
Table 2. 6- Identification, substrate utilization and <i>pmmo</i> gene identity detection of the methanotrophs isolated from enrichment cultures at 37°C from FAV2 soil sampled at different depths.	51
Table 2. 7 - Growth of the isolates at different pH and temperatures. n.m. not measures. Growth was registered after 3 days of incubation.	51
Table 3. 1 - Fumaroles composition; samples were taken in the 2010 sampling campaigns.	67
Table 3. 2 - Chemical – Physical characterization of sampling area in Stephanos and kaminakia craters and methane consumptions.	79
Table 3. 3 - OD ₆₀₀ measured from M3 broth culture after a month of enrichment under 1% and 25 % of methane respectively.....	80
Table 4. 1 - Chemichal – physical characterization and methane consumption of the sampling site in Vulcano island, Santorini island, Sousaki area.	93
Table 5. 1- Comperison between studied geothermal system. a.D’Alessandro et al., 2009; b. D’Alessandro et al., 2006; c. Capaccioni et al. 2001, d. Tassi et al, 2013.....	99
Table 7. 1 - Micro GC structure and functions MS = Molesieve colums; PPU = Porous Polymer column; TDC= termal conductivity detector.....	110
Table 7. 2- primer couples used for PCRs amplification.in this study.	114
Table 8. 1 - Physical conditions and soil gases composition of the samples from Nisyros Island. a. Temperaure measured at 20 cm of depth; b. temperature measured at 50 cm of depth.	121
Table 8. 2 – methane flux measured using the accumulation chamber.	124

LIST OF CONTENT

<i>PREFACE</i>	x
ABSTRACT.....	xi
SOMMARIO.....	xiii
1. INTRODUCTION	1
1.1 METHANE (CH ₄).....	2
1.2 METHANE CYCLE ORIGINS AND SOURCES	4
1.3 METHANE SINKS	8
1.4 METHANE OXIDIZING BACTERIA (MOB) AND THEIR ECOLOGY	9
1.5 TYPE I, TYPE II AND TYPE X METHANOTROPHS: PHYSIOLOGY AND BIOCHEMISTRY.....	12
1.6 GEOTHERMAL SYSTEMS	16
1.7 HYDROTHERMAL GASES	18
1.8 SOIL (GEO)CHEMISTRY	19
1.9 AIM.....	21
2. PANTELLERIA ISLAND.....	25
2.1. GEOLOGICAL SETTING	26
2.2. SAMPLING AREA	29
2.3. RESULTS	31
2.3.1. CHEMICAL–PHYSICAL CHARACTERISTIC OF THE SAMPLED SITES...31	
2.3.2. SOILS GASES.....	36
2.3.3. CLUES OF METHANOTROPHIC ACTIVITY	39
2.3.4. MICROBIOLOGY AND MOLECULAR DETECTION OF METHANE OXIDIZING BACTERIA.....	42
2.3.5. SOIL BACTERIAL DIVERSITY	45
2.3.6. DETECTION OF METHANE OXIDATION GENES	46
2.3.7. DIVERSITY OF METHANOTROPHS	48
2.3.8. ISOLATION OF METHANOTROPHIC BACTERIA FROM THE GEOTHERMAL SITE.....	50
2.4. DISCUSSION	54
3. NISYROS ISLAND.....	58
3.1. GEOLOGICAL SETTING	59
3.2. SAMPLING AREA	62

3.3.	RESULTS	66
3.3.1.	TEMPERATURE DISTRIBUTION.....	66
3.3.2.	FUMARoles	67
3.3.3.	SOIL GASES	68
3.3.4.	METHANE FLUX.....	76
3.3.5.	GEOCHEMICAL EVIDENCES OF METHANE MICROBIAL OXIDATION	78
3.4.	DISCUSSION	80
4.	VULCANO ISLAND, SOUSAKI, NEA KAMENI.....	83
4.1.	VULCANO ISLAND	84
4.2.	SOUSAKI	86
4.3.	NEA KAMENI (SANTORINI)	90
4.4.	RESULTS	93
4.4.1.	METHANE CONSUMPTION	93
4.5.	DISCUSSION	94
5.	GENERAL DISCUSSION AND CONCLUSION	96
6.	REFERENCES	101
7.	MATERIALS AND METHODS.....	106
7.1.	SOIL AND GAS SAMPLING.....	106
7.2.	PHYSICAL-CHEMICAL SOIL CHARACTERIZATION.....	108
7.2.1.	TEMPERATURE, PH, OM AND WATER CONTENT.....	108
7.2.2.	MAJOR ELEMENTS	108
7.2.3.	ISOTOPES	109
7.2.4.	METHANE OXIDATION POTENTIAL RATE	109
7.2.5.	GAS ANALYSES BY USING MICRO GAS CHROMATOGRAPHY	110
7.3.	DNA EXTRACTION METHODS	112
7.4.	TEMPORAL GRADIENT GEL ELECTROPHORESIS	113
7.5.	DETECTION OF METHANE OXIDATION GENES AND CONSTRUCTION OF A <i>pmoA</i> LIBRARY	115
7.6.	CLONE LIBRARY CREATION.....	115
7.7.	ISOLATION OF METHANOTROPHIC BACTERIA	116
7.8.	PRINCIPAL COMPONENTS ANALYSIS (PCA).....	117
7.9.	REFERENCES	119
8.	APPENDIX I	120

8.1.	NISYROS SOIL GASES COMPOSITON	120
8.2.	NISYROS METHANE FLUX.....	122
9.	APPENDIX II	125

PREFACE

This PhD Project was developed in collaboration with three departments: Dpt. of the Science of the Earth and of the Sea head office of the PhD in Geochemistry, in the Environmental Microbiology and Microbial Ecology of the department STEBICEF - Biological Chemical and Pharmaceutical Science and Technology where microbiology experiments were carried out, and INGV- sez. Palermo, where most of the geochemical analyses were performed. This project born from an intuition of my supervisors Prof. F. Parello and Dr. W. D'Alessandro that on the basis of previous data understood the importance of investigating bacterial communities in geothermal areas to explain anomalies in measured methane flux values. Competence and always new approach of science of my supervisor Dr. P. Quatrini started my challenge in carrying on this multidisciplinary, relatively new, fascinating project. The most difficult challenge was to merge competences in different subjects and reach the correct approach to work in a bio-geochemical (or geo-microbiologic) environment.

These pages are an attempt to summarize all the work done during my PhD. In the 1) introduction it is possible to find a rapid summary on methane, focusing the attention on methane microbial oxidation by methanotrophs, and a very synthetic description of geothermal sites to retrieve some concepts on this type of system. The second part of the dissertation reports on the results obtained followed by a general discussion and conclusions. It is divided in four chapters focusing the attention on 2) Pantelleria Island, 3) Nisyros Island, and 4) other areas. The different areas were not studied with the same extension and that is the explanation of this chapter subdivision.

At the end of the results, 5) a general discussion was made to compare all the studied areas and to reach a conclusion of the work.

My choice was to group materials and methods at the end, to help the reader to immediately reach the core of our work.

ABSTRACT

Yearly, 22 Tg of CH₄ are released in to the atmosphere from several natural and anthropogenic sources. Methane plays an important role in the Earth's atmospheric chemistry and radiative balance being the most important greenhouse gas after carbon dioxide. Volcanic/geothermal areas contribute to the methane flux, being the site of widespread diffuse degassing of endogenous gases. Preliminary studies estimated a total CH₄ emission from European geothermal and volcanic systems in the range 4-16 kt a⁻¹. This estimate was obtained indirectly from CO₂ or H₂O output data and from CO₂/CH₄ or H₂O/CH₄ values measured in the main gaseous manifestations. The total estimated CH₄ emission from geothermal/volcanic areas is still not well defined since the balance between emission through degassing and consumption through soil microbial oxidation is poorly known. Moreover, methane soil flux measurements are laboratory intensive and very few data have been collected until now in these areas. Such methods, although acceptable to obtain order-of-magnitude estimates, completely disregards possible methane microbial oxidation within the soil carried on by the methanotrophs. At the global scale, microbial oxidation in soils contributes for about 3-9% to the total removal of methane from the atmosphere. But the importance of methanotrophic organisms is even larger because they oxidize the greatest part of the methane produced in the soil and in the subsoil before its emission to the atmosphere. Environmental conditions in the soils of volcanic/geothermal areas (i.e. low oxygen content, high temperature and proton activity, etc.) have long been considered inadequate for methanotrophic microorganisms. But recently, it has been demonstrated that methanotrophic consumption in soils occurs also under such harsh conditions due to the presence of acidophilic and thermophilic Verrucomicrobia. These organisms were found in Italy at the Solfatara at Pozzuol (Italy), at Hell's Gate (New Zealand) and in Kamchatka (Russia), pointing to a worldwide distribution. Here we report on methane oxidation rate measured in Pantelleria Island (Italy), Vulcano Island (Italy), Sousaki (Greece), Nea Kameni (Santorini) and Nisyros (Greece) soils. Clues of methane microbial oxidation in soils of these areas can be already found in the CH₄/CO₂ ratio of the flux measurements which is always lower than that of the respective fumarolic manifestations indicating a loss of CH₄ during the travel of the gases towards earth's surface. Laboratory methane consumption experiments made on soils collected at Pantelleria, Vulcano, Nea Kameni, Nisyros and Sousaki revealed for most samples consumption rates up to 950, 48, 15, 39 and 520 ng CH₄ h⁻¹ for each gram of soil (dry weight), respectively. Only few soil samples displayed no methane consumption activity. Analysis on soil gases and chemical-physical characteristics of the soils allowed us to discriminate the main factors that influenced the methanotrophs presence and the methane consumption rate. Soil gases composition, and in particular the amount of the CH₄ and H₂S, represent the main discriminating factor for methanotrophs. In fact, Vulcano and Nisyros Island, whose soil gas contained up to 250000 ppm of H₂S, showed the lowest consumption rate. Moreover, in geothermal/volcanic soils H₂S contribute to the soil pH lowering; highest methane consumption were recorded in Pantelleria island where H₂S is less than 20 ppm and pH close to the neutrality were measured. Microbiological and molecular analyses allowed to detect the presence of methanotrophs affiliated to Gamma and Alpha-Proteobacteria and

to the newly discovered acido-thermophilic methanotrophs belong to the Verrucomicrobia phylum in soils from Pantelleria. Culturable methanotrophic Alphaproteobacteria of the genus Methylocystis and the Gammaproteobacteria Methylobacterium were isolated by enrichment cultures. The isolates show a wide range of tolerance to pH and temperatures and an average methane oxidation rate up to 450 ppm/h. A larger diversity of (α - and γ -) proteobacterial and verrucomicrobial methanotrophs was detected by a culture-independent approach based on the amplification of the methane mono-oxygenase gene pmoA. This is the first report describing coexistence of both the methanotrophic phyla (Verrucomicrobia and Proteobacteria) in the same geothermal site. The presence of proteobacterial methanotrophs, in fact, was quite unexpected because they are generally considered not adapted to live in such harsh environments and could be explained by not really low pH values (> 5) of this specific geothermal site. Such species could have found their niches in the shallowest part of the soils of Favara Grande where the temperatures are not so high and thrive on the abundant uprising methane. Understanding the ecology of methanotrophy in geothermal sites will increase our knowledge of their role in methane emissions to the atmosphere.

SOMMARIO

Ogni anno, 22 Tg di CH_4 vengono rilasciati in atmosfera da numerose sorgenti sia naturali che antropiche. Il metano riveste un ruolo molto importante nella chimica dell'atmosfera terrestre e nel bilancio dell'energia radiante assorbita, essendo il secondo gas serra più potente dopo la CO_2 . Le aree vulcaniche e geotermali contribuiscono al flusso di metano in atmosfera, essendo vaste aree di degassamento. Studi preliminari hanno stimato che le emissioni globali di metano dai sistemi geotermali e vulcanici europei sono nel range di 4-16 kt a^{-1} . Questa stima è stata ottenuta indirettamente dai dati delle emissioni di CO_2 o H_2O e dal rapporto del flusso CO_2/CH_4 oppure $\text{H}_2\text{O}/\text{CH}_4$ misurati nelle principali fumarole. La stima del metano emesso globalmente dalle aree vulcaniche e geotermali non è ancora ben definita in quanto il bilancio tra le emissioni per degassamento dai suoli e il consumo di metano per ossidazione microbica è ancora poco noto. Inoltre, le misure di flusso di metano sono molto difficili da eseguire e si hanno a disposizione pochi dati. Alcuni metodi, seppur accettabili al fine di ottenere stime sul flusso di metano, escludono completamente la possibilità che il metano venga rimosso per via microbica dai batteri metanotrofi. A scala globale, l'ossidazione microbica del metano contribuisce alla rimozione di circa il 3-9% del metano dall'atmosfera. Ma l'importanza dei batteri metanotrofi è ancora maggiore in quanto questi ossidano la maggior parte del metano prodotto nel suolo e nel sottosuolo prima che questo raggiunga l'atmosfera. Le condizioni ambientali dei suoli vulcanici e geotermali (ad esempio scarso contenuto in ossigeno, alta temperatura, attività protonica, ect.) sono stati da sempre considerati inospitali per i batteri metanotrofi. Tuttavia, di recente è stata dimostrata la presenza di batteri acidofili e termofili appartenenti al phylum dei Verrucomicrobia. Questi organismi sono stati individuati alla Solfatarina di Pozzuoli (Italia), ad Hell's gate (Nuova Zelanda) ed in Kamchatka (Russia).

Qui riportiamo l'attività metanotrofa riscontrata nei suoli dell'Isola di Pantelleria (Italia), dell'Isola di Vulcano (Italia), di Sousaki (Grecia), di Nea Kameni- Santorini (Grecia), e dell'Isola di Nisyros (Grecia). Evidenze di rimozione microbica del metano in questi suoli era già stata riscontrata nel rapporto dei flussi di CO_2/CH_4 , che risultava sempre inferiore rispetto a quello atteso, indicando una perdita di CH_4 durante il suo movimento verso la superficie. Esperimenti per la misura del consumo di metano sono stati eseguiti usando i suoli di Pantelleria, Vulcano, Nea kameni, Nisyros e Sousaki.

Questi esperimenti hanno rivelato tassi di consumo fino a 950, 48, 15, 39 e 520 ng $\text{CH}_4 \text{ h}^{-1}$ per ogni grammo di suolo (peso secco), rispettivamente. Solo pochi campioni non hanno indicato consumo di metano. L'analisi dei gas del suolo e le caratteristiche chimico-fisiche del suolo ci hanno permesso di discriminare i fattori principali che influenzano la presenza dei metanotrofi e il tasso dei consumi del metano. La composizione del gas dai suoli, e in particolare il contenuto di CH_4 e di H_2S rappresentano il fattore discriminante per i metanotrofi. Infatti, l'isola di Vulcano e di Nisyros, il cui contenuto in H_2S raggiunge circa 250000 ppm, mostrano i consumi più bassi. In aggiunta nei suoli geotermali e vulcanici l' H_2S contribuisce all'abbassamento del pH dei suoli. I valori di consumo maggiori sono stati misurati nell'isola di Pantelleria dove l' H_2S è meno di 20 ppm e il pH è vicino alla neutralità. Analisi microbiologiche e molecolari hanno permesso di riscontrare nei suoli di Pantelleria la presenza di batteri metanotrofi affiliati ai Gamma ed agli Alfa-Proteobatteri

ed agli acido-termofili Verrucomicrobia. Il metanotrofo coltivabile appartenete al genere Methylocystis (Alfaproteobatterio) e il Gammaproteobatterio Methylobacterium sono stati isolati attraverso colture di arricchimento. Gli isolati mostrano ampi range di tolleranza di pH e temperatura e un tasso di ossidazione fino a 450 ppm/h. Attraverso l'amplificazione del gene pmoA, basandosi sui metodi coltura-indipendenti è stata rivelata un'ampia diversità di batteri metanotrofi appartenenti ai Proteobatteri (α - e γ -) ed ai Verrucomicrobia.

Questo è il primo report in cui si dimostra la coesistenza di entrambi i phyla di metanotrofi in un sito geotermale/vulcanico. La presenza dei metanotrofi Proteobatteri era inaspettata perché le condizioni di sito sono state considerate inadeguate e può essere spiegata del pH non eccessivamente basso (>5) di questo specifico sito geotermale. Queste specie possono aver trovato la loro nicchia negli strati più superficiali dei suoli di Favara Grande a Pantelleria dove le temperature non sono così alte ed è presente una forte risalita di metano. capire l'ecologia dei metanotrofi nei siti geotermali e vulcanici aumenterà le conoscenze nel loro ruolo nelle emissioni di metano in atmosfera.

1. INTRODUCTION

1.1 METHANE (CH₄)

Methane, the most abundant hydrocarbon in the atmosphere, plays a key role in the abrupt climate change being the second most important greenhouse gas after the CO₂. Over the last three centuries the methane mixing ratio increased from 700 – 750 ppb in the 18th century to a global average of 1750 ppb in 2000s (Fig. 1.1). The rate of increase was close to 16 ppb per year in 1700s, but it started to decrease in 1990s, this variation in the rate was attributed to the climate-altering variations in emissions from biomass burning (Van der Werf et al., 2004), wetlands (Walter et al., 2001) and changes in the chemical sink after the eruption of Pinatubo (Dlugokencky et al., 1996).

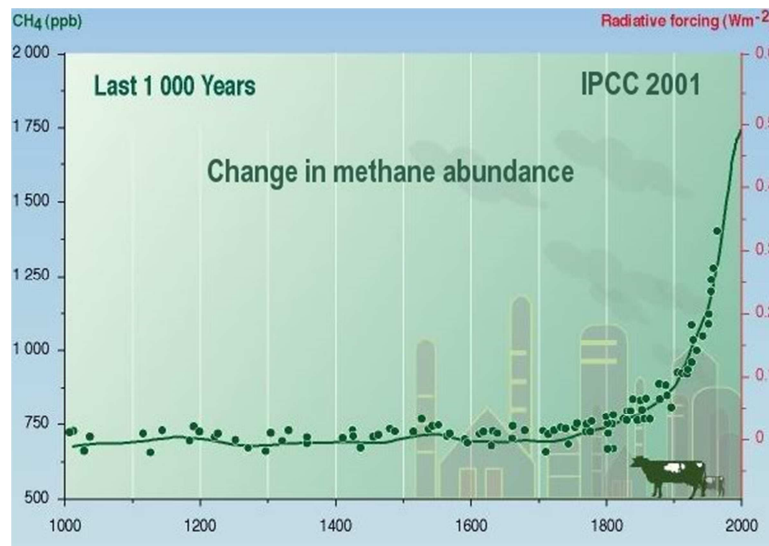


Fig. 1. 1- Variation of methane abundance in the atmosphere (IPCC, 2001).

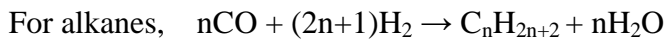
The increased amount of methane in the atmosphere has important implications for the energy balance and the chemical composition of the atmosphere. These effects are due to the chemical and physical properties of the methane molecule. In fact, methane absorbs and emits longwave radiation at the wavelengths of 3.31 μm and 7.66 μm ; the difference between the vibrational states of the CH₄ molecule corresponds to the energy of photons that can be absorbed by a CH₄ molecule. This energy allows the transition of the CH₄ bend-vibrational state to one of a higher energy. The vibrational transitions are associated with rotational transitions. This process is reversed by the emission of a photon or by the transfer of energy to other molecules by collision. The Earth emits energy at wavelengths as determined by the local temperature. This energy transfer is most efficient at wavelengths that are intensively emitted by the Earth, and at

wavelengths that are in a relatively transparent part of the absorption spectrum of the atmosphere. Both criteria are met between 7 μm and 12 μm , known as the atmospheric infrared window. Because the longwave absorption of CH_4 at 7.66 μm occurs within the atmospheric window region, CH_4 is an important greenhouse gas (Herzberg, 1945). Even if the atmospheric abundance of CH_4 is about 200 times smaller than CO_2 , it contributes significantly to the enhanced greenhouse effect owing to a relatively high warming efficiency. This efficiency is quantified by the Greenhouse Warming Potential (GWP), defined as the induced radiative forcing relative to CO_2 ($\text{Wkg}^{-1}/\text{WkgCO}_2^{-1}$) integrated over a certain time period. If the direct (radiative) and indirect (chemical) contributions of CH_4 are added, a GWP of 21 is calculated for a 100 year integration time. The contribution of CH_4 to the enhanced greenhouse effect is estimated at 0.57 W m^{-2} , or 22% of all greenhouse gases (36% for CO_2) for the period 1850–1992 (Lelieveld et al., 1998). Since the recent decline of the CH_4 growth rate is poorly understood, future contributions are difficult to predict (Houweling, 1970).

1.2 METHANE CYCLE, ORIGINS AND SOURCES

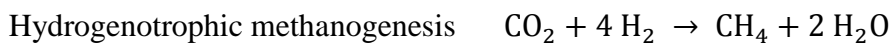
In the carbon cycle, methane plays an important role being one of the most important greenhouse gases (Fig. 1.2). The total source strength for CH₄ amount at 598 Tg a⁻¹, while the total global sink is 576 Tg a⁻¹ (IPCC, 2001); the imbalance produces 22 Tg of methane added in atmosphere every year, increasing the total abundance (5000 Tg, IPCC 2001). Methane is produced by multiple mechanisms grouped in abiotic, biotic and thermogenic origins.

Abiotic methane can be considered CH₄ produced via Fischer-Tropsch-type reactions:



The reactions consist in a reduction of the carbon monoxide by the hydrogen at the temperature range of 170-220°C and at the pressure of 20 bar. This type of methane is formed in few systems like mid-ocean-ridge (MOR) hydrothermal systems, volcanic hydrothermal systems and low temperature serpentinisation of ophiolythic sequences, and predominate where organic matter deposits are depleted. Nevertheless, Giggenschbach (1995) and Hernandez et al. (1998) highlighted some exceptions in methane origin's mechanism in these systems; in fact, methane can be produced in some low temperature (<100 °C) geothermal areas and in some volcanic soils by biogenic processes by archaea bacteria.

Biogenic methane originates from the degradation of the organic matter by microbial communities (methanogens), following two different patterns - Hydrogenotrophic methanogenesis and Acetoclastic methanogenesis - depending by on soils and climatic conditions:



In absence of primary electron acceptors like O₂, NO₃⁻, SO₄²⁻ and Fe³⁺, the final step in degradation of organic matter by microbial communities is the oxidation of small

molecules, such as acetate and H₂ coupled to the reduction of CO₂, or the methyl group of methane (Op den Camp et al, 2009). Thermogenic methane is produced via non-microbial decomposition of the organic matter; it is considered biogenic because the last source is organic material, but it is formed as a result of abiotic reactions, so it can be considered abiogenic but not abiotic methane; this type of methane predominates in tectonic subduction zones where organic matter is continually buried. It is possible to discriminate the origin mechanism of the methane because methane molecules maintain an isotopic fingerprint left by the origin mechanism as shown in Fig 1.2.

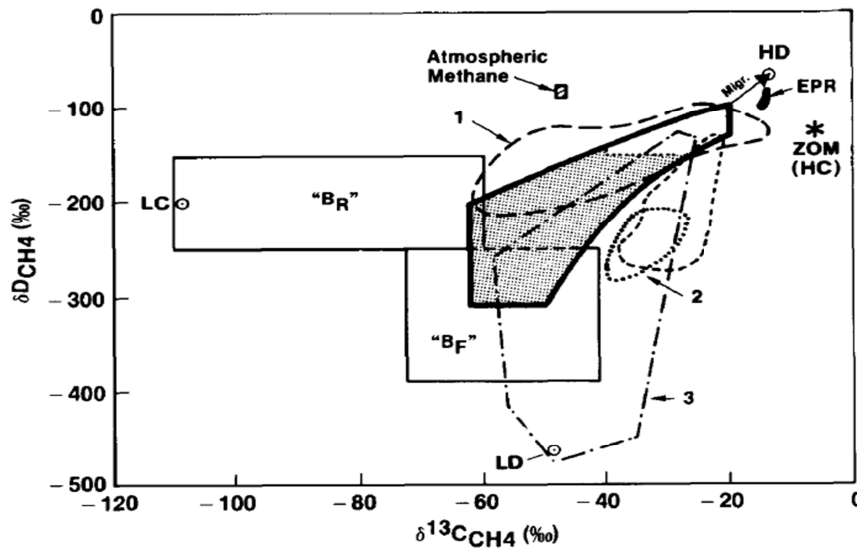


Fig. 1. 2 - ¹³C and deuterium concentrations in naturally occurring methane. Fields BR and BF are the areas which encompass bacterial methanes that form by CO₂ reduction and fermentation, respectively (see Fig. 1). The heavy outlined area encompasses methane of thermogenic origin, wherein the shaded part depicts methane associated with oils and the unshaded part the non-associated methane. 1 = Sacramento Basin, California (Jenden and Kaplan, 1988); 2 = Cooper Basin, Western Australia (Rigby and Smith, 1981); 3 = Canadian Shield gases (Sherwood et al., 1988); 4 = geothermal methane (Des Marais et al., 1981; Lyon and Hulston, 1984; Welhan, 1988 in this special issue); EPR=East Pacific Rise (Welhan, 1981); ZOM= Zambales Ophiolite methane Philippines (Abrajano et al., (1988 in this special issue); Migr. = migrated Rotliegend gases, G.D.R. (Runge, 1980); LC and HC and LD and HD are highest and lowest concentrations for ¹³C and deuterium, respectively, found so far in natural methane, Atmospheric methane (Wahlen et al., 1987). (Schoell, 1988).

A wide range of sources, both natural (wetlands, termites, ocean, fresh water, wild ruminants, forest burning, gas hydrate and geological sources) and anthropogenic (energy use, landfill, waste treatment, rice agriculture and biomass burning) emit a large amount of methane in to the atmosphere every year or store it as solid methane hydrate on the sea floor or in terrestrial sediment (Fig. 1.3). This latter case creates an unstable reservoir in face of future global warming.

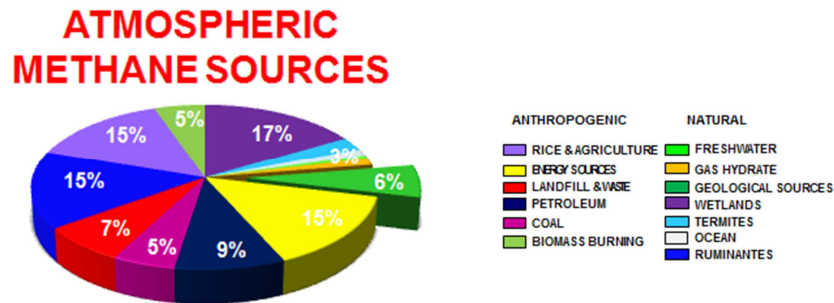


Fig. 1. 3 - Methane emission from different sources (Kvenvolden et al., 2005).

Natural sources contribute emitting 170 Tg of methane per year in the atmosphere, while anthropogenic sources emit at about 540 Tg of methane per year (Kvenvolden et al., 2005).

In this thesis, attention is focused on the geological sources of methane and in particular on geothermal/volcanic sources. The estimation of the total CH₄ emission of geogenic methane is currently not well defined since the balance between emission through degassing and sink within the soils is not well known.

Methane is an important constituent of geothermal gases, but the origin is quite controversial. The main origin mechanism of methane in geothermal area is the inorganic synthesis in geothermal reservoirs is by the Fischer-Tropsch reaction in which temperature dictates the equilibrium of the reaction (Giggenbach, 1980) and represents most of the methane production in geothermal area. Extensive faults and fractures in geothermal environments enhance the rate of the methane flow. The mantle source of methane is not really clear; These CH₄ origin seems to be related to mineral phase transitions with the liberation of volatiles, instead of any primordial gas (Etiope et al., 2002).

The biogenic methane in geothermal systems is limited and can be associated with organic-rich sediments (Gunter, 1978). In any case, methane emitted from geothermal areas is released from aqueous hydrothermal solutions by boiling or degassing and escapes from localized sites such as gas vents, mofettes, fumaroles, crater exhalation or as pervasive leakage throughout large areas. Methane in volcanic areas escapes from magma and emanates diffusely to the surface (Fig. 1.4.).

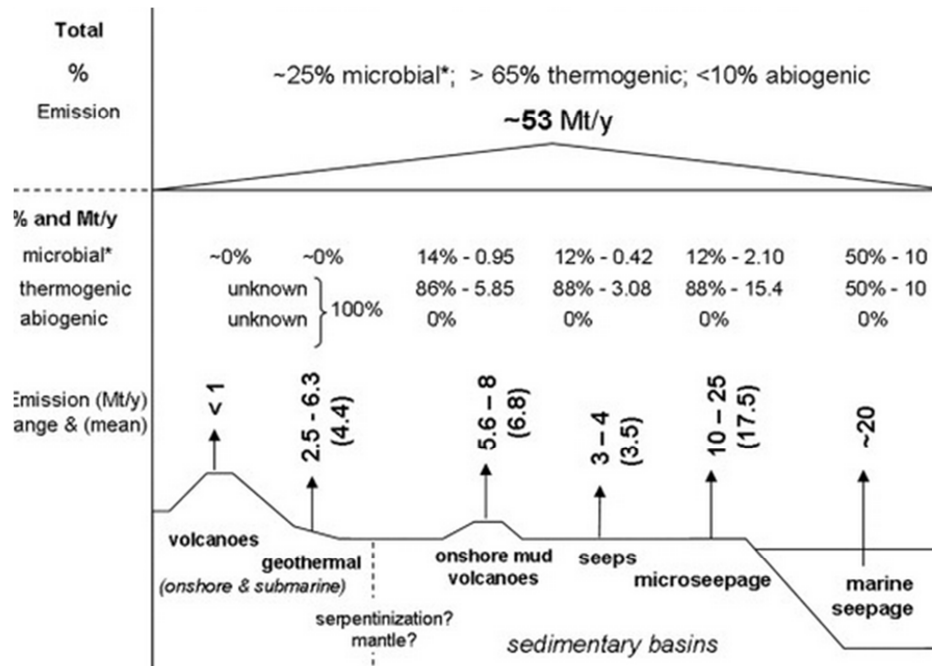


Fig. 1. 4 - Geological sources of methane.

	Area (Km ²)	CH ₄ output (ton/yr)
Czech Rep.	1500	~0.3
Germany	900	2
Greece	34	~800-3500
Italy	~100	1600-11500
Iceland	577	1300
Spain	-	2
Total		~4000-16000

Table 1. 1 - Methane output from European country (Etiopie et al, 2008) .

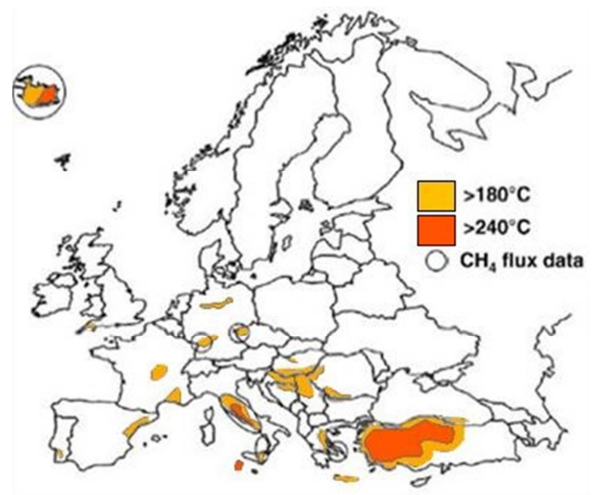


Fig. 1. 5 - Main European geothermal (modified by Etiopie et al., 2008).

On the global scale methane emissions from geothermal/volcanic areas contribute on the order of 1.7 – 9.4 Tg a⁻¹ (Kvenvolden et al., 2005; Lacroix et al, 1993). The

geothermal emissions vary depending on the geo – tectonic setting of the area: in the region of crustal rifting and plate subduction, geothermal and volcanic methane are predominant.

Geological history suggests that at least 10 European countries host geothermal manifestations with methane emissions, and Italian and Hellenic territories are the most active geothermal sites (Fig 1.5 and Table 1.1.). The amount of methane emitted from geothermal/volcanic areas is currently not well estimated because the methane output is usually measured not directly but using indirect method.

1.3 METHANE SINKS

Methane removal takes place mainly in the atmosphere by photochemical depletion and in the soils by microbial oxidation (Fig. 1.6). Methane is a molecule relatively stable under standard conditions and direct reactions of molecular oxygen with gaseous hydrocarbons are difficult under atmospheric conditions, owing to the large activation energies required. Instead, most reactions of methane removal from the atmosphere are driven by highly reactive radicals such as OH and H₂O. In the global methane cycle the largest atmospheric sink is represented by hydroxyl radicals reaction in the troposphere. Further destruction takes place in the stratosphere by hydroxyl reactions and by chlorine oxidation and by electronically excited oxygen atoms. These reactions remove 90% of the methane emitted in atmosphere. Microbial oxidation is the main sink of methane in soils. The uptake of atmospheric methane in soils has been estimated to be 30 – 45 Tg per year (Ehhalt and Prather, 2001). Microbial oxidation is a remarkable biological filter for methane because this process in the earth intercept and remove more than 50% of the methane coming up through the soil before it reaches the atmosphere (Reeburgh et al., 2003). The soil consumption of methane occurs via oxidation by aerobic bacteria (methane oxidizing bacteria or methanotrophs) several varieties of which have been identified (Hanson and Hanson, 1996). Methane microbial oxidation occurs in a small subsurface region (3-15 cm of depth). The key factors that influence the methane uptake and consumption rate are the rate of diffusion in the substrates of CH₄ and O₂, the rate of biological oxidation and the soil properties (Whalen and Reeburgh, 1996; Savage et al., 1997).

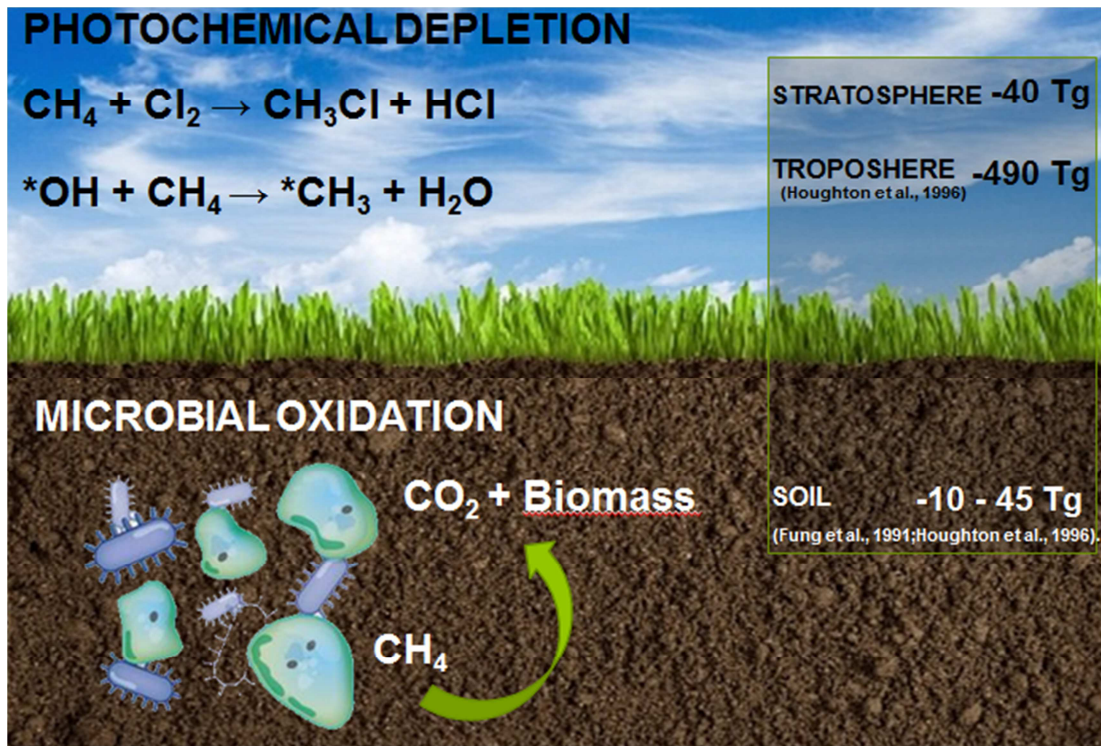


Fig. 1. 6 - Methane sinks in soil and in atmosphere.

1.4 METHANE OXIDIZING BACTERIA (MOB) AND THEIR ECOLOGY

Methane oxidizing bacteria (or methanotrophs) are microorganisms with the ability to use methane as the sole source of carbon for energy and biomass production. Methanotrophs represent a subgroup of Methylophilic bacteria, aerobic bacteria that use one-carbon compounds (methane, methanol, methylated amines, haloethanes, and methylated compounds containing sulfur) as a major source of cellular carbon (Hansen and Hansen 1996). Distribution, ecology and activity of methanotrophs are important to understand the global methane cycle, and the management to reduce methane emissions in the atmosphere. Methane oxidizing bacteria (MOB) are ubiquitous and play an important role in the global carbon cycle acting as a natural filter between the underground and the atmosphere. They were isolated from several environments such as, soils, wetlands, freshwater, marine sediments, water columns, groundwater, rice paddies, and peat bogs (Kolb and Horn 2012, McDonald et al., 2005, Cebon et al., 2007).

Methanotrophs are, from an ecological point of view, grouped on the basis of their affinity for methane. A first group are identified as “high affinity oxidation” and are able to consume methane at atmospheric concentration (1.7 ppm). This group is ubiquitous in soils that have not been exposed to high NH_4^+ concentrations (Chowdhury et al., 2013, Bender and Conrad, 1992). High affinity methanotrophs contribute at about 10% of the total atmospheric methane consumption by methanotrophs in soils. The second group, low affinity oxidation, are capable of oxidizing methane in concentrations higher than 40 ppm. Low affinity methanotrophs live mainly in soil with neutral pH (Chowdhury et al., 2013, Bender and Conrad 1992). CH_4 oxidation by aerobic methanotrophs is ecologically controlled by multiple factors including oxygen availability, NH_4^+ concentration, pH, water availability, temperature and other abiotic factors. Most common and favorable conditions for methane microbial oxidation are water content of 20-35%, temperature in the range of 25-35°C, pH 5.8 – 7.5, NH_3 concentration between 12 and 61 mM and Cu less than 4.3 mM (Bender and Conrad, 1995).

Methanotrophic bacteria were overall grouped in three different phyla: *Proteobacteria*, *Verrucomicrobia* and *NC10*. Commonly, methanotrophs fall within the phylum *Proteobacteria*, but recently methanotrophs in the phylum *Verrucomicrobia* have been discovered in geothermal areas (Dunfield et al., 2007; Pol et al., 2007; Islam et al., 2008). The novel phylum, NC10 represents bacteria capable of anaerobic methane oxidation coupled to denitrification (Ettwig et al., 2009). Methanotrophs belonging to *Proteobacteria* were usually grouped in Type I (*Gammaproteobacteria*), Type II (*Alphaproteobacteria*) and Type X, based on morphological, physiological and phylogenetic characteristics (Hansen and Hansen 1996) (Table 1.2). Proteobacterial methanotrophs are adaptable to several environmental conditions; they can grow in a temperature range between 3.7 and 67 °C) (Tsubota et al., 2005) and in a range of pH from 4.5 and 7.5 (Dedysh et al., 2007). Verrucomicrobial methanotrophs were identified for the first time (2008) in three different geothermal areas. They are thermo-acidophilic bacteria and are able to grow in very low pH (0.8) and at temperatures up to 65°C (Islam et al., 2008).

Phylum and class	<i>Proteobacteria</i> (<i>Gammaproteobacteria</i>)	<i>Proteobacteria</i> (<i>Alphaproteobacteria</i>)	<i>Proteobacteria</i> (<i>Alphaproteobacteria</i>)	<i>Verrucomicrobia</i>
Family	<i>Methylococcaceae</i> <i>Methylococcus, Methylocaldum,</i> <i>Methylohalobius, Methylothermu,</i> <i>Methylobacter,</i>	<i>Methylocystaceae</i>	<i>Beijerinckiaceae</i>	<i>Methylacidiphilaceae</i>
Genera	<i>Methylomicrobium, Methylomonas,</i> <i>Methylosarcina,</i> <i>Methylosoma, Crenothrix,</i> <i>Clonothri, Methylosphaera</i>	<i>Methylocystis, Methylosinus</i>	<i>Methylocella, Methylocapsa</i>	<i>Methylacidiphilum</i>
Lowest reported growth pH	5.0	4.4	4.2	0.8
Highest reported growth pH	11	7.5	7.5	6.0
Lowest reported growth temperature (°C)	3.5	5.0	4.0	37
Highest reported growth temperature (°C)	67	40	30	65
sMMO	+/-	+/-	+/-	-
pMMO	+	+	+/-	+
Carbon fixation pathway	Ribulose monophosphate pathway, Calvin-Benson-Bassham Cycle (rarely)	Serine cycle	Serine cycle, Calvin-Benson- Bassham Cycle	Serine cycle, Calvin- Benson-Bassham Cycle

Table 1. 2- Comparison of all described families of methanotrophic bacteria. + = presence; - =absence.

1.5 TYPE I, TYPE II AND TYPE X METHANOTROPHS: PHYSIOLOGY AND BIOCHEMISTRY

Despite their diversity, methanotrophic bacteria share several characteristics that allow them to be classified as either a Type I, a Type II or Type X methanotrophs. Type I methanotrophs, which fall under the Gamma subdivision of *Proteobacteria*, typically have intracytoplasmic membranes throughout the cell that occur as bundles of vesicular disks, utilize the ribulose monophosphate (RuMP) pathway (Fig. 1.7) for carbon assimilation, and have signature phospholipid fatty acids that are 4 and 16 carbons in length. Type II strains, which fall under the Alpha subdivision of the *Proteobacteria*, typically have intracytoplasmic membranes that are aligned along the periphery of the cell, utilize the serine pathway for carbon assimilation, and have signature phospholipid fatty acids of 18 carbons in length. Type X as type I methanotrophs, utilized ribulose monophosphate as the primary pathway for formaldehyde assimilation. But they also have low levels of the serine pathway enzyme, ribulosebiphosphate carboxylase, an enzyme present in the Calvin- Benson cycle (Hanson and Hanson 2006).

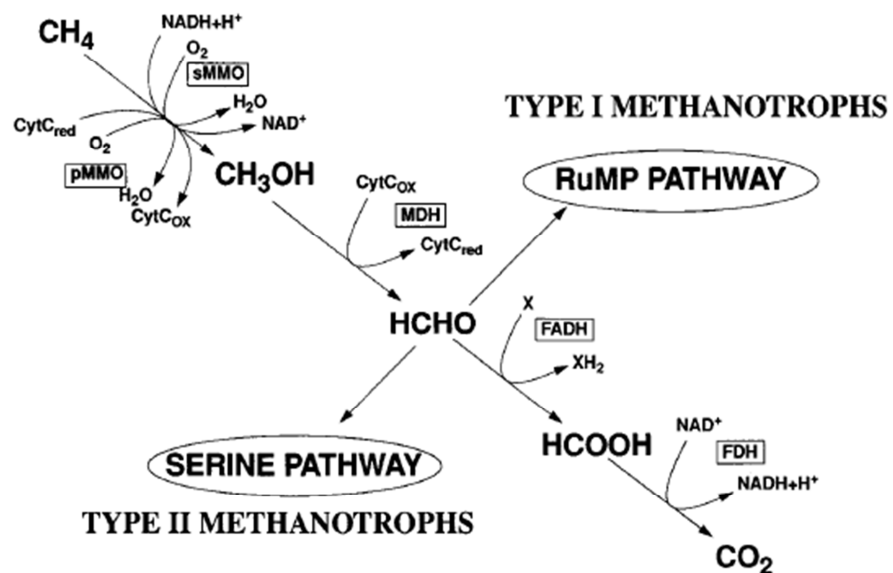


Fig. 1. 7 -Pathways for the oxidation of methane and assimilation of formaldehyde. Abbreviations: CytC, cytochrome c; FADH, formaldehyde dehydrogenase; FDH formate dehydrogenase (Hansen and Hansen, 1996).

Despite the wide methanotrophs diversity, the methane conversion pathway is common to all the methanotrophs and consists of four reactions in which methane is

oxidize intermediate products (methanol, formaldehyde, formic acid to form carbon dioxide. The remarkable reaction, in methane metabolism is the first step, in which methanol is produced from the methane molecule. This step is catalyzed by an important enzyme, methane mono-oxygenase (MMO) (Fig. 1.8 a, b and c).

MMO exists in two different forms: soluble MMO (sMMO, located in the cytoplasm) and membrane bound (to the cytoplasmatic membrane) particulate MMO (pMMO). The sMMO is well characterized by three enzyme components consisting of an hydroxylase, a B component and NAD(P)H reductase. The hydroxylase (MMOH, 285 KDa), is an oligomer of three different subunits (α , β and γ) and contains non-heme iron. The sMMO Operon contains six genes that codify for the hydroxylase α , β , and γ subunit (*mmoX*, *mmoY*, *mmoZ*), the reductase enzyme (*mmoC*), and the regulatory protein (*mmoB*), that permits the assembling of the unique di-iron center of the sMMO enzyme.

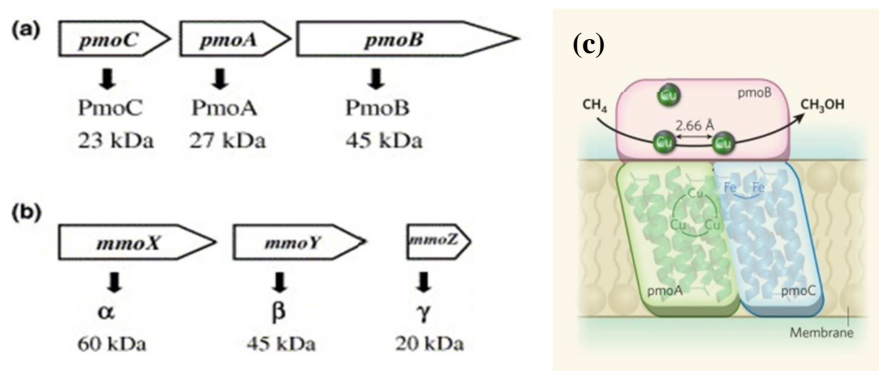


Fig. 1.8 – a) pMMO and b) sMMO encoding genes and subunits; c) pMMO: methane conversion in methanol.

The B component (MMOB) is a protein without cofactors, involved in engagement – release processes (Colby & Dalton 1978); while the NAD(P)H reductase (MMOR) is 38.4 kDa in size and contains flavin adenine dinucleotide and an Fe₂S₂ cluster (Hansen and Hansen 1996).

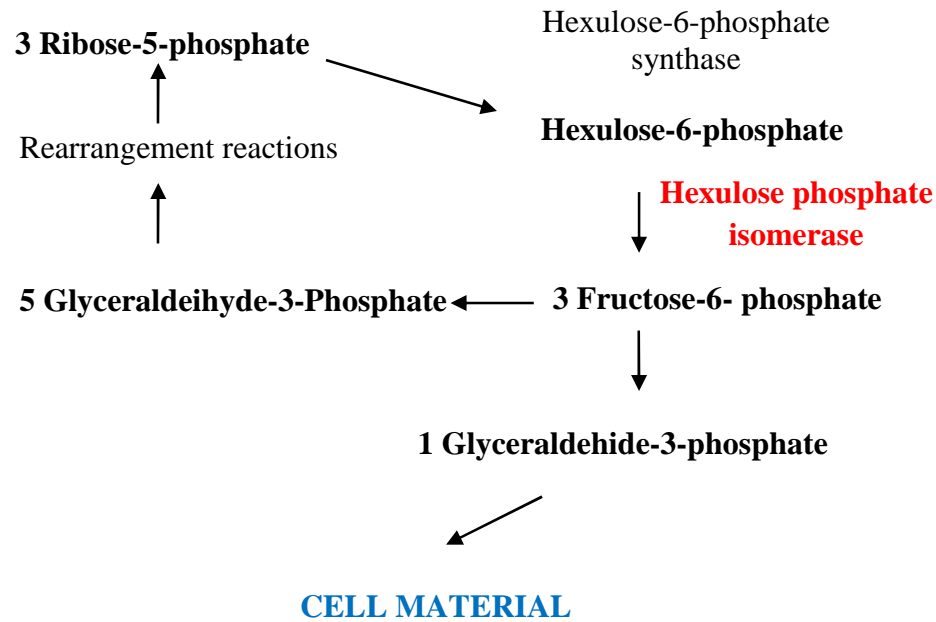
In contrast to sMMO, little is known about the molecular properties of pMMO; however, it is understood that this enzyme consists of three, integral-membrane, polypeptide subunits (ABC) and has a catalytic center containing copper. The A, B and C subunits constitute one monomer of the enzyme. The pMMO operon contains three genes that code for the A, B, and C-subunit (*pmoB*, *pmoA*, *pmoC*).

Even if both sMMO and pMMO are involved in methane oxidation, their aminoacidic sequence of their protein are quite different; moreover sMMO and pMMO differ in the metals used as cofactors, in their location inside the cells and in electrons donors used. Methane microbial oxidation by aerobic methanotrophs is triggered by the bond $\text{CH}_4 - \text{MMO}$, this requires two reducing equivalents to split the O_2 bond. One atom of oxygen is reduced to form H_2O and the other is combined with the methane to form methanol.

Methanol is oxidized in formaldehyde by MDH (*Periplasmatic methanol dehydrogenase*). Electrons from the reaction are transferred at the CL cytochrome, the electron acceptor, that is oxidized by a C cytochrome. Formaldehyde is converted to formate by a system of several enzymes (Anthony, 1991). Finally, formate is oxidized in CO_2 by the enzyme NAD-dependent formate dehydrogenase.

The steps following the formaldehyde production are different in methanotrophs expressing sMMO and pMMO and it is possible to distinguish the ribulose pathway and the serine pathway (Fig. 1.9).

a) RuMP PATHWAY FOR FORMALDEHYDE FIXATION



b) SERINE PATHWAY FOR FORMALDEHYDE FIXATION

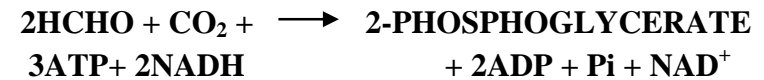
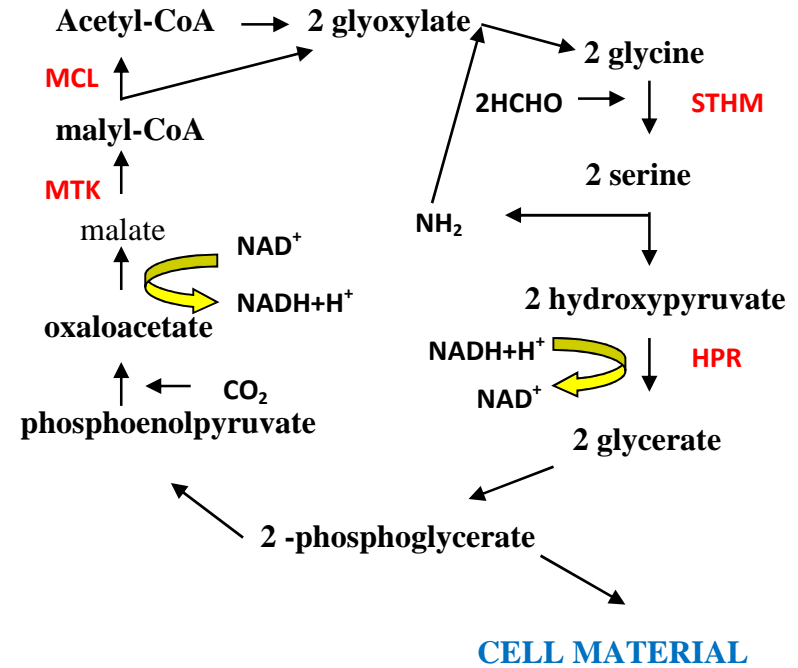


Fig. 1. 9 - a) RuMP pathway for formaldehyde fixation. The reaction is catalyzed by the unique enzymes of this pathway, hexulose - 6- phosphate synthase and hexulose-phosphate isomerase, are indicated. b) Serine pathway for formaldehyde fixation. Unique reactions catalyzed by serine hydroxymethyl transferase (STHM), hydroxypyruvate reductase (HPR), malate thiokinase (MTK), and malyl coenzyme A lyase (MCL) are identified (modified by Hansennand Hansen, 1996).

1.6 GEOTHERMAL SYSTEMS

Geothermal areas have been the subject of this project due to their unique characteristics in geo-biosphere. Geothermal areas occur frequently in regions of active or recently active volcanism and consist in a series of systems in which heat is transferred from within the Earth to the surface through rocks by conduction or by transfer of heat involving water, either in liquid or vapor state (hydrothermal areas). Three geological components are required for the formation of a geothermal/hydrothermal system: fluid (liquid or gas), heat, and permeability through rocks to permit the fluid to flow in the subsurface and rise to or near the land's surface (geothermal field). Meteoric water, or water that entered in a geothermal system at Earth's surface, such as rainfall, snowmelt, rivers, lakes, and seawater forms most of hydrothermal fluids. Water recharge, or the site where water soaks into the ground, may be distant (up to tens of kilometers) from the discharge site. Some waters reach several kilometers depth. The source of heat is either magma, in the case of volcano-related systems, or heat from the normal temperature increase with depth in the earth. Fractures in rocks often create permeability, but in some systems interconnected pores or large cave systems allow fluids to flow. Often, geothermal systems are associated with caldera structure because crustal fracturing occurred during the caldera formation that allowed the deep penetration of meteoric fluid, establishing the geothermal activity. A Geothermal system is generated where hot upflowing water approaches the surface in a region of anomalously high heat flow and where thermal convection dominates the behavior of ground water in the permeable crust (Elder, 1966, 1981). Thermal energy is provided by continuous intrusive activity, cooling of plutons in the upper 10 km of the crust (Larsen et al. 1979), and in minor part by mineral alteration, devitrification and decay of radioactive nuclides (Fehn et al., 1978). Geothermal systems are very different due to their chemical-physical characteristics (reservoir's temperature or enthalpy, nature and geological setting). See Table 1.3 for classification on the basis of the temperature.

TEMPERATURE	ENTHALPY	FLUID	GEOLOGY
Low-Temperature (LT): 150°C at 1 km of depth. Characterize by hot or boiling springs.	Low-enthalpy (< 800 kJ/kg).	Liquid dominated geothermal system with water temperature at boiling point and the water phase control the pressure in the reservoir.	Sedimentary basins, fracture or fault controlled convection systems, active fracture zone on land.
Medium-Temperature (MT): 150 – 200 °C			
High –Temperature (HT): temperature > 200°C at 1 km of depth; Characterize by fumaroles, steam vents, mud pools and high altered ground	High enthalpy (> 800kJ/kg)	Two-phase geothermal system where steam and water co-exist and the temperature and pressure follow the boiling point curve	Rifting zone, hotspot volcanism, compressional regime.
		Vapor-dominated geothermal systems where temperature at, or above, the boiling point at the prevailing pressure in the reservoir. Some liquid water may be present.	

Table 1. 3 - Classifications of geothermal systems on the basis of temperature, enthalpy and physical state (Bodvarsson, 1964; Axelsson and Gunnlaugsson, 2000).

Geothermal gaseous emissions consists of gases released from the aqueous hydrothermal solution, by boiling or degassing, in localized sites such as gas vents, mofettes and fumaroles (Etiopo et al., 2007). The total gas content in the steam phase varies from about 0.01% to several tens percent. CO₂ and H₂S are the main components of the geothermal gases, but they include also CH₄, N₂, H₂, NH₃ and trace gases (He, Ne, Ar, Kr, and Xe). In liquid-dominated systems gases are dissolved in the hot water, but they pass in steam phase when steam is formed by boiling.

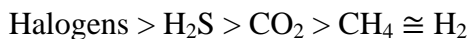
Europe is one of the most geothermally active areas in the world; 28 European countries have geothermal systems and at least 10 countries host surface geothermal manifestations (hot springs, mofettes, gas vents), including Italy and Greece.

1.7 HYDROTHERMAL GASES

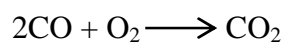
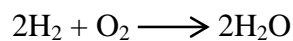
Volcanic gases are mainly composed by H₂O, CO₂, SO₂, H₂S, HCl, and HF. Gases are released both from active volcanoes when the magma is depressurized and by quiescent volcanoes by fumaroles or degassing throughout the soils. Fumarole gases rise toward the atmosphere following convective motion due to temperature that increases the kinetic energy of the molecule in the fluid. The release of the gases depends on their solubility in liquid phase. The solubility is the property of a solute (solid, liquid or gaseous) to dissolve in a solid, liquid, or gaseous solvent to form a homogeneous solution of the solute in the solvent. It depends on the physical and chemical properties of the solute and solvent as well as on temperature, pressure and the pH of the solution. Henry's law relates the solubility and "at a constant temperature, the amount of a given gas that dissolves in a given type and volume of liquid is directly proportional to the partial pressure of that gas in equilibrium with that liquid." Henry's law is expressed as:

$$p = k_H c$$

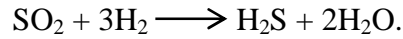
where p is the partial pressure of the solute in the gas above the solution, c is the concentration of the solute and k_H is a constant with the dimensions of pressure divided by concentration. The constant, known as the Henry's law constant, depends on the solute, the solvent and the temperature. Gas solubility in hydrothermal fluids, usually is:



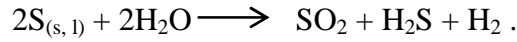
Halogens, H₂S, and CO₂ are the most soluble gases while, CH₄ and H₂ are less soluble. Liquid H₂O content increases with its a decrease in temperature (condensation); CO₂, the second most important volcanic gas, follows a similar tendency. H₂ and CO gas concentrations drop upon cooling in accordance with the reactions:



Sulfur in the fumarolic gas exists in two major species: SO₂ and H₂S. The variations in SO₂ and H₂S contents at temperatures above 573 K are controlled by the reaction:



At lower temperatures, where elementary sulfur is stable, the equilibrium is governed by the reaction:



Cl, F, Br, and, possibly, I are transported in volcanic gases in the form of their compounds with hydrogen: HCl, HF, and HBr. The behavior of HCl, HF, and HBr is due to the fact that they do not take part in redox reactions, and that the amount of precipitated solid halogen-bearing phases is incommensurably small as compared with their concentrations in the gas. As temperature decreases, CH₄, CO₂, and S₂ pass their maxima (1213 K for CH₄ and 1073 K for CO₂ and S₂), and then their concentrations gradually decrease. These components are subordinate and their contents are controlled by proportions of the major gas constituents H₂O, CO₂, SO₂, H₂S, and H₂ (Churakov et al., 1998).

1.8 SOIL (GEO)CHEMISTRY

Soils are multicomponent biogeochemical systems which reflect the influences of weathering and living organisms on the parent material. Soil is more complex than simply ground-up rock; in fact, it contains a large population of macro-, meso-, and microscale animals, plants, and microorganisms. Soil is characterized by solid inorganic and organic compounds in various stages of decomposition and disintegration, an aqueous solution of elements, inorganic and organic ions and molecules, and a gaseous phase containing nitrogen, oxygen, carbon dioxide, water vapor, argon, and methane plus other trace gases. It represents the interface between geosphere atmosphere and it is important because all life supporting components derive, either directly or indirectly even from the soil. Chemistry and geochemistry of the soils are very relevant because they rule the presence or the absence of life in soils (both in term of plant, microorganisms and animals). The key chemical characteristic of the soils is the pH. In geothermal areas, chemistry and pH of the soil are mainly influenced by the composition of fumarolic gases (H₂S, HCl, HF, and so on). Considering that halogens

are very soluble and their concentration in fumarolic flux is really low, H₂S represents the main contributor to soil acidification in this situation (Tedesco and Sabroux, 1987; Tedesco, 1994). Hydrogen sulphide is a weak acid, however, when it reaches the surface it is firstly oxidized to sulphur and then to sulphuric acid (pK₂ = 1.92), hence lowering the pH of soil (Brock, 1978). This gradient of pH can also be accompanied by a temperature gradient. Soil pH and temperature are the main limiting factors in volcanic areas for microorganisms and vegetation.

1.9 AIM

Geothermal and volcanic areas have long been considered limiting for methanotrophs life. Their harsh environmental conditions such as high temperatures, low pH and high concentrations of H₂S and NH₃, seemed to be inadequate for methanotrophs range of life. Despite their unfavourable environmental conditions, several evidences acquired in different geothermal and volcanic areas remarked the possibilities of the microbial oxidation of the methane in these areas. Firstly, laboratory incubation experiments using geothermal and/or volcanic soils indicated significant methane consumptions. Castaldi and Tedesco (2005) recorded consumption values from 4.5 to 150 mg CH₄ m⁻² day⁻¹ after a series of incubation experiment using soils from the Solfatara at Pozzuoli; D'Alessandro et al. (2011 and 2009) demonstrated microbial methane oxidation; after laboratory incubation experiments with soils from Sousaki recorded consumption values up to 478 pmol CH₄ h⁻¹ g⁻¹; Moreover, they obtained negative methane flux in a degassing area at Favara Grande in Pantelleria Island, indicating the possibilities of methane microbial oxidation during the measurement period.

Secondly, a clear evidences of methanotrophs activity in geothermal and volcanic soils is given by the anomalies recorded in the expected CO₂/CH₄ flux ratio. In other words, the methane flux in a degassing area is measured by two different method (direct and indirect); the first method permit to measured directly the methane flux from a degassing area; the second is based on the methane amount and the CO₂/CH₄ flux ratio measured in the fumaroles placed in the analysed degassing areas. If no methane uptake were occur, no difference in methane flux measures would be recorded.

D'Alessandro et al. (2009, 2011) evidenced serious anomalies in the CO₂/CH₄ flux ratio in measurements at Pantelleria Island, Sousaki and Nisyros Island. Fig. 1.10 a, b and c shows the CO₂/CH₄ flux ratio obtained by direct method from these degassing areas.

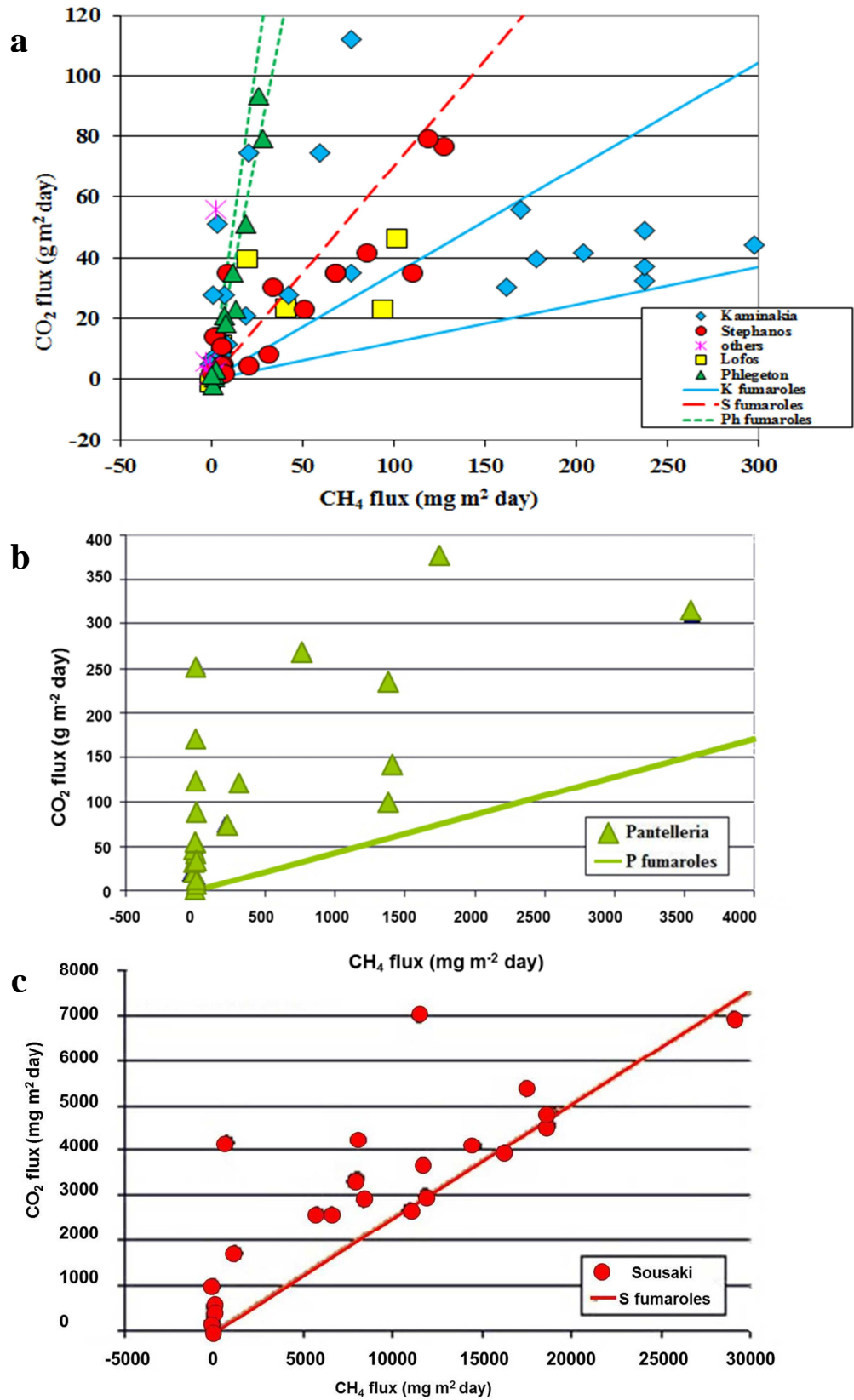


Fig. 1. 10- CO₂/CH₄ flux ratio measures at a) Nisyros island, b) Pantelleria Island and c) Sousaki. Line indicates the ratio measured in fumaroles, symbols ratio measures in degassing areas close to the fumaroles.

Measured values are shifted than the expected ratio in fumaroles, because the methane flux is lower than the expected indicating a possible methane removal mechanism during the measurement period.

Finally, confirms of the methanotrophs presence in geothermal and volcanic were given by genetic analysis on soils performed by different group of research using soils from the Solfatara (Pozzuoli – Pol et al., 2007), Hell’s Gate (New Zeland – Op den Camp et al., 2009), Kamchatka (Russia – Islam at al., 2008; Kizilova et al., 2012). These studies permitted to discover the new acido-thermophilic methanotrophs belong to the *Verrucomicrobia* phylum in all the investigated areas. Moreover, Kizilova et al., (2012) in the hot springs at Kamchatka confirm the presence of the more thermophilic *Proteobacteria* “*Methylothermus*” belong to the *Gamma-proteobacteria*.

Clues of methanotrophs activity in geothermal and volcanic soils against few confirms of the presence of these bacteria brought our interest to ascertain and add confirm on the possibilities of these bacteria to be adapt to live in extreme environment. The start point was the evidences acquired by D’Alessandro et al., (2009 and 2011) at Pantelleria, Sousaki and Nisyros, but we extended our field of search to Vulcano Island and Nea Kameni (Fig. 1.11).

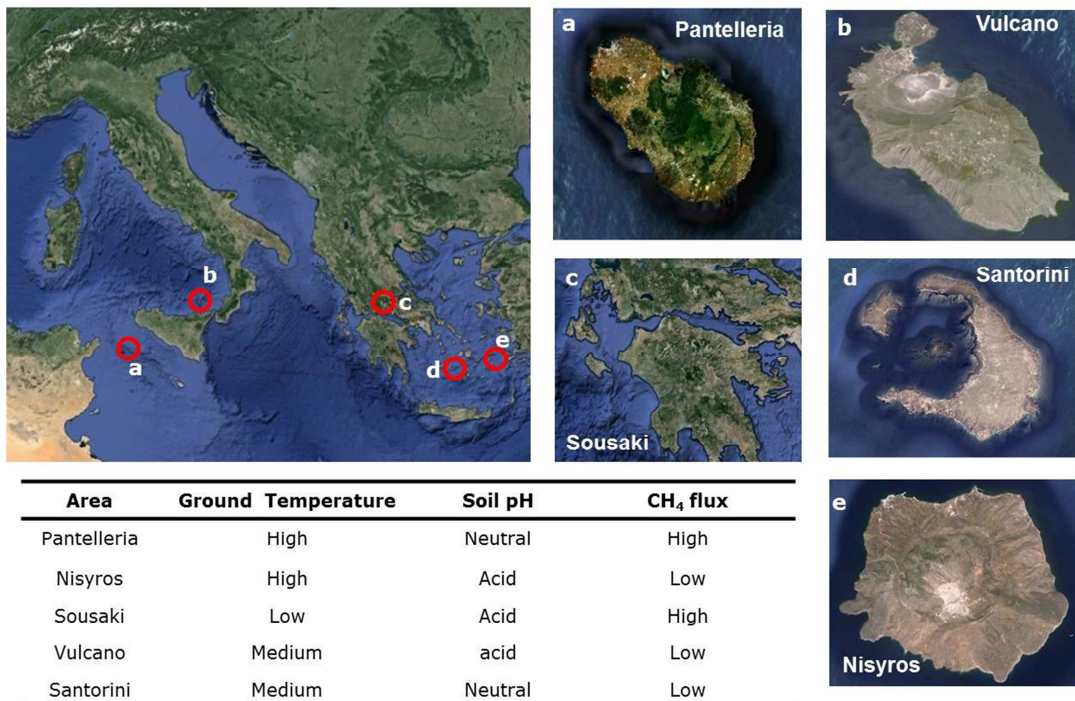


Fig. 1. 11 - Sampled areas, a) Pantelleria Island, Italy b) Vulcano Island, Italy, c) Sousaki, Greece, d) Nea Kameni - Santorini, Greece, and e) Nisyros, Greece island; table indicates chemical-physical conditions of the selected areas.

Pantelleria Island, Vulcano Island, Santotini Island, Nisyros Island and Sousaki were the five geothermal/volcanic system selected both in Italian and Hellenic territories on the basis of the methane flux from the underground, chemical-physical characteristics of the soils and H₂S content in the soil gases. Previous studies indicated that Pantelleria island and Sousaki area recorded the highest methane flux values among the selected sites. Vulcano Island and Nisyros the harsher conditions. Very high value of H₂S were recorded in Nisyros Island, Vulcano Island, the lower value were recorded at Pantelleria Island.

The first goal was to understand how the environmental conditions could influence the methanotrophic activity. The second goal was to analyze the methanotrophic potential of geothermal and volcanic soils. The third goal was to explore the methanotrophs diversity in the geothermal and volcanic soils and to evaluate their efficiency in reducing the methane released in to the atmosphere.

2. PANTELLERIA ISLAND

2.1. GEOLOGICAL SETTING

Pantelleria island is the emergent part of a quiescent Quaternary strato – volcano located at about 100 km SW of Sicily and 70 km off the Tunisia, in the Sicily Channel rift zone (Fig. 2.1 and Fig. 2.2).

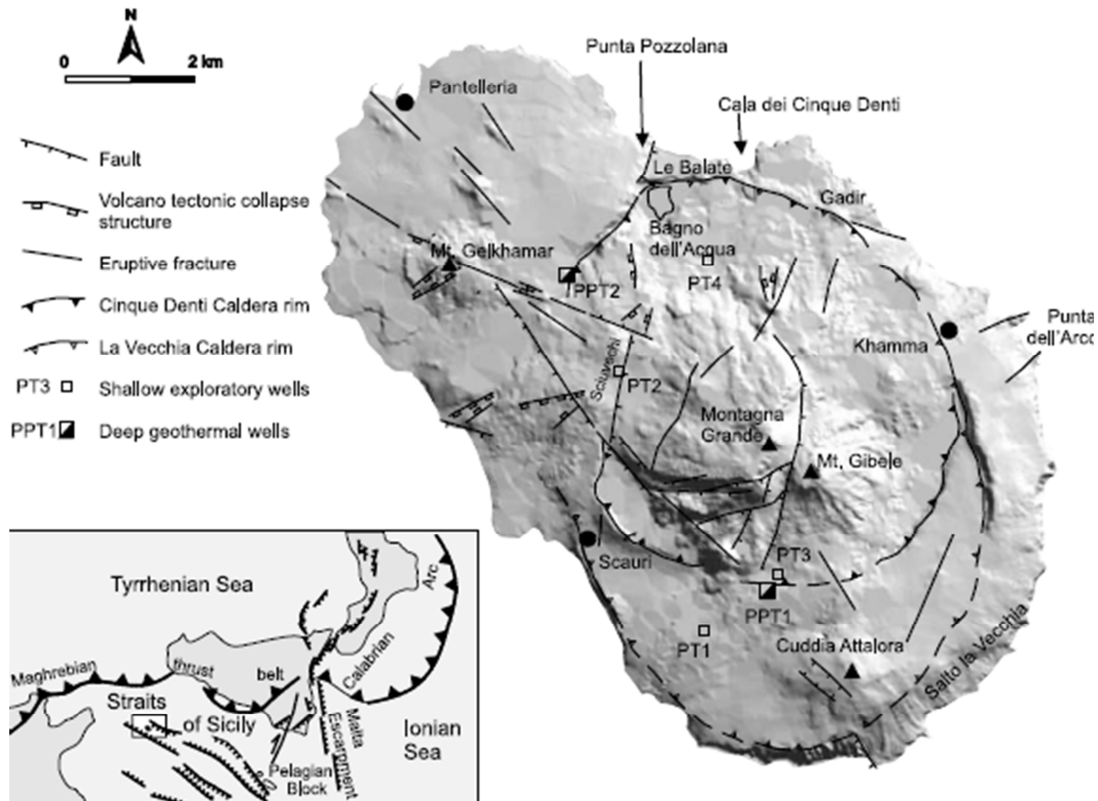


Fig. 2. 1– Geological structure of Pantelleria island.

The submergent part of the island is composed of high – density products and the subaerial products are mainly alkaline and peralkaline rhyolites (pantellerites) with a high silica content (Civetta et al 1984), true basalts occur only in the northwestern part of the island. The oldest subaerial products are dated at 320 ka, successive explosive events (114 ka and 45 ka) were followed by caldera collapses. Intra –caldera activity in the last 45 ka associated with geophysical data indicate an active magmatic chamber at crustal depth.

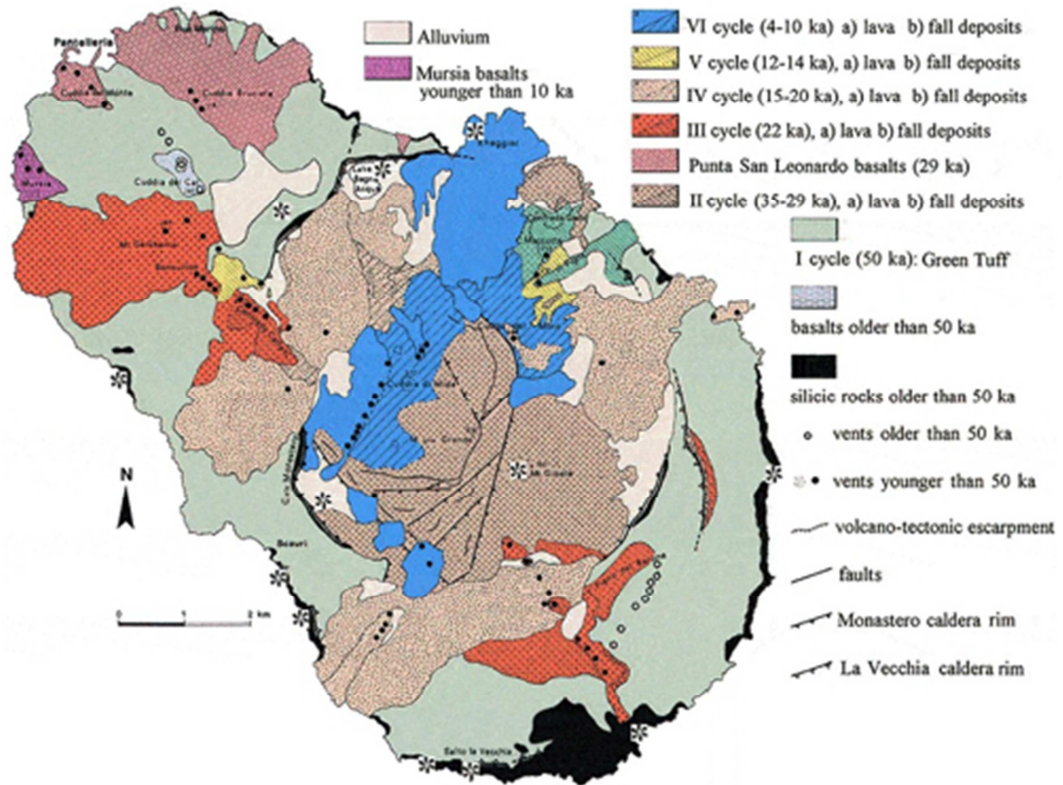


Fig. 2.2 - Geological map of Pantelleria Island.

The structural setting of Pantelleria is dominated by a resurgent active nested caldera in central south part of the island, formed during the most important volcanic episode of the island in the last 50 ka; and in the northwest the island is dominated by basaltic eruptions (Mahood and Hildreth, 1986; Civetta et al., 1988). Well drilling campaigns (Fulignati et al., 1997; Giannelli et al., 2001) distinguished a high-temperature active hydrothermal system in the caldera and the presence of a low temperature and low permeability hydrothermal system developed outside the caldera (Fig. 2.3).

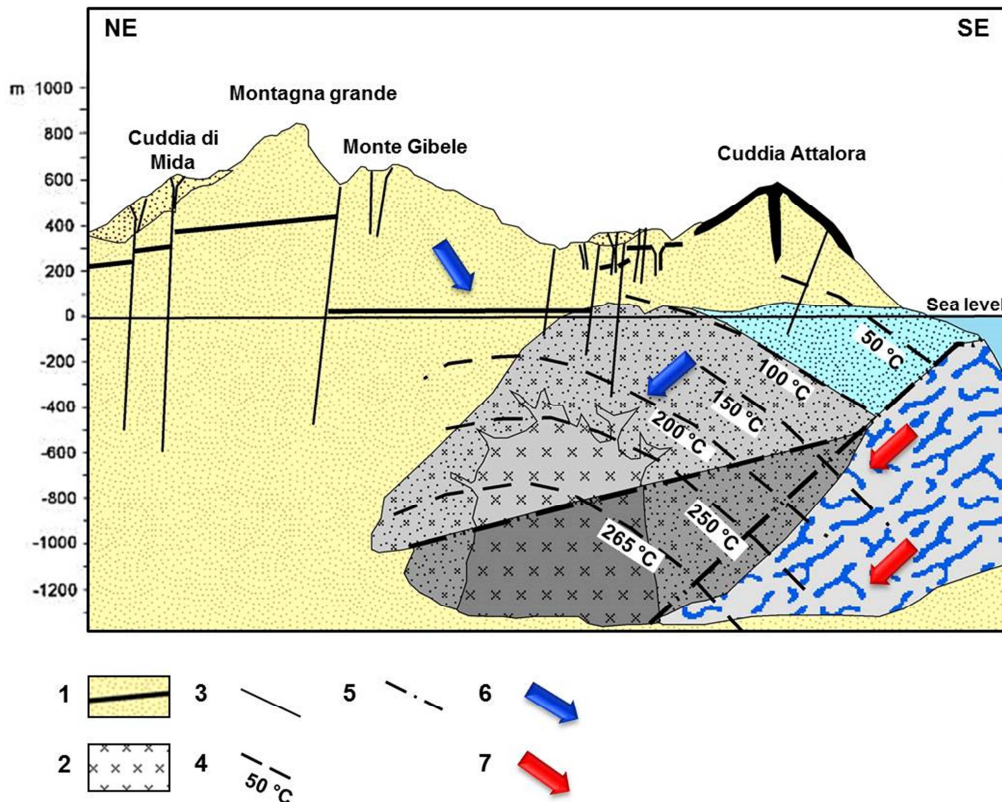


Fig. 2. 3.– Conceptual model of the geothermal system of Pantelleria ; 1. Recent pyroclastic rocks; 2. Trachyte; 3. Faults; 4. Isotherms; 5. Boundaries between zone characterized by fluids of diverse origin; 6. Direction of meteoric recharge; 7. Direction of marine recharge (Modify by Giannelli et al., 2001).

The thermal structure of the SW part accounts for the presence of a mixing zone of marine and meteoric water and volcanic gas. Geophysical data suggest that the geothermal anomaly is limited to the youngest caldera in the southern part of the island. The upper part of the geothermal field is mainly composed of rocks sealed by silica and clay minerals, that create the cover of the field (200 – 500 m). The reservoir is a water-dominated type and presents temperature close to boiling point. Trachitic – comenditic lavas with high level of fractures are very hydrothermalized. The low-temperature hydrothermal alteration (<200 °C) is developed in basaltic–hyaloclastic lithologic sequences, that occur for 700 m and then is interrupted by a sequence of altered doleritic dikes. The geothermal fluids of Pantelleria consist for the most part of seawater (Giannelli et al, 2001); according to the model of Giannelli et al. (2001) the increasing temperature depletes the fluid of Ca, Mg and SO₄ and deposits anhydrite, quartz and clay minerals. The seawater flows through fractures and faults attaining

temperatures >300 °C in the southern part of the island, where an area of volcanic gas upflow is present. Volcanic gases increase the amount of C and S, decrease the pH, temperatures and gas partial pressures. Dolomite, calcite and anhydrite should be deposited by the fluids derived from the mixing of gases with marine water.

Many hot springs and thermal wells occur in the NW and SW part of the island. Persistent fumaroles are concentrated on the young eruptive centers and/or along active faults. In the central part of the island, within the younger caldera, many fumaroles with temperatures between 40°C and 100°C are recognizable. Previous surveys identified many areas characterized by intense gas flux from the soil (Chiodini et al., 2005). The most important fumarolic manifestations of the island can be detected at Favara Grande, south of Montagna Grande. The area is located at the intersection of a regional tectonic lineament with many volcano-tectonic structures. It comprises the main fumarolic field of Favara Grande with strong steam emission and many fumarolic manifestations all with temperatures close to boiling water. Fumarolic emissions have typical hydrothermal composition (Chiodini et al., 2005; Fiebig et al., 2013) with water vapor as the main component (about $970,000 \mu\text{mol mol}^{-1}$) followed by CO_2 (about $23,000 \mu\text{mol mol}^{-1}$). Among the minor components the fumarolic gases of Favara Grande display relatively high contents of H_2 and CH_4 (about 1300 and $800 \mu\text{mol mol}^{-1}$ respectively) and low contents of H_2S ($<20 \mu\text{mol mol}^{-1}$). This leads, after condensation of water vapor, to high CH_4 concentrations in the soils (up to $44,000 \mu\text{mol mol}^{-1}$) and high CH_4 fluxes from the soil (up to $3550 \text{ mg m}^{-2} \text{ day}^{-1}$) in the area of Favara Grande (D'Alessandro et al., 2009).

2.2.SAMPLING AREA

Favara Grande, the main exhalative area at Pantelleria Island was one the areas studied in this PhD project. Favara Grande, in a previous study had offered a starting point for further investigations because of a loss in methane was recorded during the uprising (D'Alessandro et al., 2009); As above, geothermal soils are able to host methane oxidizing bacteria and the discovery of these microorganisms in Pantelleria soils could explain the methane loss in sampled gases. The sampling campaigns were conducted in June 2011 and in November 2011. Ten top-soil samples (0-3 cm), five from a field with geothermal features (from now on called "geothermal area" and five from an abandoned agricultural field (from now on called "agricultural area"- no data are recorded on the

previous conditions of the agricultural area), were collected in June 2011 from sites FAV1 – FAV10 (Fig. 2.4) - and in November from site FAV2 on a vertical profile 0-15 cm taking a sample at five different depths. Soil gas samples were collected from the same ten site at three different depths to analyze the composition of the gases in which bacteria were living when they were sampled. Temperatures were measured in situ and used to obtain a statistical temperature profile of the area to verify the possibility of a correlation between temperature and microbial presence (map were created by using the GIS software ArcMap 9.3, ESRI); pH were measured in soil suspensions either with deionised H₂O. Major oxides of the soils have been determined by XRF analyses (Table 2.2). Table 2.1 summarize results of all the analyses applied to gas and soil samples.

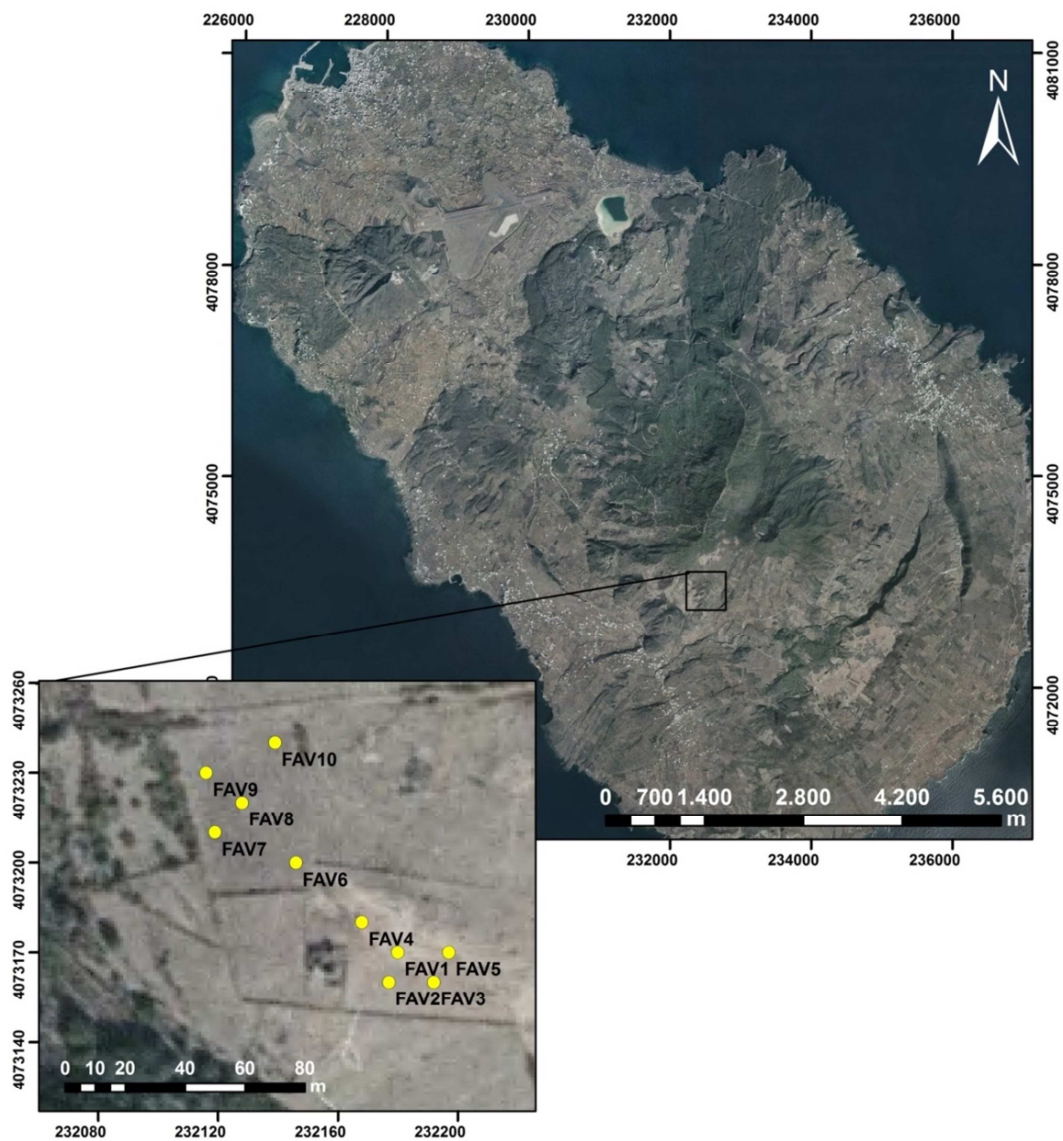


Fig. 2. 4 - Sampling site at the geothermal area (FAV1 –FAV5) and at the agricultural area (FAV6 – FAV10), Favara Grande, Pantelleria island

2.3. RESULTS

2.3.1. CHEMICAL – PHYSICAL CHARACTERISTIC OF THE SAMPLED SITES

Soil and gas samples were taken from Favara Grande, the main exhalative area in Pantelleria island. Ground temperatures were measured in situ from 2 to 50 cm of depth (Table 2.1 and Fig. 2.5 a). In the geothermal area the temperatures in surface level were between 38 and 62 °C reaching temperatures at 50 cm between 74 and 112 °C. The highest temperatures were always measured at FAV1 except for the deepest measurement which was highest at FAV2. Temperatures in the agricultural area in surface level were between 31 and 34 °C decreasing with depth (26-28 °C at 50cm) towards the annual mean atmospheric temperature of the area indicating the absence of an anomalous geothermal gradient. In the geothermal area temperatures are influenced by the geothermal gradient as remarked by the increasing of temperature with depth in FAV2 vertical profile also in November (33 – 83°C in 15 cm of depth, Fig. 2.6). The shallowest temperature was significantly lower than in June due to the lower atmospheric temperature but at 15 cm it was very close that of June. This indicates that the shallowest portion of the soil in the geothermal area is partially influenced by the atmospheric temperature while at greater depths (10 cm at FAV2) the temperature is controlled exclusively by the hydrothermal system.

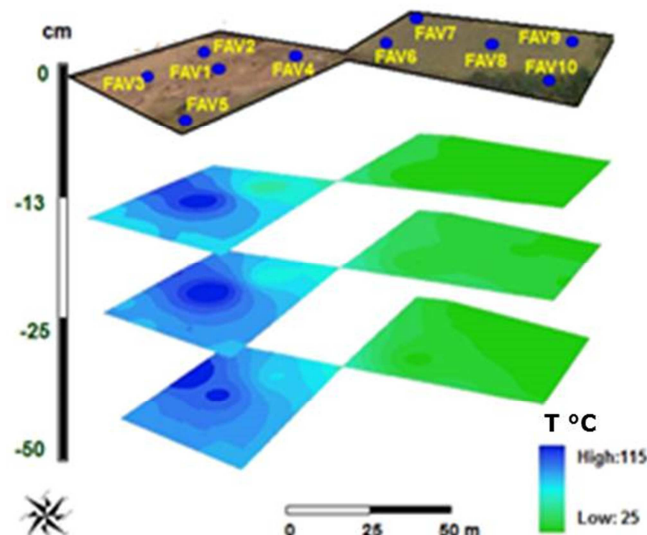


Fig. 2. 5 – Distribution map of the temperature at Favara Grande.

The soils of the agricultural area display a narrow range of pH (6.29-6.80) close to neutrality. On the contrary the soils in the geothermal area show lower values and a wider range (3.41-5.98) indicating a clear hydrothermal influence (Table 2.1). As indicated in Fig. 2.6 pH lowering with depth in site FAV2 reaching the lower value at 13 cm of depth.

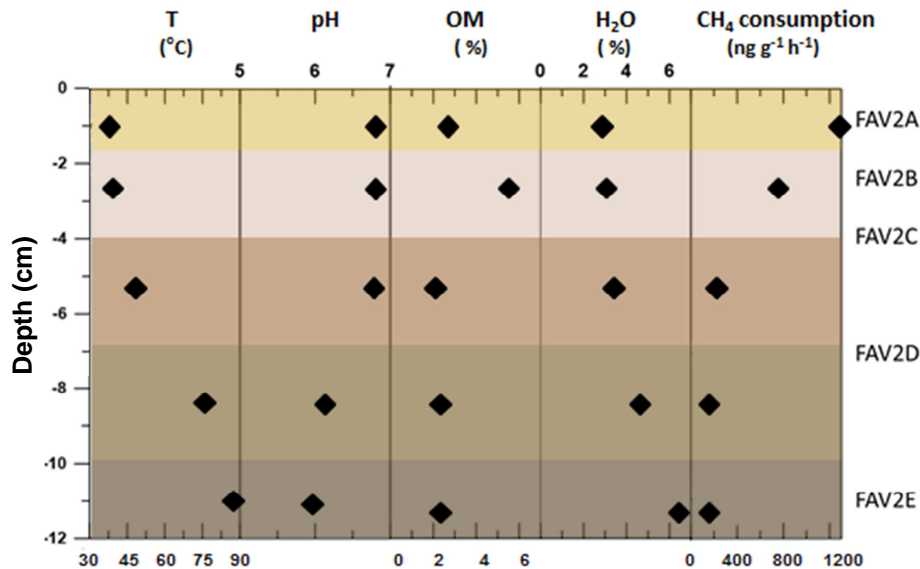


Fig. 2. 6 - Variation of Chemical –physical characteristics in FAV2 vertical profile.

Measured organic matter was in a range of 1 to 6 % by mass with the maximum value measured in the soils sampled from the shallowest layer and decreased in the deeper layers of the FAV2 vertical profile. Usually, organic matter can constitute a third or more of the mass of poorly drained soils, though fractions from 6% to 10% are more common in well-drained soils (White, 1997). Value measured at Pantelleria Island soils are lower of 6-10% indicating few amount of organic matter both in geothermal and in agricultural soils. Water content in the geothermal soils was higher in the deeper layers and decreased in the shallowest layers as clues of hydrothermal flux from the underground and the steam phase of the hydrothermal fluid. Vapor content with the decrease of temperature passes in the liquid phase and soils increase in the amount of water present (Table 2.1 and Fig. 2.6).

Difference in trace and major (oxides) element between agricultural and geothermal area has been highlighted. In samples FAV6-FAV10 major and trace elements showed

very similar values. On the contrary, value from the geothermal area showed greater differences in major and trace elements concentrations.

Oxides were used to calculate Chemical Alteration Index (CIA), which is the most accepted of the available weathering indices offering the best quantitative measure of chemical weathering (Nesbitt and Young, 1982).

It represents a ratio of predominantly immobile Al_2O_3 to the mobile cations Na^+ , K^+ and Ca^{2+} given as oxides. The CIA is defined as

$$\text{CIA} = [\text{Al}_2\text{O}_3 / (\text{Al}_2\text{O}_3 + \text{CaO}^* + \text{Na}_2\text{O} + \text{K}_2\text{O})] \times 100$$

where the major element oxides are given in molecular proportions. CaO^* represents the CaO content of silicate minerals only (Fedo et al., 1995). Kaolinite has a CIA value of 100 and represents the highest degree of weathering. (Nesbitt and Young, 1982; Fedo et al., 1995). Calculated CIA on Pantelleria rock indicate for Trachytes and Pantellerites 45 and 43 respectively (Di Figlia et al., 2007). Calculated CIA on Pantelleria soils showed the highest value in FAV1, FAV4 soil samples indicating high level of alteration with CIA up to 85; FAV2 vertical profile showed an increase of CIA with depth indicating that alteration is favored by higher temperatures and stronger interaction between hydrothermal flux and rocks. Soils from agricultural area indicated CIA values ranged from 59 to 61; Values in this range are higher than Trachytes and Pantellerites indicating alteration of soils even in the agricultural area.

Sample	X_UTM	Y_UTM	T (°C) at depth				pH	OM (%)	H2O (%)	NH ₄ ⁺ (mg/gDW)	Gas depth (cm)	He	H2	O2	N2 (%)	CH4	CO2
			2 cm	13 cm	25 cm	50cm											
FAV1	232180	4073170	62	82.7	103.7	102.2	3.41	3.77	12.93	0.0142	13	0.00	0.85	14.50	54.99	1.00	28.66
											25	0.00	7.78	4.16	9.86	3.92	74.27
											50	0.00	7.32	2.63	4.95	3.71	81.39
FAV2	232177	4073160	60	75	85.9	111.6	5.98	3.12	2.83	0.0010	13	0.00	0.30	16.02	61.08	0.86	21.74
											25	0.00	1.32	3.71	7.06	3.64	84.27
											50	0.00	4.24	3.30	6.37	3.95	82.14
FAV3	232192	4073160	50	58.2	68.5	88.2	5.24	2.95	3.34	0.0008	13	0.00	0.05	18.60	73.24	0.19	7.91
											25	0.00	0.16	16.39	63.94	0.63	18.88
											50	0.00	0.44	10.64	38.72	1.88	48.31
FAV4	232168	4073180	38	46	55.2	74.3	3.93	2.71	4.22	0.0058	13	0.00	0.01	17.14	69.38	0.28	13.19
											25	0.00	0.01	16.89	68.05	0.33	14.71
											50	0.00	0.11	19.85	76.58	0.07	3.39
FAV5	232197	4073170	46	56.1	68	86.8	4.39	3.22	4.22	0.0084	13	0.00	0.00	3.80	16.54	2.64	77.02
											25	0.00	0.02	3.44	9.05	3.52	83.98
											50	0.00	0.16	3.09	8.18	4.00	84.57
FAV6	232146	4073200	31	30.6	29.9	28.5	6.38	5.02	1.80	0.0009	13	0.00	0.00	20.30	79.41	0.00	0.29
											25	0.00	0.00	20.14	79.44	0.00	0.42
											50	0.00	0.00	20.15	79.29	0.00	0.56
FAV7	232119	4073210	34	32.7	30.6	26.3	6.41	4.99	1.61	0.0011	13	0.00	0.00	20.50	79.16	0.00	0.34
											25	0.00	0.00	20.53	79.02	0.00	0.45
											50	0.00	0.00	20.18	79.14	0.00	0.69
FAV8	232128	4073220	31	30	29.1	27.1	6.80	3.92	1.46	0.0013	13	0.00	0.00	20.96	78.72	0.00	0.32
											25	0.00	0.00	20.17	79.48	0.00	0.34
											50	0.00	0.00	20.24	79.02	0.00	0.74
FAV9	232116	4073230	32	30.9	29.6	26.8	6.29	4.44	1.74	0.0012	13	0.00	0.00	20.78	78.95	0.00	0.27
											25	0.00	0.00	20.34	79.33	0.00	0.33
											50	0.00	0.00	19.80	79.71	0.00	0.50
FAV10	232139	4073240	31	30.4	29.5	27.6	6.78	3.65	1.21	0.0012	13	0.00	0.00	19.61	80.17	0.00	0.22
											25	0.00	0.00	20.61	79.03	0.00	0.36
											50	0.00	0.00	20.55	78.91	0.00	0.54

Table 2. 1- Chemical –physical characterization of soils and gases sampled at 0-3 cm of depth at the geothermal (FAV1-FAV5) and the agricultural field (FAV6 – FAV10)

Soil sample	CIA	Na ₂ O	Mg	Al ₂ O ₃	SiO ₂	P ₂ O ₅	K ₂ O	CaO	TiO ₂	MnO	FeO ₃	L.O.I
FAV1	85	1.59	1.15	18.24	50.45	0.1	1.07	0.63	0.87	0.16	9.95	23.39
FAV2	70	3.079	0.38	15.39	59.8	0.12	2.83	0.7	0.95	0.3	9.5	8.14
FAV3	73	3.021	0.54	16.8	58.42	0.1	2.58	0.73	1.1	0.17	9.58	8.82
FAV4	81	2.128	0.25	18.88	51.38	0.09	1.72	0.48	1.07	0.17	13.22	11.22
FAV5	75	2.715	0.76	17.77	54.17	0.17	2.06	1.02	1.05	0.14	10.04	10.85
FAV6	61	3.799	0.25	13.18	61.88	0.13	3.7	0.88	0.66	0.28	8.28	7.94
FAV7	60	4.05	0.23	13.09	61.55	0.12	3.87	0.88	0.69	0.31	8.33	7.58
FAV8	59	4.264	0.22	13.26	62.32	0.11	3.95	0.85	0.7	0.27	7.8	6.89
FAV9	61	4.037	0.24	13.55	62.06	0.11	3.73	0.85	0.81	0.25	7.82	7.21
FAV10	60	4.395	0.2	14.03	62.76	0.12	3.89	0.9	0.7	0.23	7.06	5.92
FAV2A	68	3.438	0.34	15.14	60.72	0.11	3.07	0.72	0.87	0.29	8.98	6.91
FAV2B	70	3.061	0.48	15.59	59.2	0.11	2.9	0.69	1.35	0.24	10.47	6.62
FAV2C	70	3.241	0.43	15.96	59.96	0.1	2.93	0.74	1.2	0.27	9.19	7.05
FAV2D	73	2.515	0.36	14.98	55.41	0.1	2.3	0.71	0.97	0.37	13.82	9.28
FAV2E	83	1.794	0.63	20.26	50.3	0.08	1.46	0.91	1.06	0.25	11.95	12.25

Table 2. 2 - Chemical Index of Alteration, Oxides and L.O.I. (loss on ignition) in %

2.3.2. SOILS GASES

Soil gases were sampled from three different depths at FAV1- FAV10 sites. As first result, Fig. 2.7 shows wide differences in the gas composition in samples from geothermal and agricultural area.

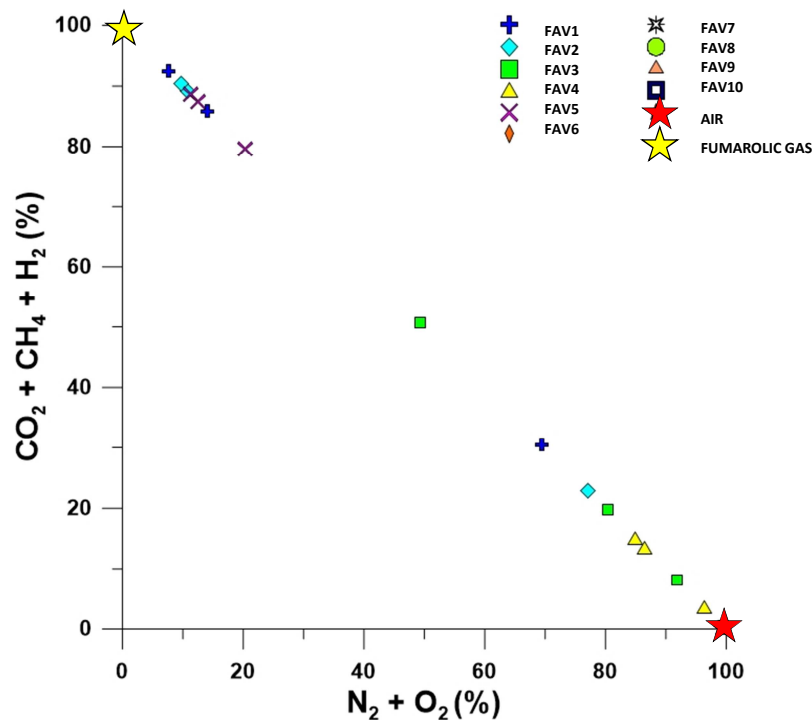


Fig. 2.7 - Fumarolic and air gas distribution in sampled soil gases from Favara Grande.

Samples from geothermal area are mainly composed by fumarolic gases, reaching the 90% of the composition in some samples (FAV1 and FAV2). On the contrary, air gases are the main contributor in the gas samples from the agricultural area (up 99%). Samples from geothermal field (FAV1-FAV5) are dominated by the fumarolic gases at each sampled depths. In samples from geothermal area, N₂ and O₂ content is very low; in particular, in site FAV5, N₂ and O₂ represent the 3.8 and 16.5 % of the gas composition at 13 cm, with an enrichment in CO₂ component (77 %); highest value of O₂ and N₂ were recorded in site FAV2 and FAV3. The O₂ and N₂ content never exceed 20% and 73%, respectively, in all the investigated depth. H₂ content is higher

in FAV1 and FAV2 samples (from 0.3 to 7%). In gas samples from geothermal area, methane content is very high, reaching value up to 4% in site FAV2 at 50 cm of depth. At all the investigated sites, CO₂ is the enriched component; its content is high in the deeper layer. Samples from the agricultura area are all mainly composed by air gases at all investigated depth. CH₄ is at the atmospheric concentration and CO₂ values are ranged from 0.22 to 0.54 %, with the high value in the deeper layer. Diagrams in Fig 2.8, show the variation in methane, carbon dioxide and nitrogen content of the FAV1, FAV2, FAV3 and FAV8 soil gases; Carbon dioxide and methane in FAV8, that represents the trend of all the agricultural samples, do not significantly vary with depth; on the contrary the amount of CO₂ and CH₄ in samples from the geothermal areas are more abundant and their amount even if vary with depth maintain high value even in the shallowest layer (Fig. 2.8).

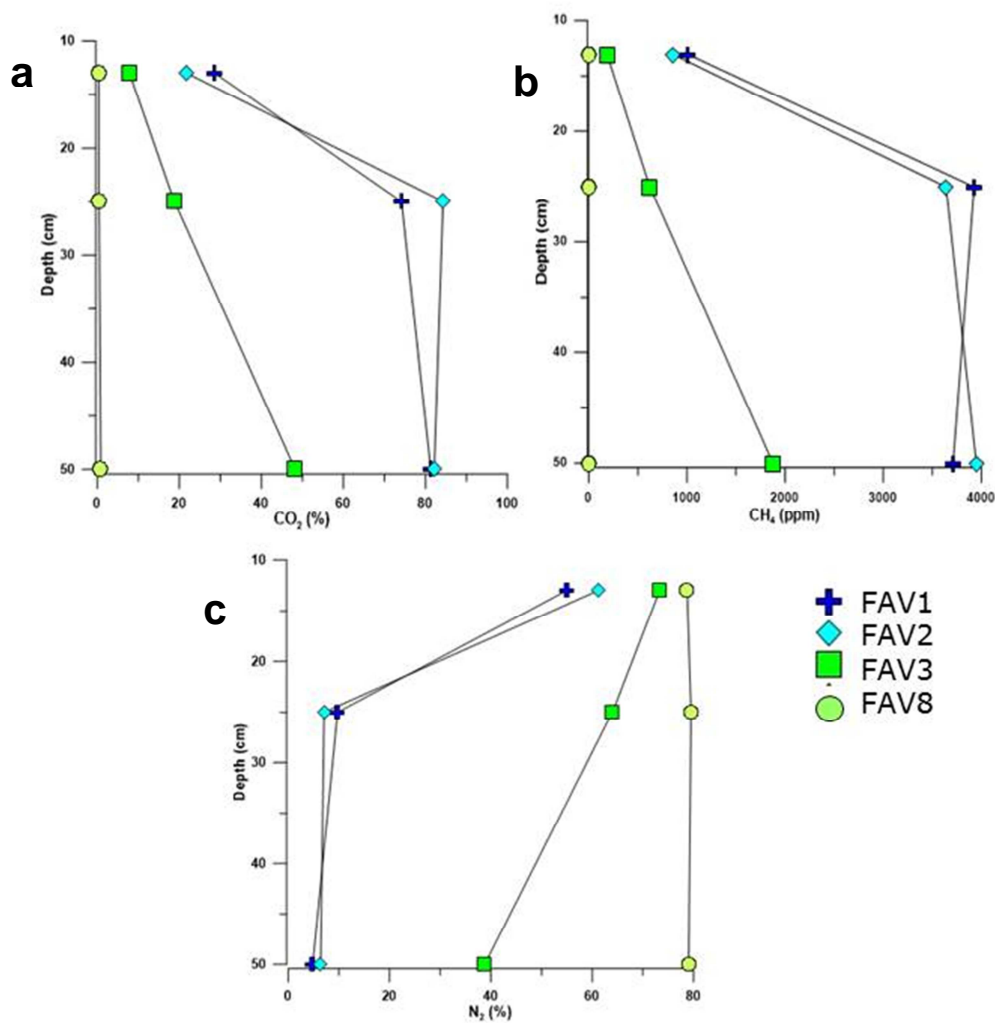


Fig. 2. 8 - Variation in a) CO₂ amount, b) in CH₄ amount and c) in N₂ amount in soil gases.

The amount of the nitrogen in sample from agricultural field does not vary with depth and maintains value similar to the air composition. In soil gases from geothermal field nitrogen reach the highest value in the shallowest layer reaching the 70% only in the sample FAV3. In the deeper layers nitrogen represents the 10% of the gas mixture, in samples FAV1 and FAV2, where the highest amount of CO₂ and CH₄ were measured.

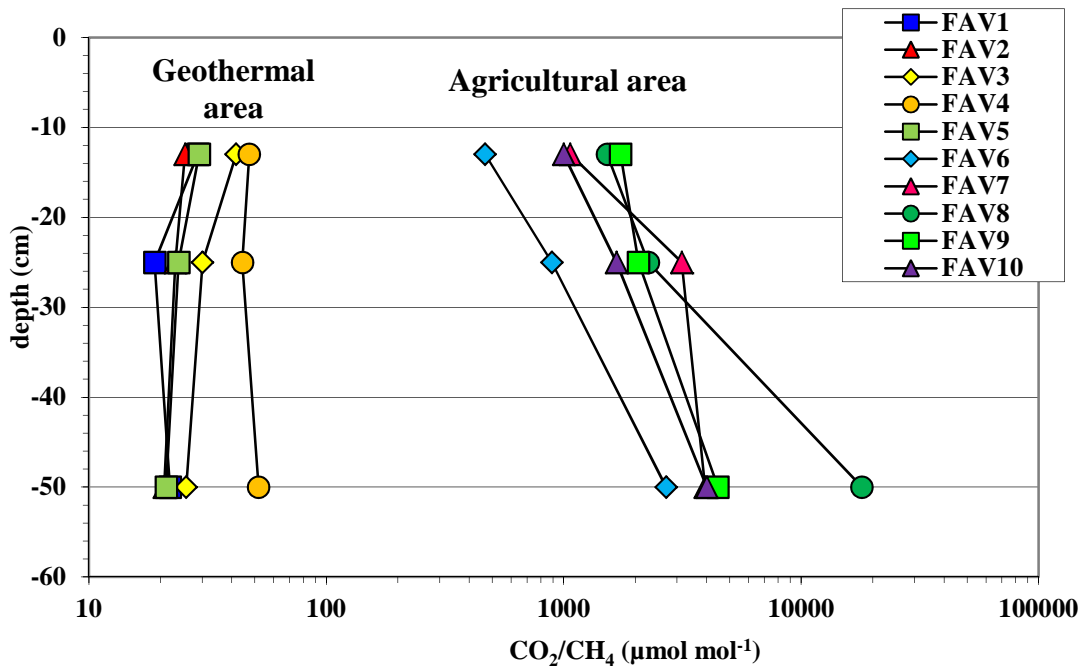


Fig. 2.9 - Variation in CO₂/CH₄ ratio with depth.

Fig. 2.9 shows the variation in CO₂/CH₄ ratio with depth of the soil gases sampled at Favara Grande. Samples from FAV1 to FAV5 indicate a low CO₂/CH₄ ratio (25 – 30, typical of the fumaroles). In all the five sites, CO₂ and CH₄ content does not significantly vary between 25 and 50 cm of depth; instead the ratio decreases in the shallowest level (13 cm). In the right part of the graph, CO₂/CH₄ ratio (FAV6 – FAV10 samples) is higher in the shallowest layer and increases with depth. This ratio depend on the CO₂ content: as data on table 2.1 indicate, methane amount is at atmospheric concentration at all investigated depth, but the CO₂ content increases in the deeper layers.

2.3.3. CLUES OF METHANOTROPHIC ACTIVITY

During this PhD study, evidences of microbial methane oxidation activity were provided by incubation experiments carried on soils sampled at Favara Grande, in both sampling campaigns. Aliquots of samples, sealed in serum battles, were used for incubation experiment (see par. 7 for material and methods); At the end the incubation period, methane oxidation, in serum bottle, were measured by GC in regular time and consumption were recorded (Fig.2.10 a and b, and Table 2.4).

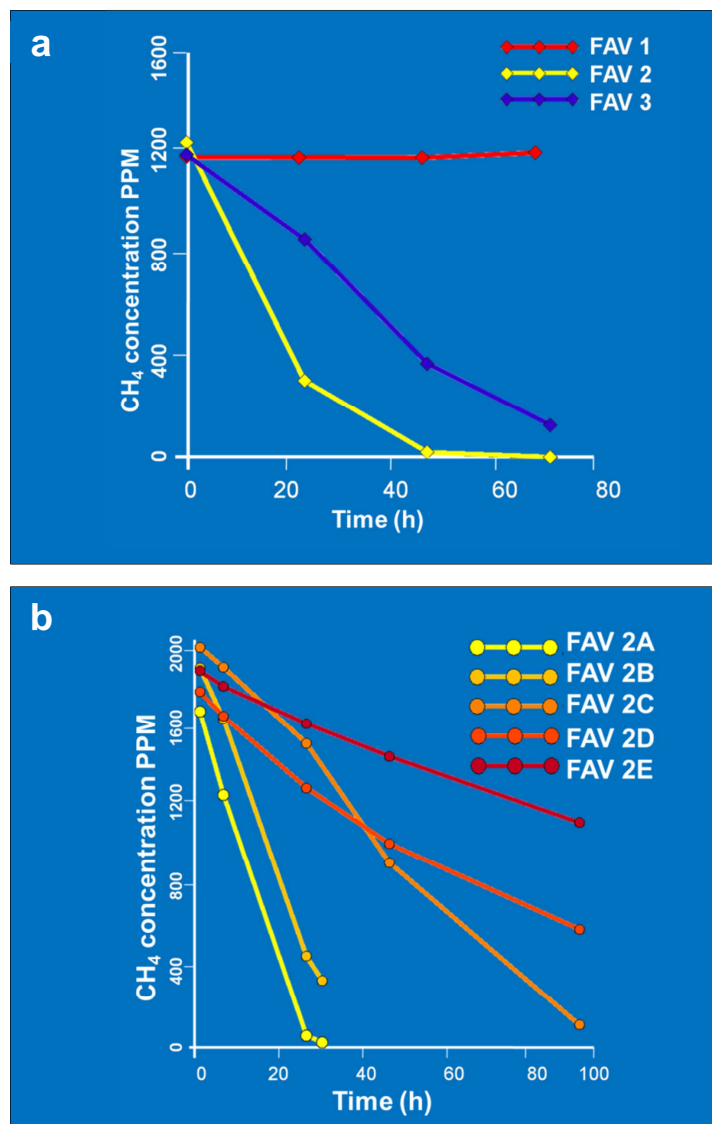


Fig. 2. 10 - a) variation of methane in laboratory incubation experiments using FAV1, FAV2 and FAV3 soil samples; b) variation of methane in laboratory incubation experiments using soils from FAV2 vertical profile.

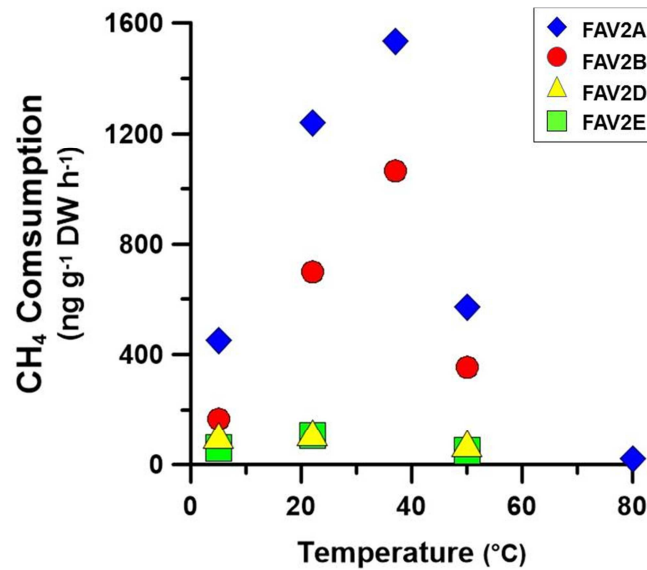


Fig. 2. 11 - methane consumption of the soils sampled at FAV2 vertical profile, incubated at different temperatures.

Samples from agricultural soils, after an the incubation in methane enriched atmosphere, did not show significant consumptions; samples from FAV1 to FAV5 revealed a different behavior. In some soils, consumptions are close to zero (FAV1, FAV4 and FAV5), and in some samples consumptions are very high (FAV2 and FAV3) up to 950 ng g⁻¹ h⁻¹. Incubation experiments on soil from FAV2 vertical profile revealed maximum methane uptake in the shallowest layers (0-2 cm, 1200 ng g⁻¹ h⁻¹) maintaining high values (more than 100 ng g⁻¹ h⁻¹) at least up to depth of 11 cm, after incubation at controlled room temperature. When samples from the vertical profile were incubated at different temperatures the CH₄ consumption increased with temperature from 5°C, to a maximum at 37° C and then decreased at 50°C. A very low but still detectable methane consumption (20 ng g⁻¹ h⁻¹) was recorded in sample FAV2A even at 80°C (Fig. 2.11). The oxidation potential of the soils, at least at FAV2, strongly depends on the initial CH₄ concentration in the serum bottles. Figure 2.12 shows that if the available CH₄ increases also the CH₄ consumption increases reaching a value of 9500 ng g⁻¹ h⁻¹ with an initial CH₄ concentration of 85,000 μmol mol⁻¹ at room temperature.

SAMPLE	CH ₄ CONSUMPTION				
	ng g ⁻¹ h ⁻¹				
	T 5 °C	T 25°C	T 37 °C	T 50°C	80 °C
FAV1	n.r	4.90	n.r	n.r	n.r
FAV2	n.r	950	n.r	n.r	n.r
FAV3	n.r	620	n.r	n.r	n.r
FAV4	n.r	3.02	n.r	n.r	n.r
FAV5	n.r	10.39	n.r	n.r	n.r
FAV6	n.r	3.55	n.r	n.r	n.r
FAV7	n.r	5.98	n.r	n.r	n.r
FAV8	n.r	2.63	n.r	n.r	n.r
FAV9	n.r	0.89	n.r	n.r	n.r
FAV10	n.r	0.23	n.r	n.r	n.r
FAV2A	450	1249	1534	573	22
FAV2B	169	701	1066	356	n.r
FAV2C	n.r	186	n.r	n.r	n.r
FAV2D	60	107	n.r	52	n.r
FAV2E	90	100.5	n.r	63	n.r

Table 2. 3 - Methane consumption value after soil incubation at different temperatures; n.r. = not recorded.

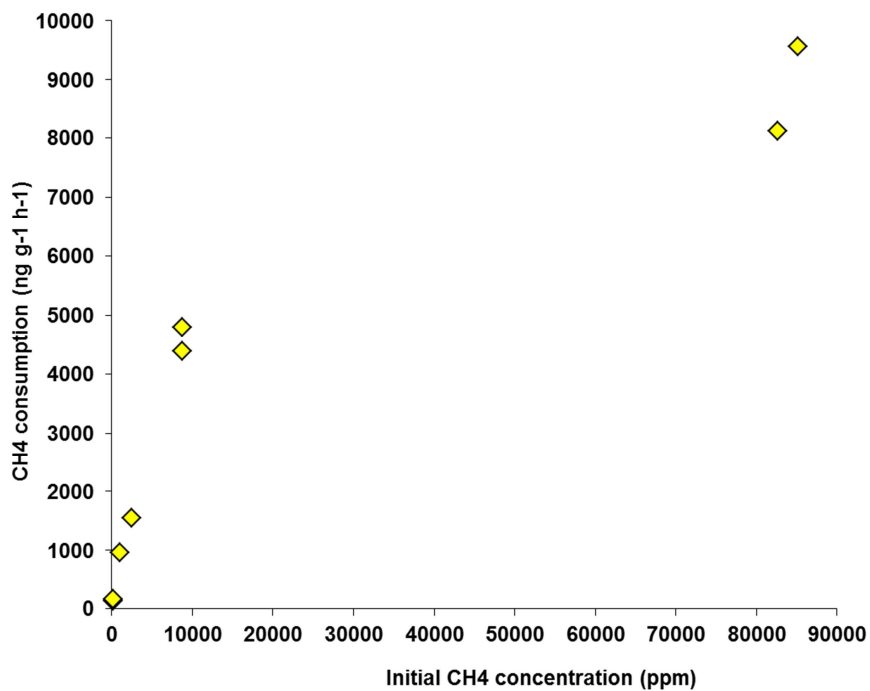


Fig. 2. 12 - FAV2A methane consumption at different methane initial concentration after 24h incubation at controlled room temperature.

Positive relation between methane initial concentration and methane consumption is significantly important because, it indicates that with the increasing of the methane flux, bacteria increase their methane oxidation rate (Fig. 2.12).

Finally, evidences of methane microbial uptake are provided from isotopic data, in fact, variations in methane isotopic ratio were measured in the headspace gases both in the serum bottles containing samples incubated in laboratory experiment and in soil gases (Fig. 2.13). Data indicated in both type of samples an enrichment in heavier isotopes as expected. Usually, methanotrophs prefer to use lighter methane for their microbial processes.

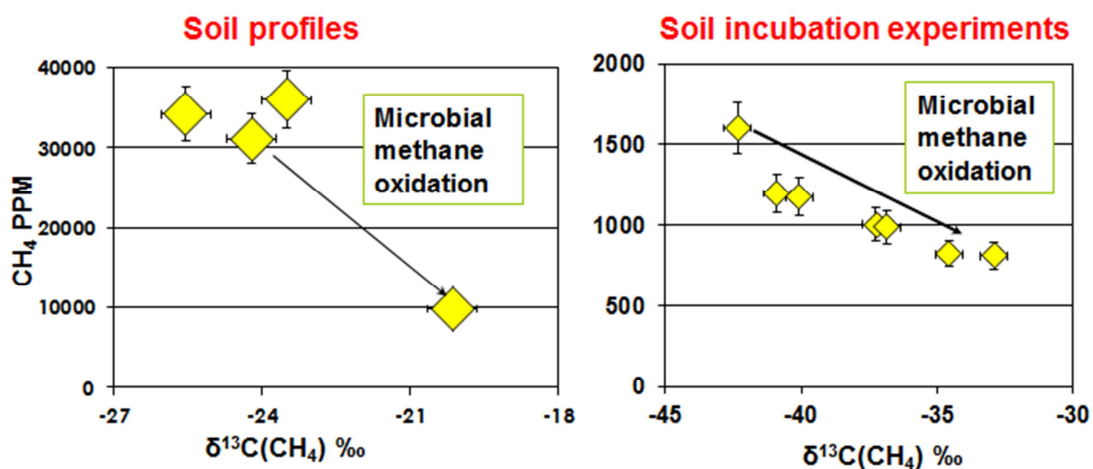


Fig. 2. 13 - Variation on CH_4 - C composition; the arrows indicate the positivization of $\delta^{13}\text{C}(\text{CH}_4)$ due to microbial methane oxidation.

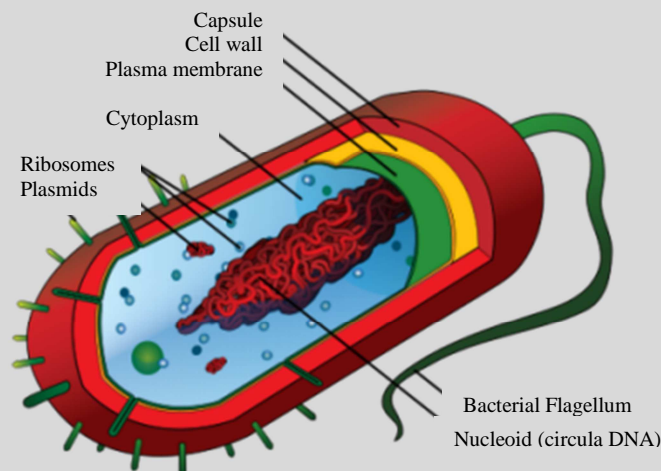
2.3.4. MICROBIOLOGY AND MOLECULAR DETECTION OF METHANE OXIDIZING BACTERIA

Methane oxidation bacteria can be detected by using microbial and molecular techniques. Classic microbiology allows to obtain isolates in laboratory to use for ecology experiments (range of temperature and pH in which isolate can grow, different medium, methane consumption rate, and so on). But only the 1% of the existing bacteria is cultivable in laboratory and molecular techniques based on genetic methods are useful to identify uncultivable bacteria living in soils. Moreover molecular techniques permit the genetic characterization of microorganism. Most common techniques are quick, relatively simple and highly replicable. Soils from Favara Grande were analyzed to investigate methanotrophs communities living in

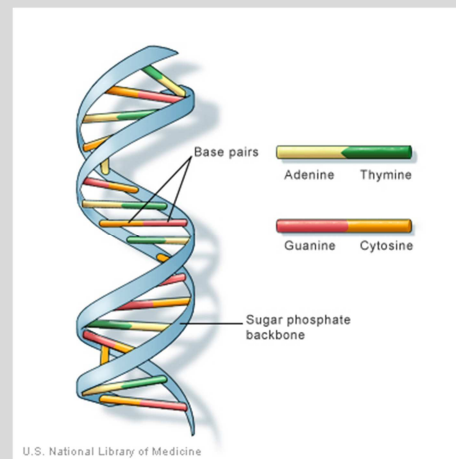
these geothermal environment by using both microbiology and molecular techniques. Polymerase Chain Reaction (PCR), Temporal Temperature Gradient Electrophoresis (TTGE), cloning and sequencing of the DNA were applied to the total soil DNA (see boxes for further information).

Box 1- Bacterial DNA

Bacteria, despite their simplicity, contain a well-developed cell structure which is responsible for many of their unique biological properties. Many structural features are unique to bacteria and are not found among archaea or eukaryotes. The bacterial chromosome is not enveloped inside of a membrane-bound nucleus, but resides inside the bacterial cytoplasm. For this reason all the cellular processes such as translation, transcription and DNA replication all occur within the same compartment and can interact with other cytoplasmic structures, most notably ribosomes. Prokaryotic chromosome exist in a unique circular and continue chain of DNA. Along with chromosomal DNA, most bacteria also contain small independent pieces of DNA called plasmids that often encode for traits that are advantageous but not essential to their bacterial host. Plasmids can be easily gained or lost by a bacterium and can be transferred between bacteria as a form of horizontal transfer. Deoxyribonucleic acid (DNA) is a macromolecule that encodes the genetic instructions used in the development and functioning of all known living organisms.

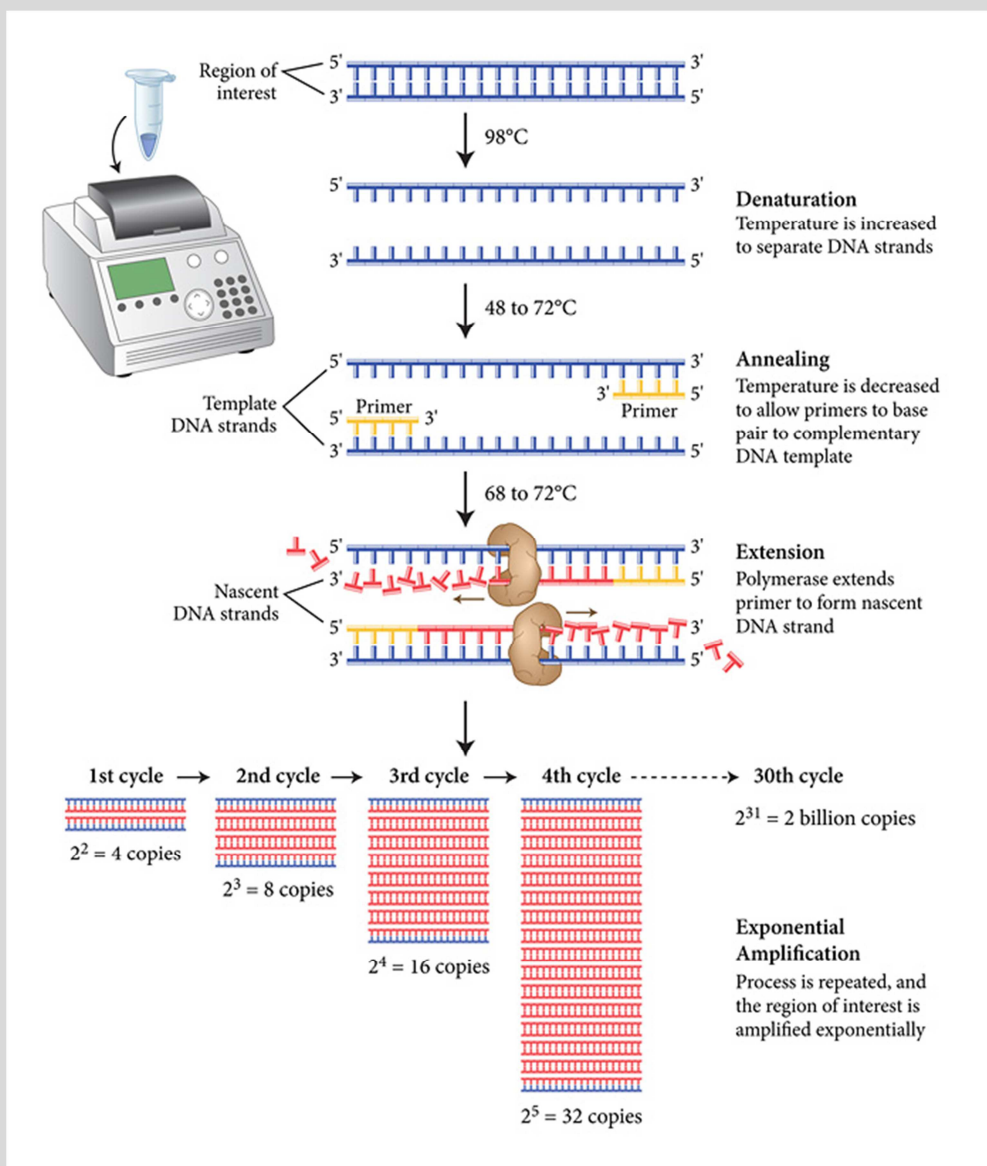


Most DNA molecules are double-stranded helices, consisting of two long biopolymers made of simpler units called nucleotides - each nucleotide is composed of a nucleobase (guanine, adenine, thymine, and cytosine), recorded using the letters G, A, T, and C, as well as a backbone made of alternating sugars (deoxyribose) and phosphate groups (related to phosphoric acid), with the nucleobases (G, A, T, C) attached to the sugars. Specific sequence of nucleotides in the DNA (gene) encode for specific proteins used by the cell.



Box 2 - Polymerase Chain reaction (PCR)

Polimerase Chain reaction (PCR) is a molecular techniques that allow to obtain multiple copies of selected part of DNA. Even if DNA is a trace PCR crate millions of copies of the specific searched fragment of DNA (gene) . Basically, it is necessary to know the target gene and the nuclides sequence of the final part of the gene that is used as specific anchorage areas for primers (complementary sequence of nuclides of the final part of the selected gene). In PCR reaction mix are also necessary free nucleotides and a DNA-Polimerase that is a thermostable enzyme that start nucleotide synthesis to create multiple copies of the target gene. Three are the main step of a PCR: Denaturation, in which double elic of DNA is opened; annealing, in which primers match with final parts of the selected gene; and extension in which free nucleotides of mix reaction were chained in correct order to copy the target gene.



2.3.5. SOIL BACTERIAL DIVERSITY

In order to evaluate the total bacterial diversity, sites FAV1, FAV2 and FAV3 were analyzed by Temporal Thermal Gradient gel Electrophoresis (TTGE) (see Box-3 for further information) of PCR-amplified bacterial *16S* rRNA gene fragments from total DNA extracted from soil samples; TTGE band profiles indicate the presence of several putative bacterial phylotypes in geothermal soils (Fig.2.14 a). Richness and diversity were determined by used the executable PAST version 2.17c, obtaining a richness in the range of 17 to 22 and a Shannon's index $H' = 2.83$. The highest diversity in term of number of bands was observed in site FAV2 (21) and in site FAV3 (22 bands); lower diversity was recorded in the sample from site FAV1 (17 bands). Most of the bands (18) at FAV3 are in common with FAV2 probably reflecting their similar chemical physical conditions. Two bands were excised from the TGGE gel from the FAV2 and FAV3 soil profiles and were sequenced (Fig. 2.14 b). The sequences were analysed with the Ribosomal Database Project using the algorithm "Classifier" and were assigned both to the Archaea in the phyla Crenarchaeota and Euryarchaeota.

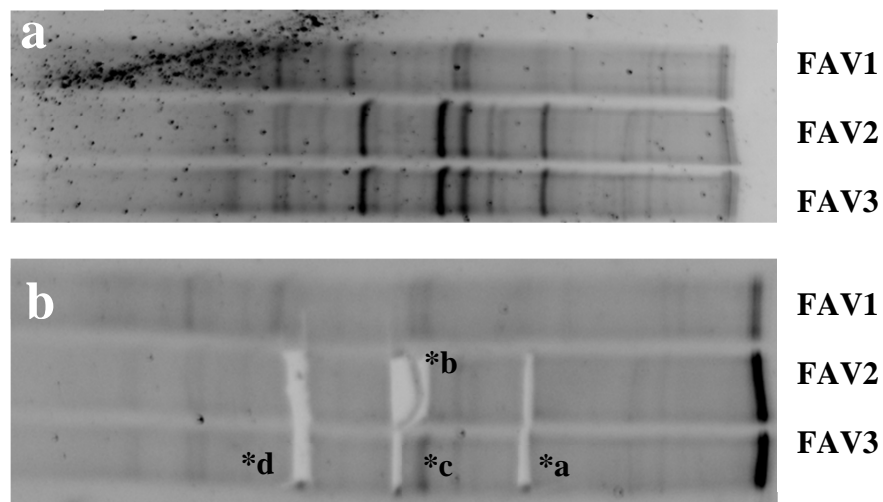


Fig. 2. 14 - a) PCR – TTGE analysis of *16S* V3; b) position of excided bands in the gel.

Box 3 – Temporal Temperature Gradient Electrophoresis (TTGE)

TTGE was first introduced by Yoshino, in 1991 and is a fingerprinting technique that allows the study of microbial communities and their dynamics. It is possible to apply this technique to every type of samples (soils, plants, sediment, skin, etc..) of which it is possible to extract bacterial total DNA. TTGE fingerprinting is based on electrophoretic separation in a denaturing acrylamide gel of PCR amplicons harboring the same length but different sequences. Separation occurs by applying a temperature gradient over time. When amplicons reach their melting temperature, they become denatured, decreasing their motility in the gel and eventually stopping their migration. TTGE is generally used for separation of low-GC species. The allocation of each amplicon to a specific species is carried out after successful electrophoresis, using two different strategies. The first one is based on a database preliminary created using reference strains. In the second, the amplicon is directly excised from the acrylamide gel, cloned and sequenced, enabling the identification of species that are not yet member of the database.

2.3.6. DETECTION OF METHANE OXIDATION GENES

The presence of methanotrophs was verified by detecting the functional methane oxidation gene *pmoA* by PCR on total DNA extracted from the three sites FAV1, FAV2, FAV3 and also in all the samples from the FAV2 vertical profile (from -1 to -12 cm). Using the couple of primers targeting *pmoA* gene encoding the β -subunit of the proteobacterial methane mono-oxygenase A682R/189F (Par. 7, Table 7.2, Fig. 2.15 a), a unique band of the expected size (580 bp) was obtained from FAV2 and FAV3 and in all vertical FAV2 samples up to -12 cm (Fig. 2.5 a, Table 2.5). Conversely, no PCR product was obtained from FAV1 (Fig. 2.15 a and b).

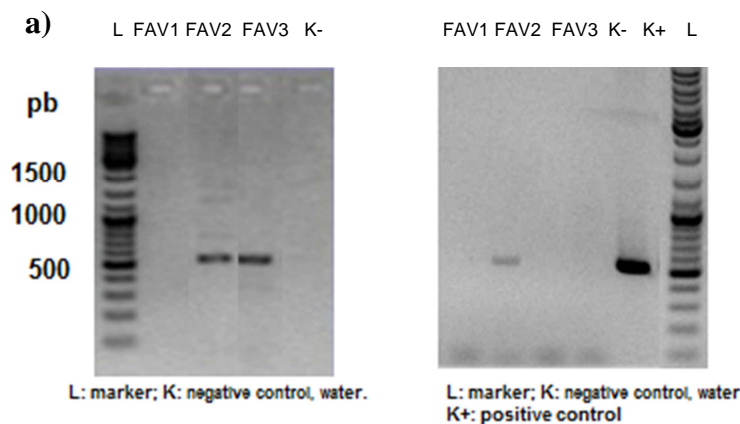


Fig. 2. 15 - Gel electrophoresis of PCR products obtained a) using primers 189F/682R targeting proteobacterial *pmoA* gene and b) using primer 156F/743R targeting verrucomicrobial *pmoA* gene.

Verrucomicrobial *pmoA* was searched by designing two newly couples of primers and targeting the Verrucomicrobial methane mono-oxygenase genes in FAV1, FAV2, FAV3 and FAV2 vertical profile DNA extracted from soil. PCR produced positive results only for FAV2 soil where PCRs product of 300 and 600 bp were obtained respectively for the couple of primers 298f/599r targeting *pmoA1-A2* and the couple 156f/743r targeting *pmoA3* (Fig. 2.15 b, Table 2.5). Accordingly soil samples from FAV2 profile showed the presence of verrucomicrobial methane monooxygenase genes with the exception of FAV2D. No amplification products were obtained from FAV1 and FAV3.

SOIL SAMPLE	PROTEOBACTERIAL <i>pmoA</i> DETECTION	VERRUCOMICROBIAL <i>pmoA</i> DETECTION ^a
FAV1	- ^b	-
FAV2	+ ^c	+
FAV3	+	-
FAV2A	+	+
FAV2B	+	+
FAV2C	+	+
FAV2D	+	-
FAV2E	+	+

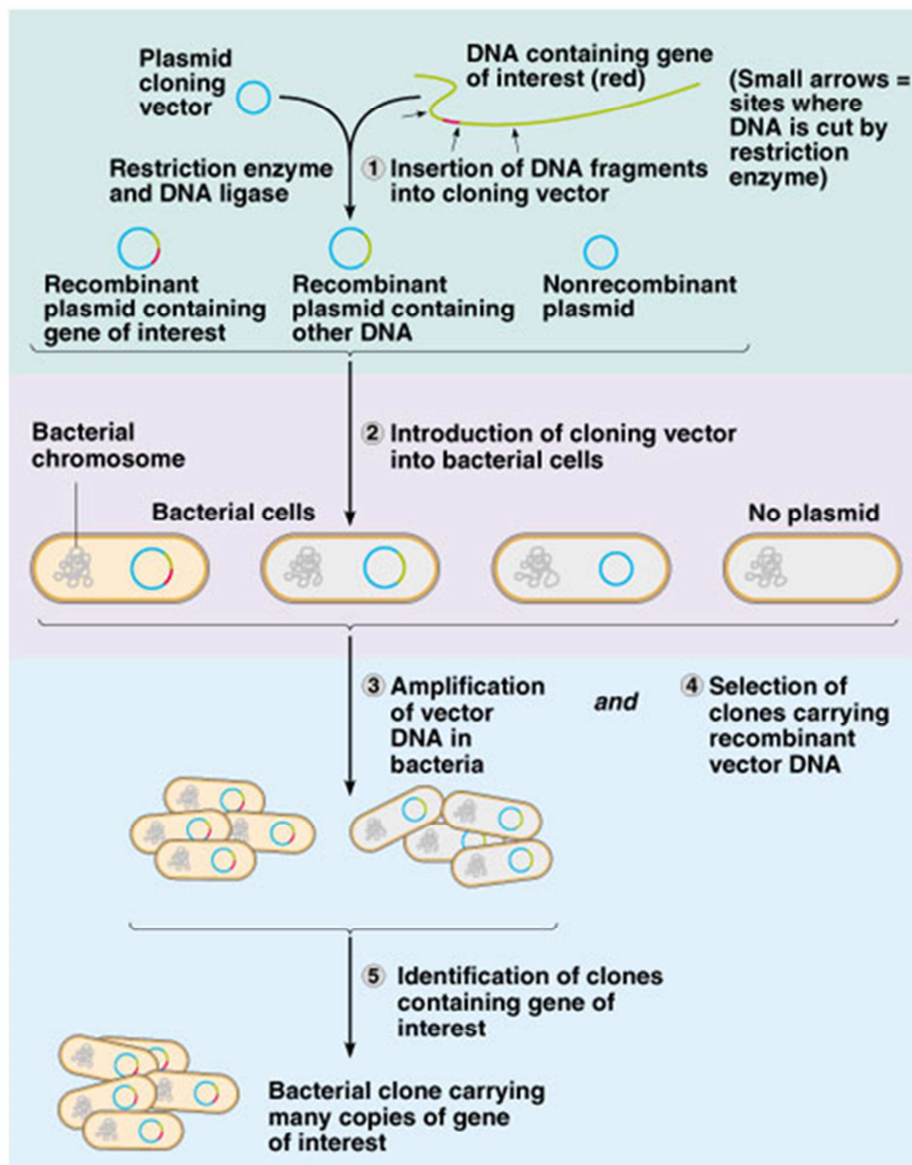
Table 2. 4 - Detection of the functional gene *pmoA*: a. amplification products with specific primer (see Table 7.2); b = absence of amplicon of the expected size; c = presence of an amplicon of the expected size.

2.3.7. DIVERSITY OF METHANOTROPHS

In order to investigate the diversity of proteobacterial methanotrophs at the most active site FAV2, a *pmoA* clone library was constructed using the PCR product obtained from sample FAV2 where the highest methane consumption was recorded (Table 2.6 and Fig. 2.16). The *pmoA* library in TOPO-TA consisted of 70 clones and sequencing of fifteen randomly chosen clone inserts revealed abundance of type I methane mono-oxygenase genes distantly related to uncultured methanotrophic bacteria and to *Methylococcus* sp. Two verucomicrobial *pmoA* clones were also sequenced and showed 99% identity with *Methilacidophilum fumarolicum*.

Name	Total length	<i>pmoA</i> gene length	Blast best match Genebank code	Identity %
Clone 10	508	504	Uncultured bacterium clone 55-2000B-661r JN591273.1	91%
Clone 6		500		
Clone 11		500		
Clone 13		496		
Clone 12		496		
Clone56	506	503	Uncultured type I methanotroph clone 05A-M40-78L EU275110.1	84%
Clone59		504		
Clone69		503		
Clone68		496		
Clone77		500		
Clone84			Uncultured type I methanotroph clone 0507-G20-76 <i>PmoA (pmoA)</i> gene, partial cds	83%
Clone76	506	503	EU275114.1	84%
Clone61	508	508	Uncultured Methylococcus sp. clone Xh_ <i>pmoA</i> _CA51 particulate methane monooxygenase protein subunit A (<i>pmoA</i>) gene JQ038178.1	83%
Clone71		528	Methylococcus capsulatus str. Bath, complete genome	82%
Clone76	530	531	AE017282.2	84%

Table 2. 5 - Methane monooxygenase gene diversity retrieved from FAV2 soil sample.



©Addison Wesley Longman, Inc.

Fig. 2. 16 - Steps of a gene cloning; 1. Selected gene fragment is amplified and inserted in a vector; 2. The vector is introduced in a bacterial cell (e.g. E. Coli).3. Vector is amplified in bacteria 4. Recombinated bacteria are selected and 5. Clone with selected gene are identified. (see Box 1)

2.3.8. ISOLATION OF METHANOTROPHIC BACTERIA FROM THE GEOTHERMAL SITE

In order to isolate methanotrophic bacteria from geothermally active site, soil enrichment cultures in methane-enriched atmosphere were set. Soil crumbles were at first incubated in an atmosphere rich in methane in order to enrich the community with the methanotrophic component (Par. 7 for details on material and methods). After 4 week 2 gr enriched soil crumbles were placed in M3 selective medium, the cultures were incubated at 37°C and 65°C; the former showed a visible increase in turbidity while no growth was observed at 65°C. The enrichment cultures were sub-cultured under the same conditions and after streaking on M3 agar-slants, in sealed serum bottles in a CH₄-enriched atmosphere, a few single colonies, apparently very similar to each other, were detected after 4-5 days. Five isolates were stably able to grow on methane as sole C source. Observation at microscope showed isolate from FAVA, FAVB, FAVC and FAVD soils were gram negative cocci (Fig. 2.17 a) and isolate from FAV2E gram negative rods.

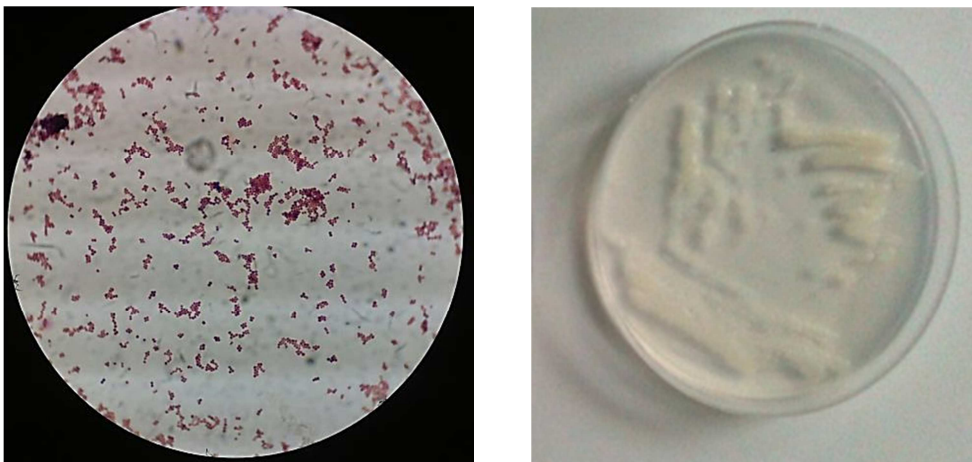


Fig. 2. 17 - a) observation at optic microscope of the GRAM test on FAV2B isolate; b) growth on methanol of FAV2B isolate.

Isolate	<i>16S</i> rRNA gene Blast best match	<i>pmoA</i> gene	Growth on methanol	Growth on fructose, glucose, ethanol
	(identity %)	Blast best match (identity %)		
FAV2A	<i>Acidobacterium</i> sp (95)	<i>Methylocystis</i> sp. 10(J459038.1) (99)	+	+
FAV2B	<i>Methylocystis parvus</i> strain OBBP(044946.1) (99)	n.d.	+	-
FAV2C	<i>Methylocystis parvus</i> strain OBBP(044946.1) (95)	<i>Methylocystis</i> sp. 10(J459038.1) (98)	+	-
FAV2D	<i>Methylocystis</i> sp. 10(AJ458500.1) (99)	n.d.	+	-
FAV2E	<i>Methylobacterium</i> sp. (HM484372.2) (92)	Uncultured bacterium clone 73-50B-682r particulate methane (96%)(JN591077.1)	+	+

Table 2. 6- Identification, substrate utilization and *pmmo* gene identity detection of the methanotrophs isolated from enrichment cultures at 37°C from FAV2 soil sampled at different depths.

Growth conditions	Samples		
	M3 broth pH	FAV2A	FAV2B, C, D
4	n.m	+	+
4.5	n.m	+	+
5	n.m	+	++
6	n.m	++	++
6.5	n.m	++	++
7	n.m	+	+
7.5	n.m	+/-	+
8	n.m	+/-	++
Incubation temperature (°C)			
18	+	+	+
22	+	+	+
30	++	++	++
37	++	++	++
45	++	+	+
65	-	-	-

Table 2. 7 - Growth of the isolates at different pH and temperatures. n.m. not measures. Growth was registered after 3 days of incubation.

Three isolates from FAV2B, FAV2C and FAV2D grew on methanol and were unable to grow on glucose, fructose and ethanol (Fig. 2.17b, Table 2.7). They all could grow

on a pH ranging from 3.5 to 8 and could grow up to 45°C but were unable to grow at 65°C. Their rRNA *16S* gene sequence revealed that three FAV2 isolates are all affiliated to the Alphaproteobacterium species *Methylocysts parvus* (id from 98 to 99%, with *Methylocystis parvus* strain OBBP, Table 2.7). Isolate from FAV2B was used to create a growth curve, results indicate a correlation between methane consumption and the turbidity measured as OD₆₀₀. Methane concentration decrease exponentially with increase of the OD₆₀₀ and the average oxidation rate of the culture is of 52 $\mu\text{mol mol}^{-1} \text{h}^{-1}$ (Fig. 2.18).

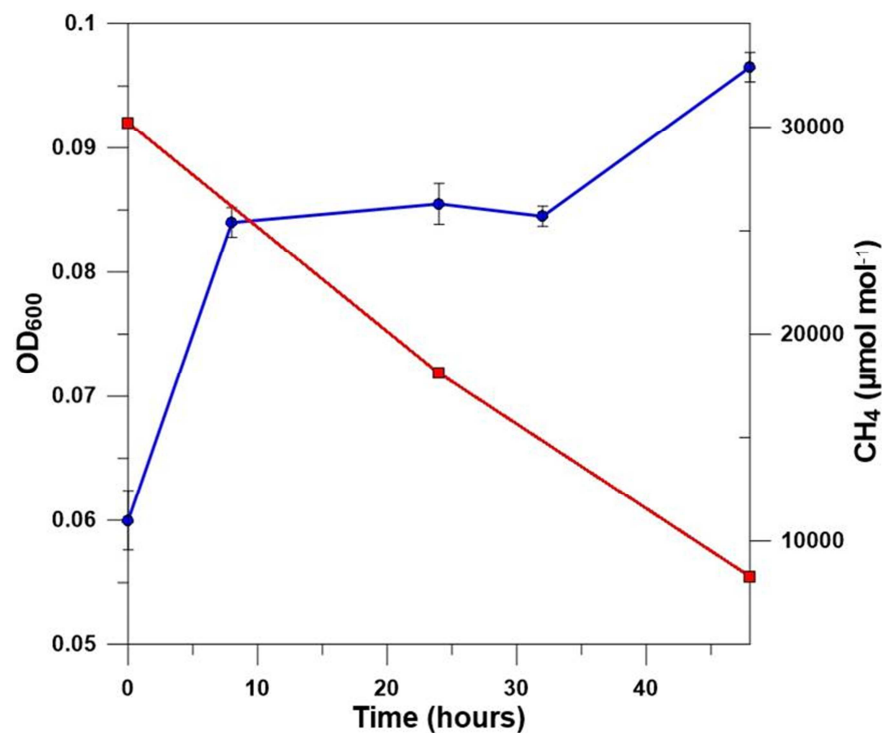


Fig. 2. 18- Growth (blu line) and corresponding methane consumption (red line) of *Methylocystis* sp strain after 3 days of incubation. Average of the optical density (OD₆₀₀)± standard error are shown in five duplicate 150 serum bottles at 37°C. The pH was 5.

The fourth CH₄ consuming isolate was obtained from the deepest soil layer (FAV2E) and beyond methane and methanol it could grow on glucose, fructose and ethanol and also at a temperature of 45°C. Its *16S* rDNA sequence is close to that of the facultative methanotrophic genus *Methylobacterium* although with a low identity. The *pmoA* gene was successfully amplified in all the five isolates and in three of the five isolates (FAV2B, FAV2C and FAV2D) the sequence of *pmoA* gene is coherent with the *16S* rRNA phylogeny (Table 2.7). Isolates from FAV2A soil are able to grow in all the investigate pH (4 – 8), temperatures (18 – 65 °C), in methane and in

methanol; FAV2A and FAV2E also growth on fructose, glucose and ethanol (Table 2.8). Analyses on *16S* rRNA reveal a similarity with *Acidobacterium sp.*, this result does not correspond with the *pmoA* gene sequence that is close to that of *methylocystis sp.* *Acidobacterium* is typical soil bacterium that often was found in co-culture with methanotroph and a co-culture of methanotrophs with *Acidobacterium* was hypothesized. Attempts to isolate the strain with microbiological techniques were carried on; FAV2A colonies were transferred for 3 week in selective medium M3 with fructose without any methane to select only the *Acidobacterium*; after 3 week colonies were re-transferred in medium with methane as only source of carbon and bacteria were still able to grown. Microbiological attempts to separate the two strain were unsuccessful; *16S* rRNA and *pmoA* sequencing of colony amplicons gave always the same results of apparent co-culture.

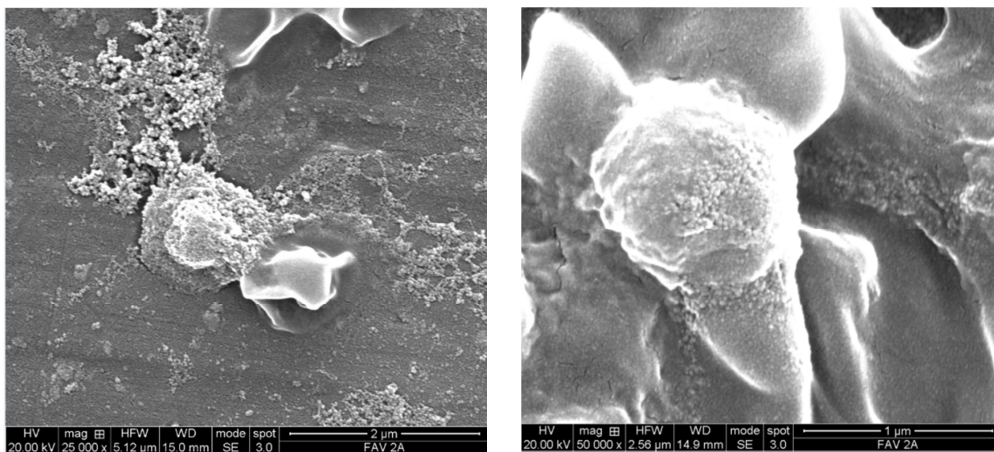


Fig. 2. 19 - SEM micrographs of FAV2A isolate.

To better investigate if FAV2A culture, *16S* rRNA product of colony PCR were used to create a clone library of the FAV2 strains and a clone libraries with 57 clone were obtained; all plasmid were extracted and digested with *afal* restriction enzyme; digestion profile indicates that all clone were the same and four of these plasmids were sequenced resulting in positive match with *Acidobacterium sp.* Sample were also observed with eSEM (Fig. 2.19). Further analyses on FAV2A culture are in progress.

2.4. DISCUSSION

Pantelleria island has a geological feature that permits very high fluxes of geothermal gases enriched in methane (D'Alessandro et al., 2009; Parello et al., 2000) releasing 5 – 10 Tons of CH₄ into the atmosphere by widespread diffuse degassing. The total emissions obtained from methane flux measurements are up to one order of magnitude lower than those obtained through indirect estimations (D'Alessandro et al., 2009). Clues of methanotrophic activity within the soils of these areas can be found in the CH₄/CO₂ ratio of the flux measurements which is always lower than that of the fumarolic manifestations indicating a loss of CH₄ during the travel of the gases towards earth's surface (D'Alessandro et al., 2009).

The CO₂/CH₄ ratio in soil gas samples from the geothermal area is more or less constant between 25 and 50 cm of depth, because convective motion of the hydrothermal gas prevails on air dilution. The decreasing in CO₂/CH₄ ratio, in the shallowest layer, is accompanied by a decrease in the CO₂ and CH₄ amount in soil gases. The decrease of both gases is mainly due to the air dilution, but the CH₄ content decreases also because of the bacterial activity uptake. On the contrary, the increasing the CO₂/CH₄ ratio recorded in samples from agricultural area could be due to the increases of CO₂ with depth as a consequence of organic activity that produces CO₂ in the soil. The Chemical Alteration index measured from samples soils is higher (up to 85) than that of the original rocks (Trachyte and Pantellerites reach 45, Di figlia et al., 2007); in geothermal soils alteration is due to hydrothermal flux and to weathering process. Micronutrient concentration in Pantelleria soils were in the range of not toxicity for methane oxidation bacteria.

The five different sites in the geothermal area at Favara Grande analyzed in this PhD thesis differ for temperature and pH from the above mentioned geothermal soils where *Verrucomicrobia* were found. FAV1 has higher temperature and lower pH than FAV2 and FAV3 sites that show temperatures < 75°C and only slightly acidic pH (5.24-5.98). These latter conditions seem more favorable for methanotrophs that were detected by PCR amplification of the methane mono-oxygenase gene, the key enzyme of methane oxidation (McDonald et al., 2008), in sites FAV2 and FAV3 but not in FAV1. Both proteobacterial and verrucomicrobial MMO gene could be

detected in FAV2 and FAV3 while no amplification product was obtained from FAV1. This microbiological result is coherent with the extremely low methane consumption detected in site FAV1 and this is probably due to the high temperatures and high fumarolic gas flux that prevent survival and activity of methanotrophs, even for the most thermo-acidophilic *Verrucomicrobia*. FAV1, in fact, has a temperature of at least 10°C higher than the hottest hot spring in Kamchatka where methanotrophic *Verrucomicrobia* were isolated (Islam et al., 2008). The extreme physical chemical conditions however do not prevent totally the bacterial life as assessed by TTGE analysis of the bacterial *16S* rRNA-amplified gene carried out on total soil DNA. FAV1 site hosts a low complexity bacterial community that thrives in those conditions. Measurements of the soil gases indicate a very high variation in methane concentration in the first measured layer that are associated with an increasing atmospheric content (air gases contribution in site FAV2 and FAV3 is more than 50% in first 13 cm). This creates a very favorable environment for methanotrophic bacteria allowing atmospheric O₂ to sustain microbial CH₄ oxidation. Many studies have, in fact, highlighted that aerobic methanotrophs increase their efficiency in very aerated soils with high methane fluxes from the underground.

Chemical-physical analysis and total bacterial diversity analyzed by TTGE confirmed that sites FAV2 and FAV3 are very similar for environmental conditions and microbial diversity.

In both sites Proteobacterial methane mono-oxygenase genes were detected, however *Verrucomicrobial pmoA* was only detected in FAV2. Considering this preliminary results and also that FAV2 shows the highest methane oxidation activity, further investigations were carried out on this site.

Enrichment cultures with methane as sole C and energy source and culture-independent techniques based on functional gene probes were used to describe the diversity of methanotrophs at FAV2. Matching the results obtained from the *pmoA* clone library and the isolation by enrichment cultures on the soil profile, site FAV2 at Favara Grande recorded the highest diversity of methanotrophs recorded in a geothermal area (Pol et al., 2007; Islam et al., 2008; Op den Camp, 2009; Kizilova et al., 2012). In the same soil, in fact, we could isolate and cultivate pure culture type II

Gammaproteobacterial methanotrophs of the genus *Methylocystis* and the facultative methanotrophs distantly related to *Methylobacterium*; contemporarily we detected, by amplification of the functional methane mono-oxygenase gene, a yet uncultivated type I *Alphaproteobacteria* and type X *Gammaproteobacteria* related to *Methylococcus capsulatus*. Moreover using the newly designed primers we detected the presence of Verrucomicrobial methane mono-oxygenase genes of *Methilacidiphilum fumarolicum* SolV isolated for the first time at Solfatara di Pozzuoli in Italy (Pol et al., 2007). This is an extraordinary high diversity of methanotrophs that could ever be expected in a geothermal soil and this is the first report in which the presence of both phyla of methanotrophs, *Proteobacteria* and *Verrucomicrobia* is recorded and their coexistence is demonstrated (Op den Camp et al., 2009). Different groups of methanotrophs are generally associated to their ability to survive, grow and oxidize methane in different environments. While the presence of *Verrucomicrobia* in a geothermal soil was predictable due to their thermophilic and acidophilic character, the presence of both *Alpha* and *Gamma Proteobacteria* was unexpected and suggests that high CH₄ fluxes and differences in environmental conditions shape the complex methanotrophic community structure at this geothermal area. Interestingly the results obtained from the clone library of proteobacterial *pmoA* genes do not overlap with those from enrichment cultures. Type I and Type X were only detected in the clone library from soil DNA, while only type II and facultative methanotrophs could be isolated after enrichment in a highly concentrated methane atmosphere. This would indicate a preponderance of type I and type X methanotrophs in the geothermal soil, while Type II methanotrophs take over in the presence of high methane concentrations at 37°C. It has also been observed that Type I methanotrophs *pmoA* sequences could be preferentially amplified over those from Type II methanotrophs due to variations in GC content (Bodelier et al., 2009 in Murrel and Jetten 2009). Type I methanotrophs are reported to be dominant in environments that allow the most rapid growth while Type II methanotrophs that tend to survive better, are more abundant in environments with fluctuating nutrient availability (Hansen and Hansen 2006). The conditions used for enrichment culture setting were those described for *Verrucomicrobia* isolation by Islam and colleagues (2008). Our results confirm that methanotrophic

Verrucomicrobia dominate highly acidic geothermal sites and are the only group to be isolated in culture, while soil pH above 5 allows colonization by a diverse group of both cultivable and uncultivated methanotrophs. In particular high CH₄ concentration and a temperature of 37°C favored the growth of *Methylocystis* from the first three top soil layers (1-13 cm) and of the facultative *Methilobacterium*. Moreover, we can affirm that *Methylocystis* has a range of growth wider than that reported in literature (Op den Camp et al., 2009). No isolates could be obtained from enrichments at 65°C notwithstanding a slight methanotrophic activity has been detected in soils up to 80°C. No attempts were made to set enrichments at intermediate temperatures, such as 45°C that is limiting for *Methylocystis* and would probably allow growth of more thermophilic strains.

3. NISYROS ISLAND

3.1. GEOLOGICAL SETTING

The island of Nisyros is a quiescent volcano belonging to the Dodecanese and it is located in the easternmost volcanic group of the South Aegean active volcanic arc.

It was built up during the last 200 ka and is considered still active though at present in quiescent status (Vougioukalakis and Fytikas, 2005) (Fig. 3.1). The island of Nisyros belongs to the Dodecanese and is located in the easternmost volcanic group of the South Aegean active volcanic arc. It was built up during the last 200 ka and is considered still active though at present in quiescent status (Vougioukalakis and Fytikas, 2005). Its volcanic activity has been characterized by an early submarine stage, a subaerial cone-building stage, culminating in the formation of a central caldera, and a post-caldera stage, when several dacitic-rhyolitic domes were extruded (Keller, 1982). No historical magmatic activity is known on Nisyros and the most recent activity was of hydrothermal character (Marini et al. 1993). Such activity concentrated in the southern Lakki Plain and on the southeastern flank of the Lofos dome both within the caldera. This hydrothermal activity formed a series of hydrothermal craters whose age decreases from southeast to northwest. The last events took place in 1871–1873 and 1887 partially destroying the small Lofos dome. A large fumarolic field is now present in this area mainly within the hydrothermal craters strongly controlled by fracturing along the main NW- and NE-trending active fault systems (Papadopoulos et al. 1998). Two deep explorative geothermal wells drilled in the Lakki Plain revealed the existence of two distinct hydrothermal aquifers. The shallowest at about 500 m depth has temperatures around 150 °C while the deeper one (> 1500 m) reaches temperatures up to 340 °C (Brombach et al., 2003) (Fig. 3.2).

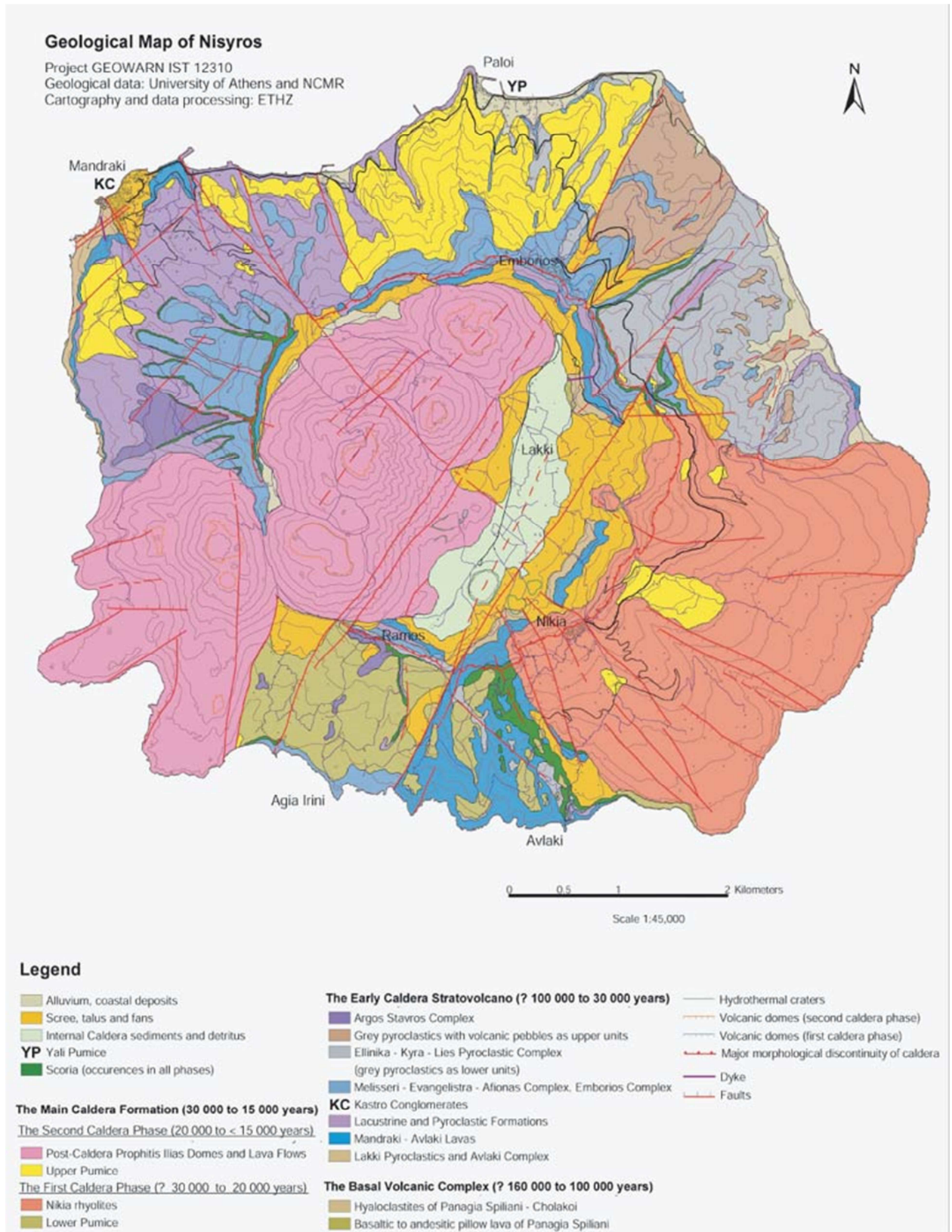


Fig. 3.1 - Geological map of Nisyros island.

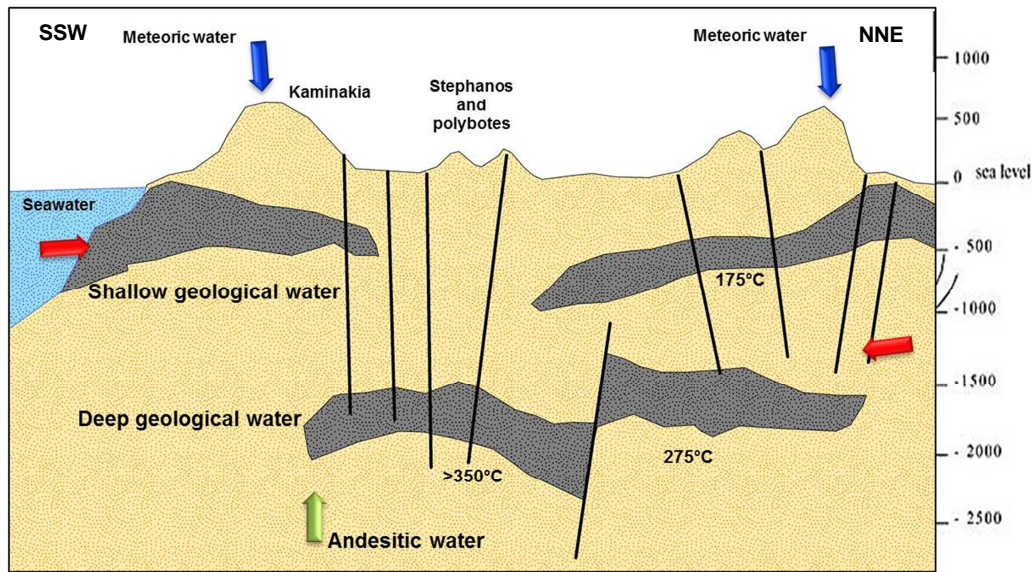


Fig. 3. 2 - Conceptual model of the geothermal system of Nisyros; blue arrows represent meteoric contribution of reservoir recharge, red arrow the marine contribution and green arrow the andesitic water contribution.

3.2. SAMPLING AREA

Nisyros island is a currently quiescent active volcanic system with strong fumarolic activity due to the presence of a high geothermal enthalpy. Previous studies assessed a widespread CO₂ degassing in the SW sector of the island (Lakki Plain) and in the nearby areas (Caliro et al., 2005). The highest CO₂ fluxes (> 300 g m² day) were measured within the hydrothermal craters in Lakki Plain. Methane flux, gases from fumaroles, soil gases and soils were sampled during tree campaigns of sampling. Two sampling campaigns were carried on 2010, before the starting of this PhD work, and the third sampling campaign and the elaboration of the previous data completed the work already started. In the first two campaigns, measurements were used to estimate the total CH₄ output of this hydrothermal system and to analyze gases from fumaroles. In the last campaign, methane flux measurement were carried out to improve the methane flux net of measurement, soil gases were sampled and soils were sampled to analyzed methanotrophic communities. Results of the first campaigns were summarize in the full paper published (D'Alessandro et al. 2013).

Basing on previous results, we decided to concentrate CH₄ flux measurements in the most representative craters (Kaminakia, Stefanos and Phlegeton) with some additional measurements in the fumarolic field of Lofos (outside any crater) and a few points in the low flux areas on 2010 campaigns, and in Micro Pyvoties, Lofos, Kaminakia, Ramos and Phlegeton in the campaign in 2013 (Fig. 3.3).

Soil gases from craters in Lakki Plain were sampled in June 2013 from 50 cm of depth and analysed by micro-GC (Par. 7 for materials and methods and Appendix I, Fig. 3.4). At each sampling site the soil temperature was also measured at 20 and 50 cm of depth.

Methane flux was measured by using accumulation chamber method; 50 site were sampled in 2013 integrating the 77 sites samples in previous campaigns (D'Alessandro et al, 2013) to increase the net of samples and better investigate methane emission from Lakki Plain. On the basis of the CO₂/CH₄ ratios and methane fluxes previously obtained (D'Alessandro et al. 2013), ten top-soils were sampled during the campaign on June 2013. Five in the crater of Kaminakia and five in that of Stefanos (Fig. 3.5).

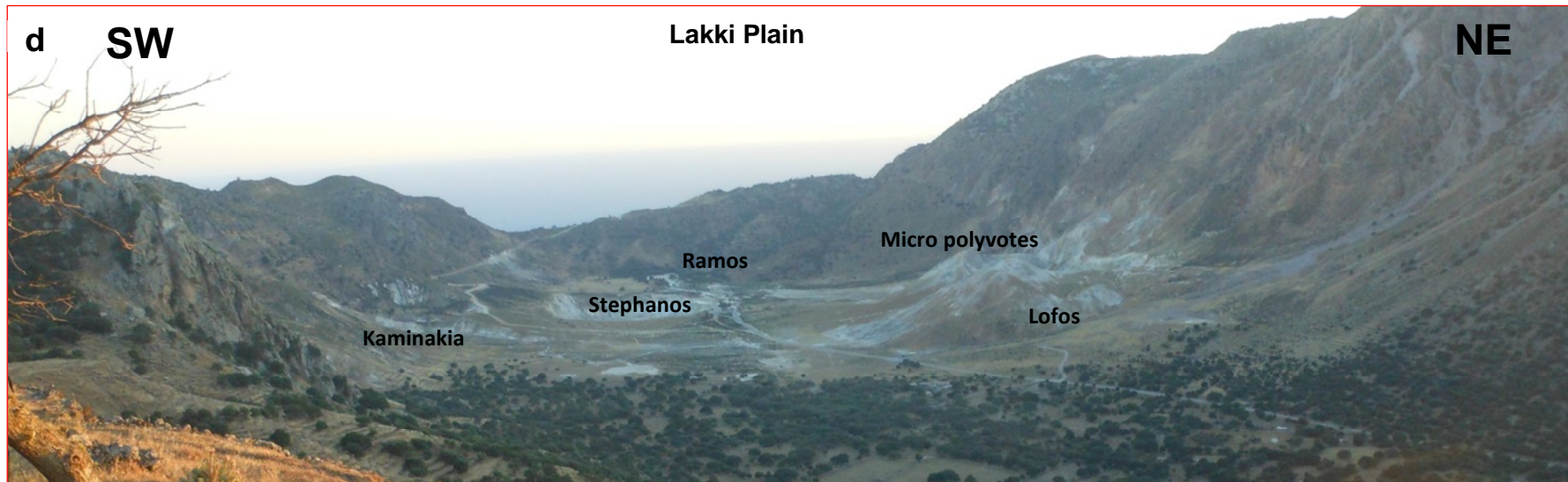


Fig. 3. 3 – a) Nisyros Island, Greece; b) Micro polyvotes, crater; c) holes in the Stephanos crater; d) Lakki plain and distribution of craters and degassing areas.

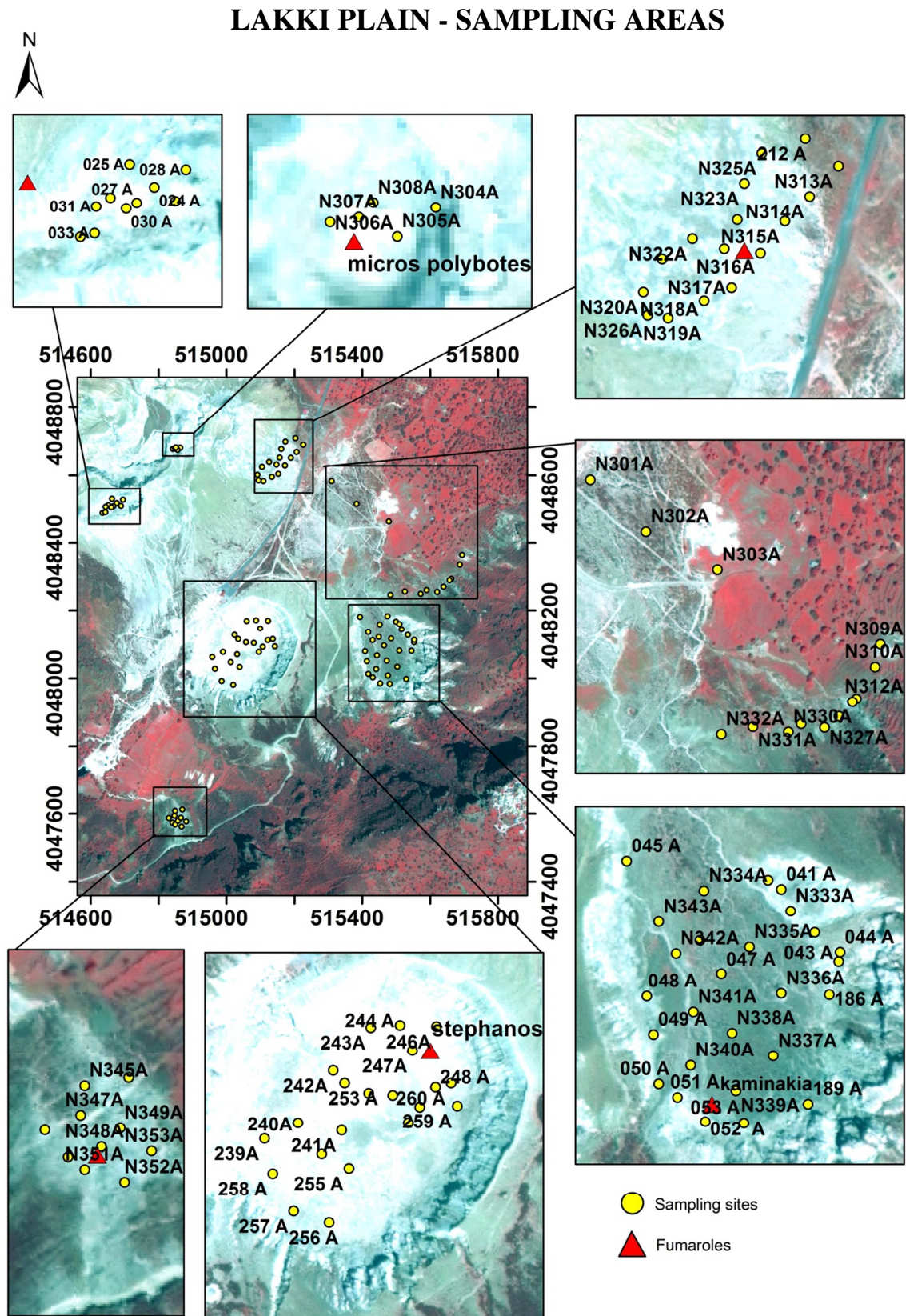


Fig. 3. 4 – Distribution of gas sampling areas in the Lakki Plain.

LAKKI PLAIN - SAMPLING AREAS

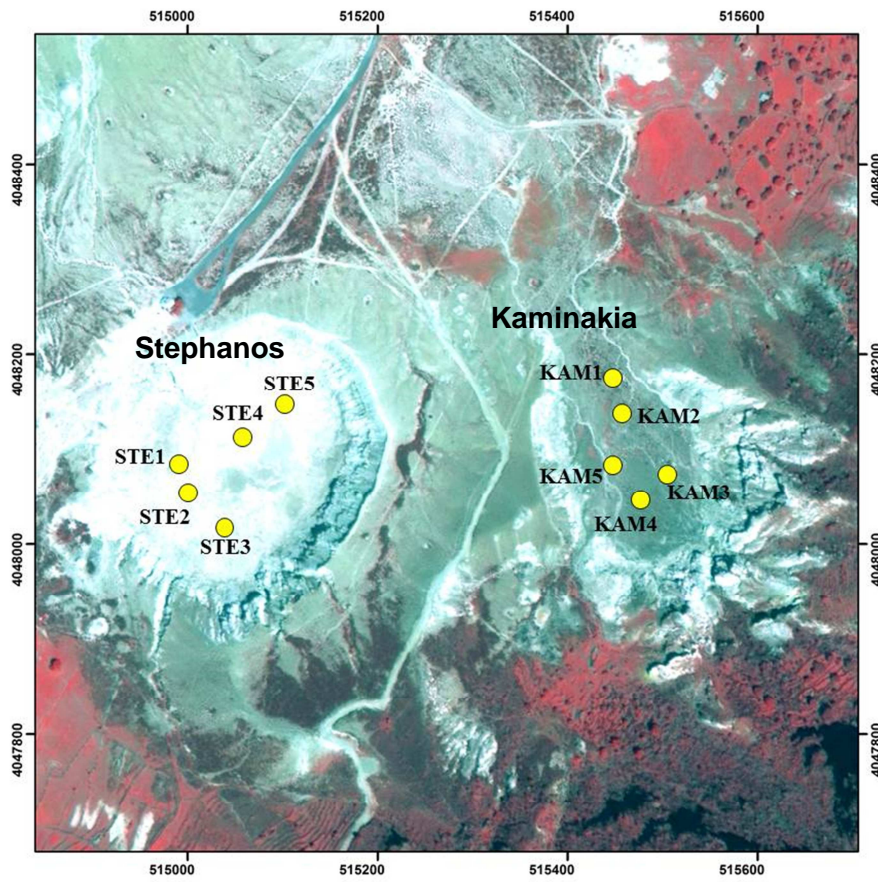


Fig. 3. 5 - Soil sampling area in Lakki plain.

3.3. RESULTS

3.3.1. TEMPERATURE DISTRIBUTION

Temperature measurements were made in 105 different sites at Lakki plain; ground temperatures were measured both at 20 and 50 cm of depth by using a digital thermometers as described in Par. 7.

Temperatures obtained were used to create distribution map of the temperature both with temperatures measured at 20 and 50 cm of depth (Fig. 3.6).

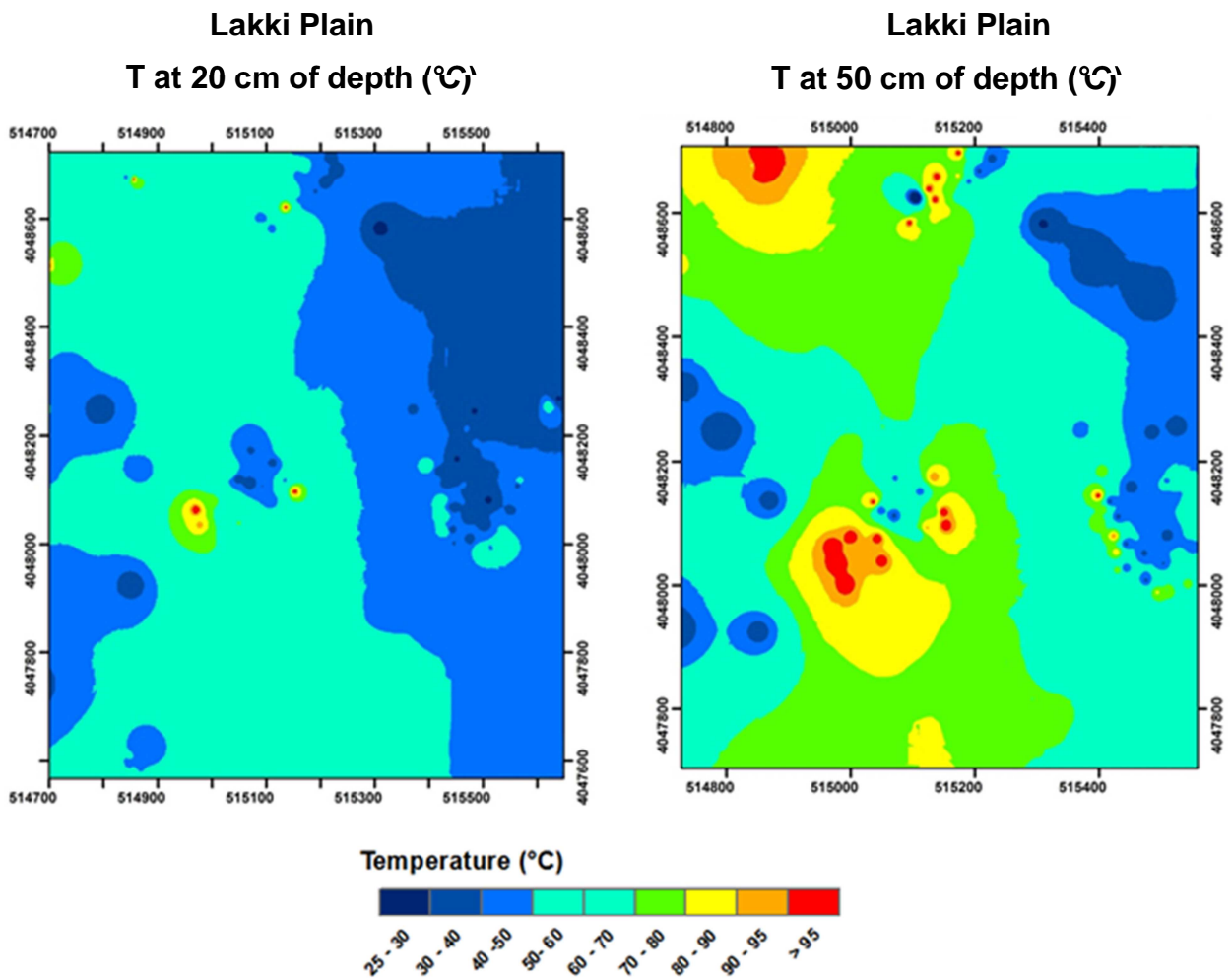


Fig. 3.6 - Temperature maps at 20 and 50 cm of depth , Lakki Plain. Maps were created by the geostatistical tool of ArcMap 9.3.

Higher temperature were measured in Stephanos where value reached 95°C even at 20 cm of depth; at Lofos and Micro polyvotes, highes temperature were recorded at 50 cm, but they significantly decrease at 20 cm. High value were also recorded in circus areas at Kaminakia, in corrispondenza of the main fumarolic manifestation.

3.3.2. FUMAROLES

Samples of the many fumarolic manifestations were collected during both campaigns in 2010 with soda filled bottles (Giggenbach and Goguel, 1989) and analysed in the laboratory for H₂O, H₂S, He, H₂, O₂, N₂, CH₄ and CO₂ (Table 3.1). Two fumaroles for each of the craters investigated for soil CH₄ fluxes were sampled both in 2009 and 2010.

sample	H ₂ O	CO ₂	H ₂ S	He	H ₂	O	N ₂	C	CH ₄	CO ₂ /CH ₄
	%	μmol mol ⁻¹								
K6	95.6	874811	96343	18	12572	0	3979	6	12272	71
K6	91.2	890317	90278	28	7914	7	8006	2	3448	258
K7	92.2	890682	73796	22	5217	8	7045	5	23226	38
K7	94.7	890636	78563	51	10974	18	13386	1	6370	140
S15	98.3	774458	211925	29	6640	8	4213	3	2723	284
S15	99.0	740627	217953	22	7515	27	30830	1	3026	245
S4	98.3	794665	190003	28	5372	13	6910	3	3006	264
S4	99.1	736916	223931	24	6169	41	29539	1	3380	218
A13	98.0	753938	227194	24	10830	0	7186	2	826	912
A13	98.6	738197	245342	28	10303	3	5543	1	582	1268
AM	97.9	755731	225266	25	11190	0	6968	2	818	924
AM	97.9	739933	204683	25	8751	3	46073	47	485	1525

Table 3. 1 - Fumaroles composition; samples were taken in the 2010 sampling campaigns.

Results of the chemical composition of the fumarolic gases are shown in Table 3.1. All samples are dominated by water vapour that accounts for 91 to 99% of their composition. For the remaining gases the composition generally follows the order CO₂ > H₂S > H₂ ≈ N₂ ≈ CH₄ » He > O₂ ≈ CO. Methane displays a wider range in composition with respect to the other gases which is reflected in the wide range in CO₂/CH₄ ratios. The main difference between the three fumarolic areas can be summarised in a lower content in H₂O and H₂S and a higher CO₂ and CH₄ content in the fumaroles of Kaminakia (K6 and K7). This has been explained by previous

authors (Marini and Fiebig, 2005) with condensation of water vapour close to the surface. Dissolution in the liquid phase changes the relative concentrations of the remaining gases depending on their solubility. This results in a depletion of the more soluble species (H_2S) and a relative increase of CO_2 and especially of CH_4 .

3.3.3. SOIL GASES

Previous studies, on Nisyros Island, assessed a widespread CO_2 degassing in the whole fumarolic area and in the nearby areas (Caliro et al., 2005). The highest CO_2 fluxes ($> 300 \text{ g m}^2 \text{ day}$) were measured within the above described hydrothermal craters in Lakki Plain.

Soil gases from craters and degassing area in Lakki Plain were sampled in June 2013 from 50 cm of depth and analysed by micro-GC (Appendix II).

Preliminary QQ Plots of CH_4 , CO_2 and H_2S , obtained from Micro-GC analyses (Appendix I) gave indication on their distribution in Lakki plain (Fig. 3.7, 3.8, 3.9). Result indicate that, on the basis of CO_2 content in sampled gases can be divided in two main families respectively with moderate/high (up to 60%) and very high content of CO_2 (up to 75%); a third family shows value of CO_2 close to the atmospheric concentration.

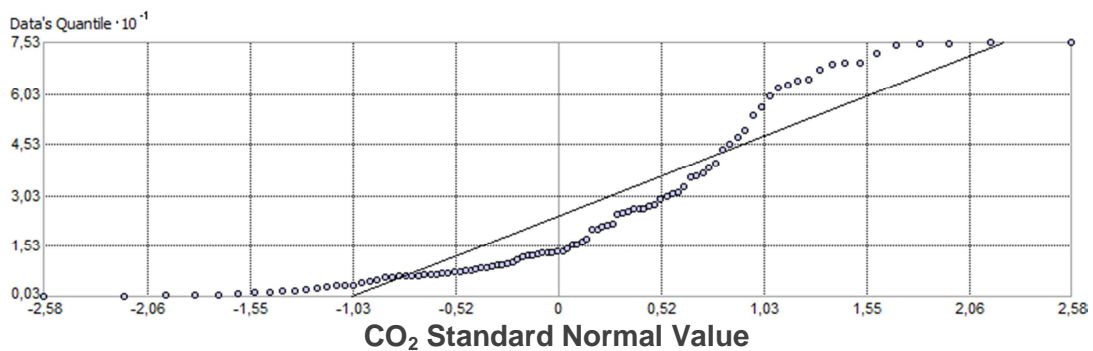


Fig. 3. 7 - QQ plot of CO_2 content in soil gases sampled at Nisyros.

The H_2S QQ plots indicated that sample it samples fall in two different groups. The first group include samples with very low or absent content of H_2S and the second samples with H_2S up to the 17%

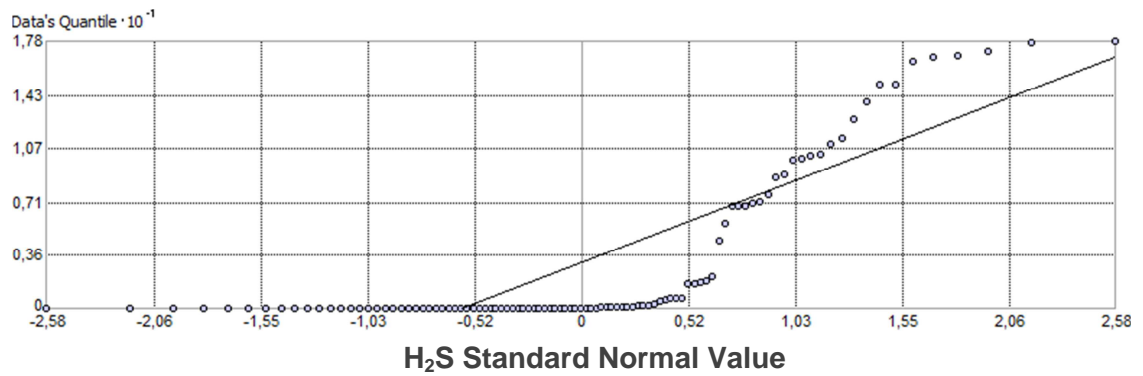


Fig. 3. 8 - QQ plot of H₂S content in soil gases sampled at Nisyros.

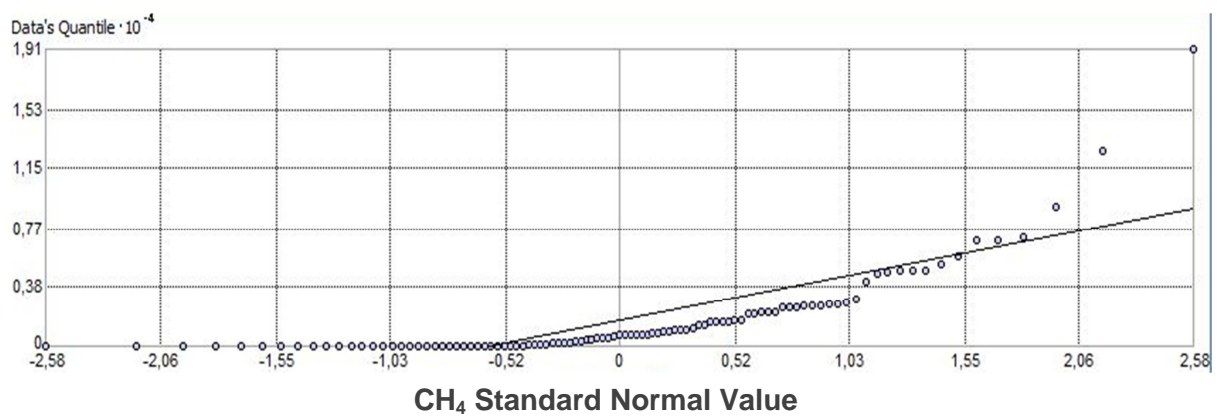


Fig. 3. 9– QQ plot of CH₄ content in soil gases sampled at Nisyros.

As shown in Fig. 3.10, gas composition in samples is mainly due to hydrothermal gases (CO₂, CH₄, H₂, H₂S); few samples of Stephonos, Kaminakia and Lofos were reached in of air gases (from 90 to 99%).

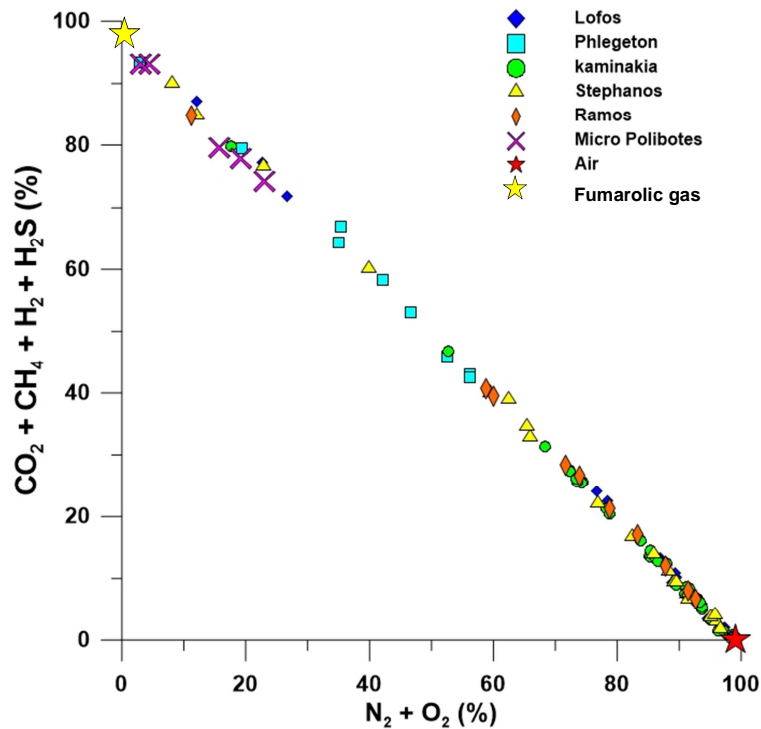


Fig. 3.10 - Fumarolic and air gas distribution in sampled soil gases.

Fumarolic gases are more abundant in Micro Polyvot, Phlegeton, Stephanos and Kaminakia. But some of the samples from Kaminakia and Stephanos recorded high content of air gases. In triangular diagram of CO_2 - CH_4 - H_2S in which it is possible to evaluate distribution of these hydrothermal components in the soil gases (Fig. 3.11). CO_2 is the main gas in all the samples like in the dry component of the fumarolic gases. High concentrations of H_2S are found at Phlegeton and Micro Polyvot close to the fumarolic compositions. Lofos and Stefanos show variable concentrations of H_2S going from high concentrations, close to the composition of the relative fumarolic composition, down to concentrations sometimes below the detection limit. Finally samples taken at Ramos and Kaminakia all show low to very low H_2S concentrations. The compositional trend of the fumarolic gases has been previously explained as due to vapor condensation close to the surface and subtraction of the most soluble gases from the mixture. The most soluble of the three gases (H_2S) is the more depleted while the least soluble (CH_4) is the most enriched. While the remaining gases plot almost all along the CH_4 – CO_2 axis. These samples are those

most contaminated by atmospheric air and modify their CH_4/CO_2 probably due to microbial CH_4 oxidation.

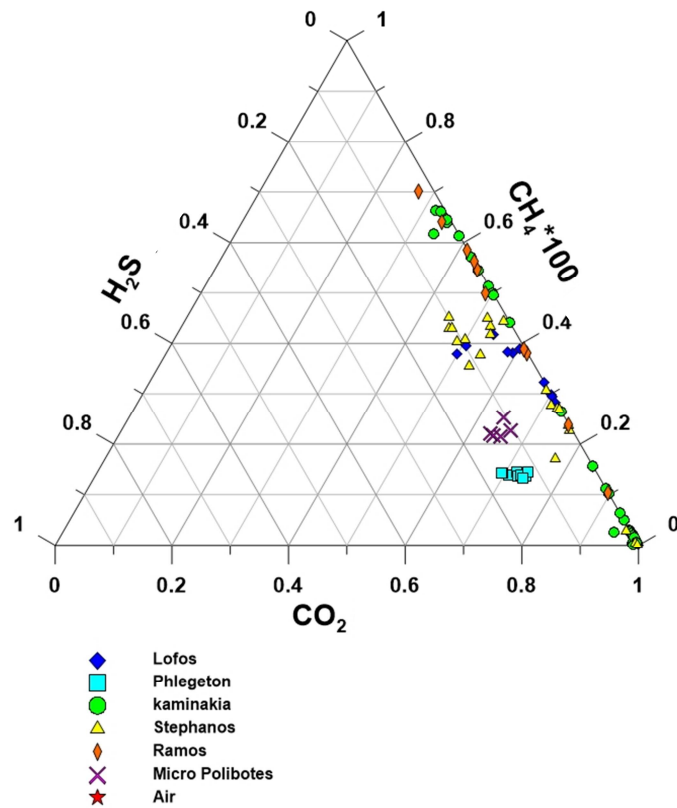


Fig. 3.11 - Triangular plot of the distribution of fumarolic gases of soil gases at the Lakki plain craters.

Fig. 3.12 to 3.14 distribution maps of the gas concentrations in Lakki Plain soils and are useful to identify areas in which gases composition is more or less influenced by the hydrothermal gas upflow.

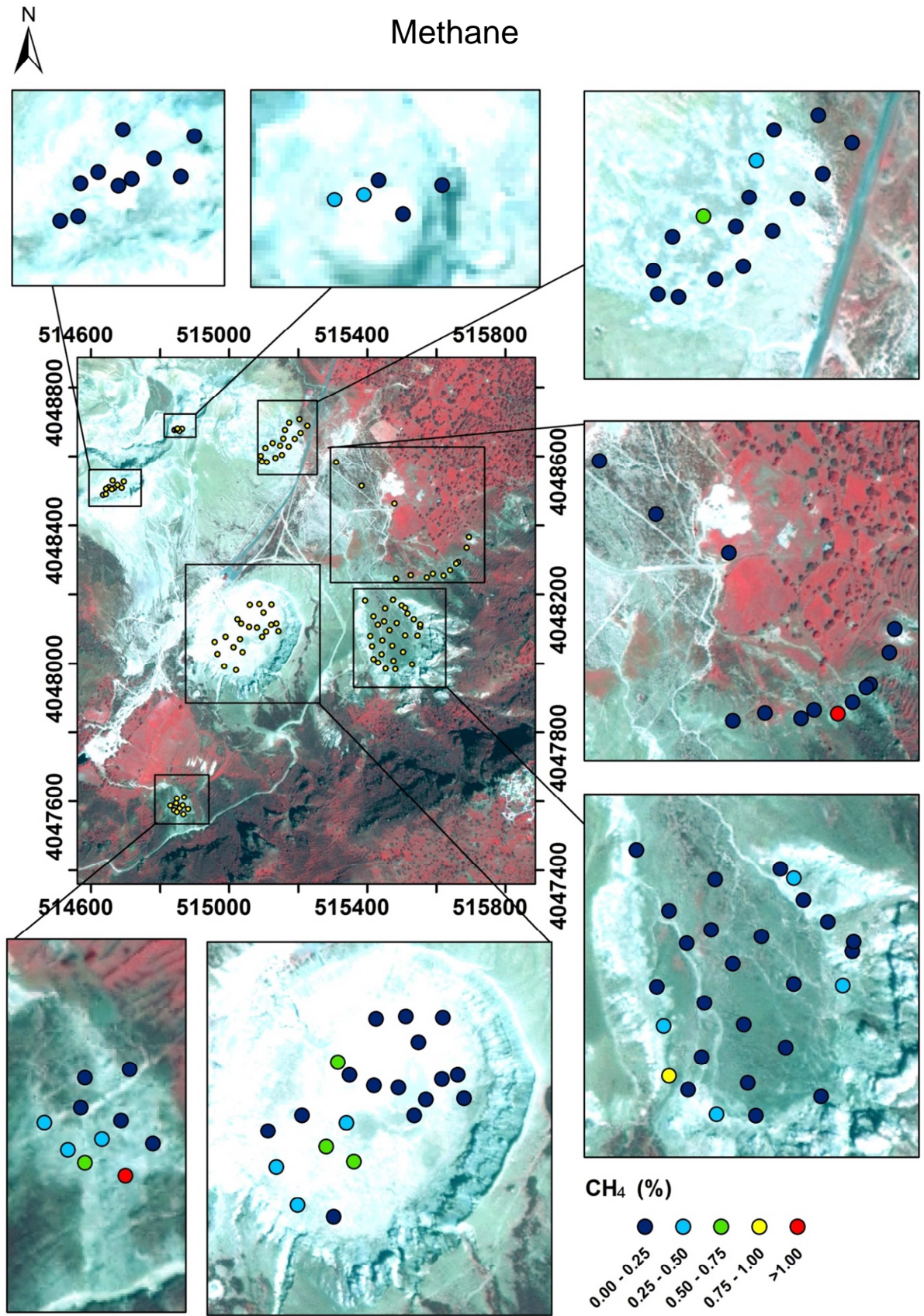


Fig. 3. 12 - CH₄ distribution in soil gases at sampled areas.

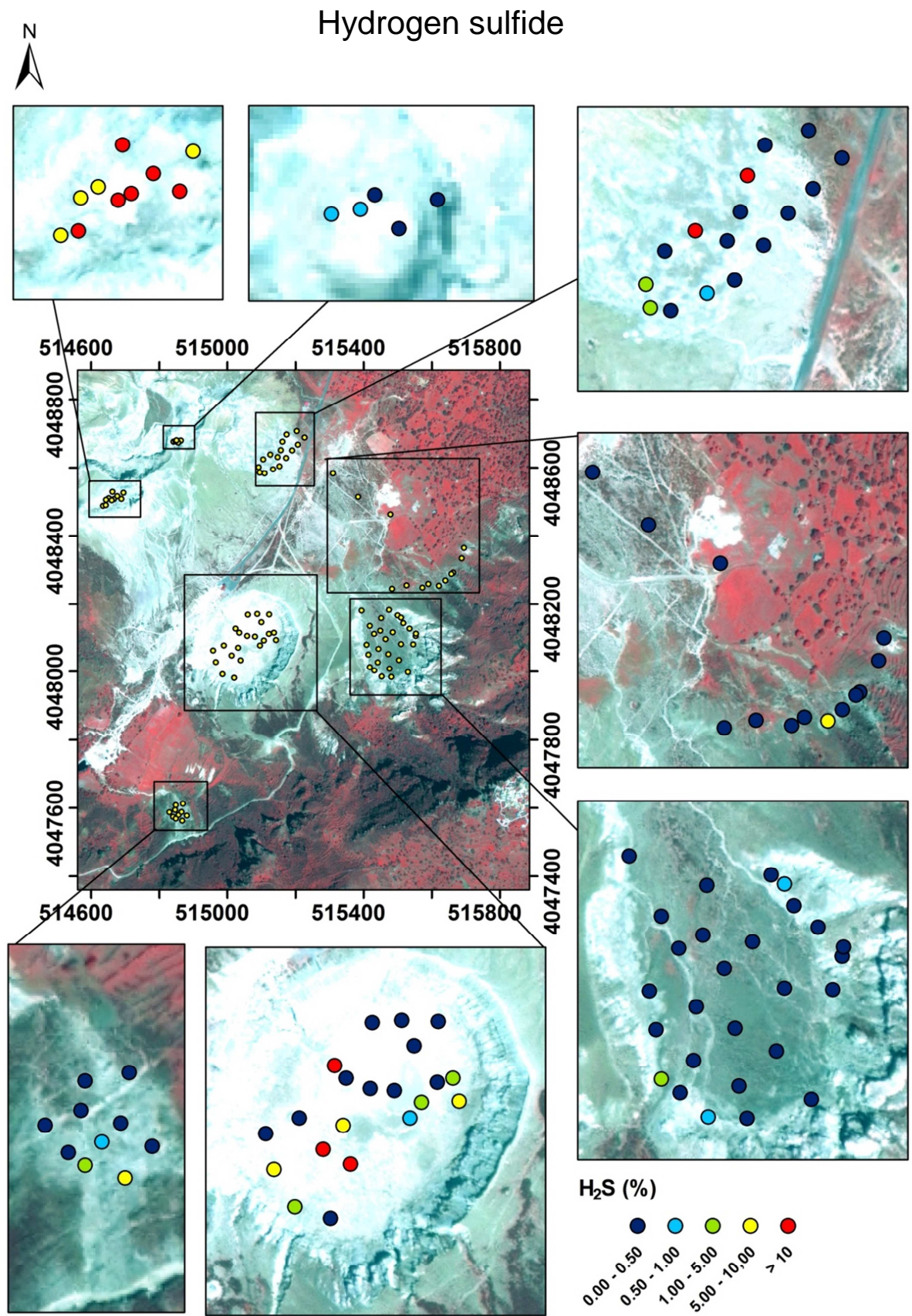


Fig. 3. 13 - H₂S distribution in soil gases at sampled areas.

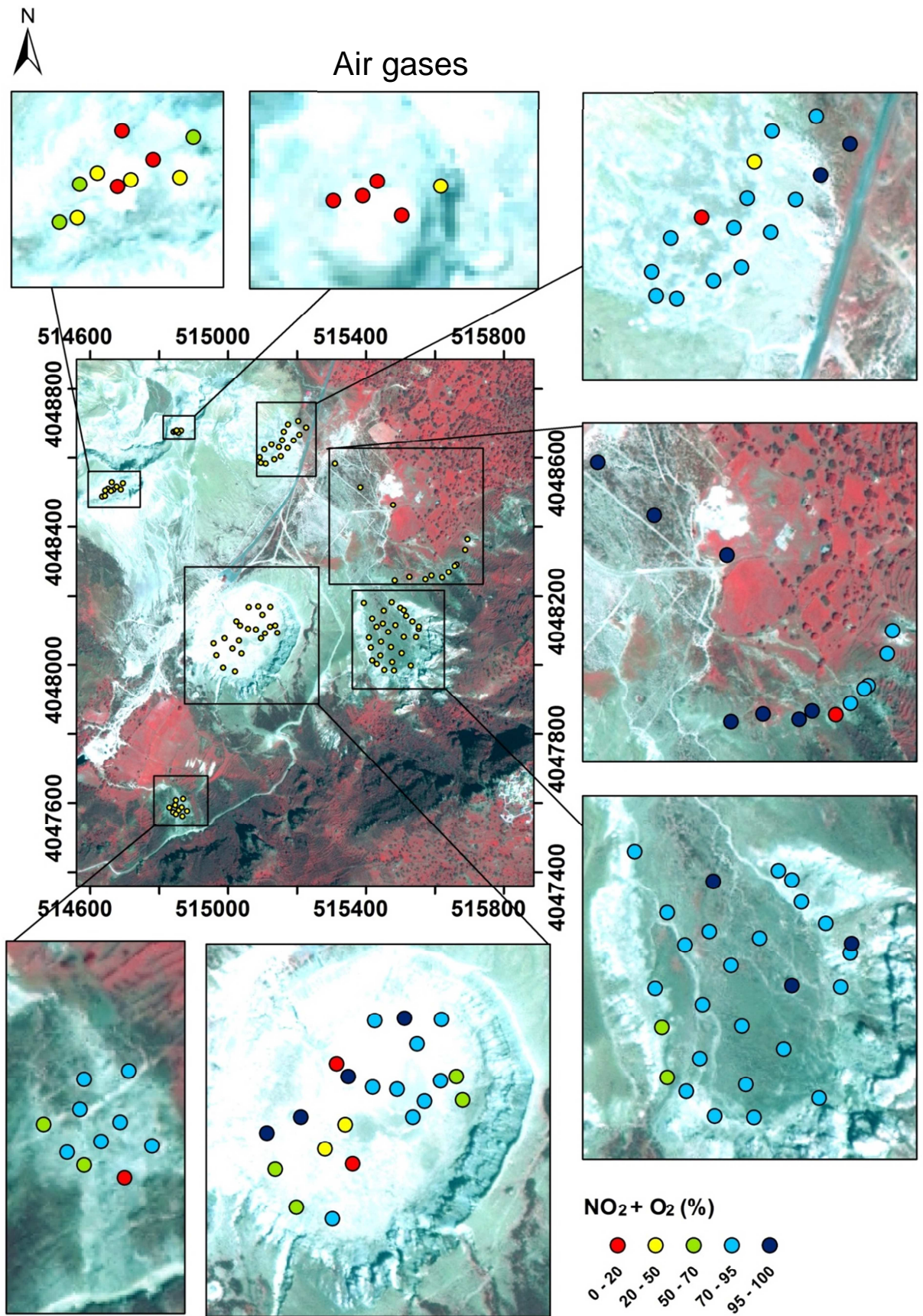


Fig. 3. 14 - Air gases distribution in soil gases at sampled areas.

CO₂ and H₂S are correlated in the binary diagram in Fig. 3.15; the general trend indicates that when CO₂ values are lower than 30% H₂S content does not exceed 2% due to the influence of the diffusive flux. On the contrary in samples with CO₂ higher than 30%, H₂S can reach value up to 18%, indicating that gas content is influenced by convective motion and reducing condition.

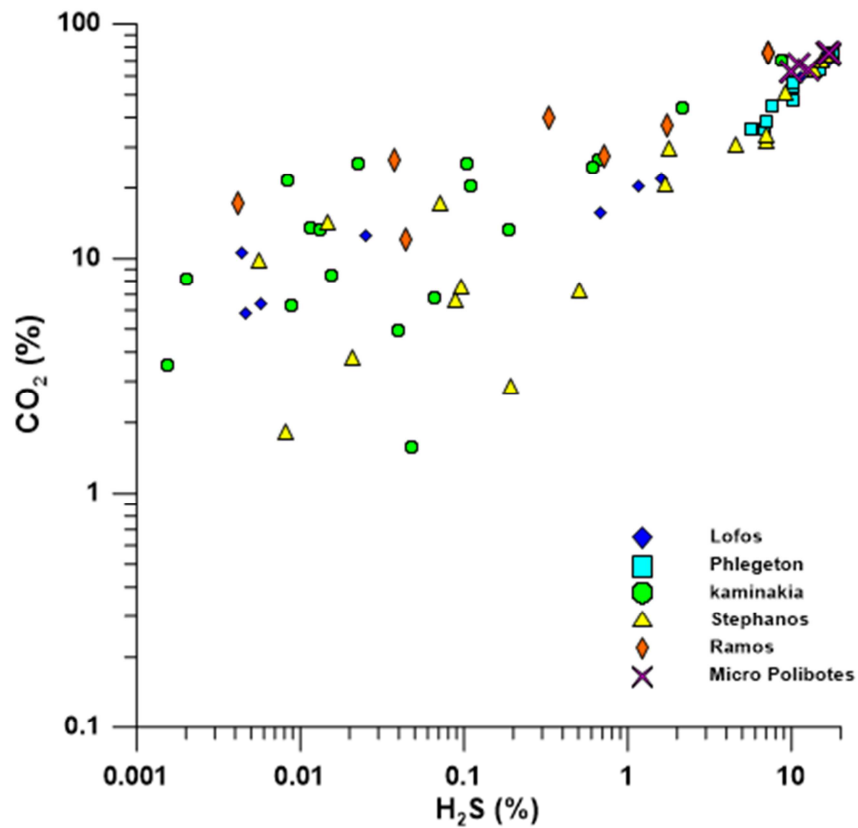


Fig. 3. 15 - Hydrogen sulfide vs carbon dioxide in Nisyros soil gases.

3.3.4. METHANE FLUX

Basing on previous results, we decided to concentrate CH₄ flux measurements in the most representative craters (Kaminakia, Stefanos and Phlegeton) with some additional measurements in the fumarolic field of Lofos (outside any crater) and a few points in the low flux areas on 2010 campaigns, and in Micro Pyvoties, Lofos, Kaminakia, Ramos and Phlegeton in the campaign in 2013 (Fig. 3.16). Methane flux was measured by using accumulation chamber method; 50 sites were sampled in 2013 integrating the 77 sites samples in previous campaigns (D'Alessandro et al, 2013) to increase the net of samples and better investigate methane emission from Lakki Plain.

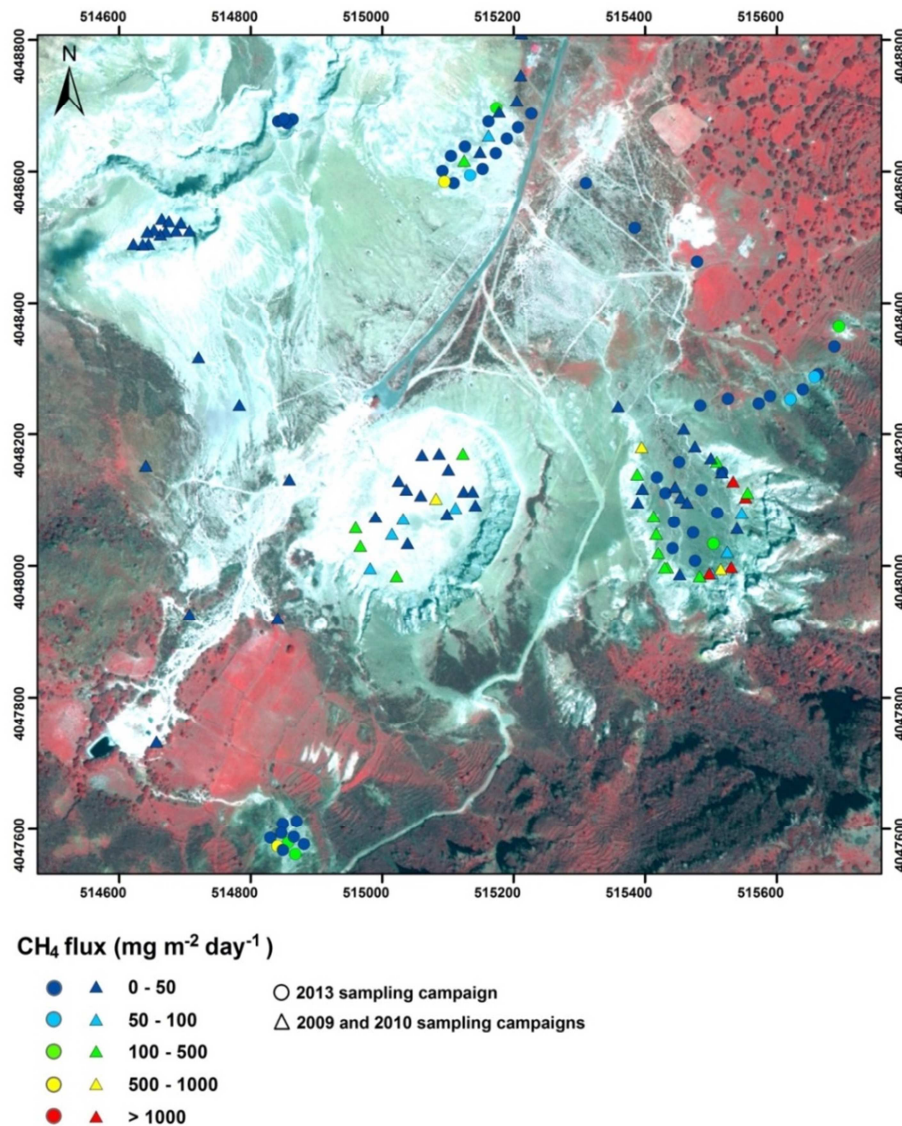


Fig. 3. 16 - Methane flux measured by accumulation chamber in the three sampling campaign; circle indicates measurements made during the field campaign in 2013; triangle indicates previous samples.

Results of the flux measurements are summarized in Appendix III. CH₄ flux values range from -33.52 to 1419 mg m⁻² d⁻¹ from 0.1 to 383 g m⁻² d⁻¹ for CO₂. Frequency histograms in Fig 3.17 show magnitude of methane flux in craters, in sampling campaign in this work and measurements by D’Alessandro et al 2013. To get insight in the methane output of the Lakki plain we focalised our measurements in restricted exhaling areas: Kaminakia, Stefanos and Phlegeton, Ramos, Micro Polyvotes craters and the southeastern flank of the Lofos dome.

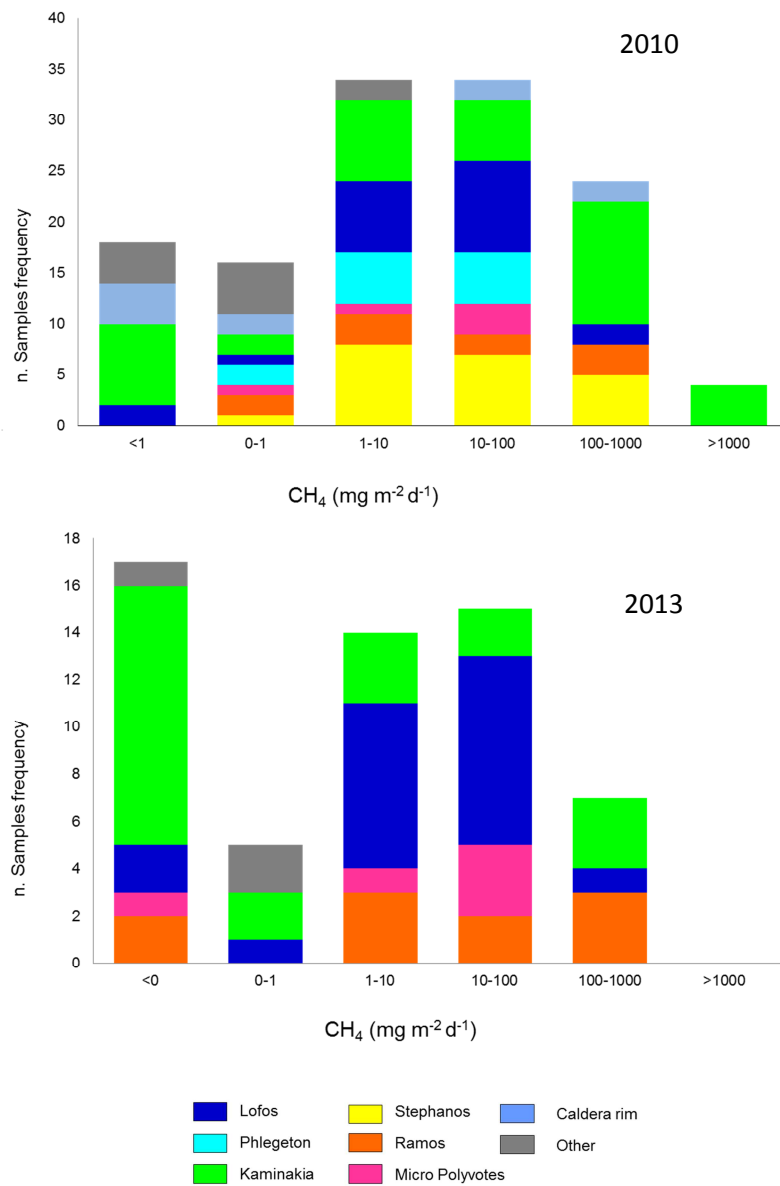


Fig. 3. 17 - Frequency of the methane flux; sampling made in 2010 were integrated with the sampling campaign in 2013.

Some measurements were also made in areas of lower hydrothermal output and indicated in the figures as other. Methane measurement in the Lakki Plain exhalative area showed that higher value of methane flux were measured at Kaminakia (up to $247 \text{ mg m}^{-2} \text{ d}^{-1}$) and at Ramos (up to $570 \text{ mg m}^{-2} \text{ d}^{-1}$). The lowest methane flux were recorded at Lofos (mean value 93, but in site flux was $930 \text{ mg m}^{-2} \text{ d}^{-1}$) and at Micro Polyvotes $30 \text{ mg m}^{-2} \text{ d}^{-1}$. Low hydrothermal sites display the lowest CH_4 flux values (Fig. 3.17, Appendix II, Table 8.2) never exceeding $2.6 \text{ mg m}^{-2} \text{ d}^{-1}$ and frequent negative values. Of the investigated exhaling areas those where the most recent activity occurred show the lowest CH_4 flux values (Lofos and Phlegeton $\sim 0\text{-}100 \text{ mg m}^{-2} \text{ d}^{-1}$) while to the older craters reach progressively higher values (Stefanos up to $714 \text{ mg m}^{-2} \text{ d}^{-1}$ and Kaminakia up to $1419 \text{ mg m}^{-2} \text{ d}^{-1}$).

3.3.5. GEOCHEMICAL EVIDENCES OF METHANE MICROBIAL OXIDATION

On the basis of the CO_2/CH_4 ratios and methane fluxes previously obtained (D'Alessandro et al. 2013), ten top-soils were sampled during the campaign on June 2013. Five in the crater of Kaminakia and five in that of Stefanos (Fig. 3.5). Samples were used for laboratory incubation experiment as described for Pantelleria soils and results of methane consumption are summarized in Table 3.2. Temperature were recorded at 20 cm of depth; higher temperature were recorded in STE1 ($70 \text{ }^\circ\text{C}$) and lower in STE4. pH is very low in all sampled site, ranging from 1.37 in STE4 to 3.67 in KAM2.

The samples collected at Stephanos display the lowest value and a narrower range (1.37-1.89) reflecting the higher H_2S values measured in the soil gases. The obtained potential methane consumptions are generally low ($4\text{-}40 \text{ ng g}^{-1} \text{ h}^{-1}$). The highest values were measured in STE4, KAM2, KAM5, with the samples coming from Kaminakia showing on average a little bit higher values. Soils were used for methanotrophs isolation experiment with the same procedure used for Pantelleria soils; methanotrophs cultures were set both with 25% and 1% of methane

considering that methane flux from Nisyros degassing area is lower than at Pantelleria, in an attempt to isolate possible high affinity methanotrophs (Fig. 3.18).

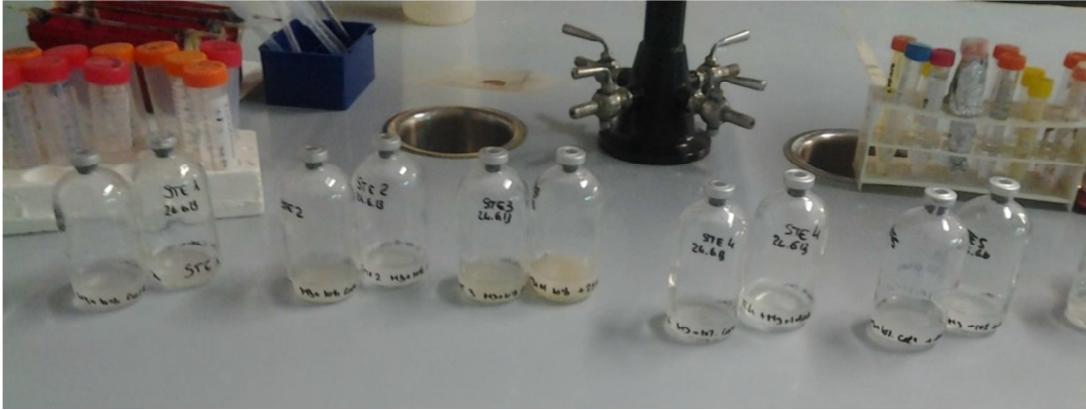


Fig. 3. 18 - Methanotrophs culture in M3 mineral medium.

Sample	X UTM	Y UTM	T(°C)	pH	Consumption (ng g ⁻¹ h ⁻¹)
STE1	515036	4048126	70	1.4	9.80
STE2	515051	4048103	70	1.66	10.90
STE3	515074	4048077	45	1.65	8.70
STE4	515081	4048120	27	1.37	37.70
STE5	515103	4048158	44	1.89	9.50
KAM1	515848	4048154	39	2.72	4.30
KAM2	515470	4048107	37	3.67	39.70
KAM3	515505	4048072	36	2.81	22.60
KAM4	515472	4048026	37	3.26	15.50
KAM5	515441	4048080	42	1.48	32.80

Table 3. 2 - Chemical – Physical characterization of sampling area in Stephanos and kaminakia craters and methane consumptions.

After a month, OD₆₀₀ of the culture in M3 broth were measured by using spectrophotometer (Table 3.3). Results indicate variability in growth in the different enrichment culture. Bacteria from M3 Broth were transferred in M3 Agar and very slow growth was observed. Bacteria show a really low growth and we observed in some samples tiny and transparent cells living with mold. Currently, isolation is in

progress and when pure culture will be obtained molecular analyses on samples will started.

Samples	Growth on M3 broth and 1% of methane (OD ₆₀₀)	Growth on M3 broth and 25% of methane (OD ₆₀₀)
STE1	0.171	0.121
STE2	0.445	0.310
STE3	0.409	0.034
STE4	0.162	0.115
STE5	0.174	0.189
KAM1	0.070	0.013
KAM2	0.027	0.014
KAM3	0.072	0.044
KAM4	0.072	0.039
KAM5	0.033	0.285

Table 3. 3 - OD₆₀₀ measured from M3 broth culture after a month of enrichment under 1% and 25 % of methane respectively.

3.4. DISCUSSION

Nisyros island is a part of an important volcanic arc system, and its present hydrothermal activity is concentrated in the Lakki Plain where gases are emitted by exhalation from several fumarolic areas (Lofos, Kaminakia, Micro Polyvoties, Mega Polyvoties, Stephanos, Ramos, Phlegeton) and diffusively along the whole area. The main fumarolic manifestation occurs at Phlegeton, Stephanos and Kaminakia. Soil gas samples display a wider range in CH₄, CO₂ and H₂S contents (from 0 to 19,142, from 9,900 to 752,707 and from 0 to 178,338 $\mu\text{mol mol}^{-1}$, respectively). This wide range is mainly due to the mixing within the soil of geogenic gases coming from depth and atmospheric gases coming from air. But also biologic processes influence soil gas composition being responsible of the large range of CO₂/CH₄ ratios. Soil gases show an enrichment in hydrothermal gases such as CH₄, CO₂, H₂S and H₂

mainly at Phlegeton and Micro Polyvototes. Less soluble gases (CH_4 and H_2) were more abundant in Kaminakia and Stephanos, where, instead, H_2S and to a lesser degree also CO_2 were solubilized with the lowering of the temperature as confirmed by measurements in the soils. The CH_4 flux distribution maps have been used to estimate the CH_4 output of the three investigated craters. The three areas according to the very different flux values show also very different CH_4 outputs. Phlegeton shows an output of about 0.01 t a^{-1} from an area of approximately 2500 m^2 , that of Stefanos is about 0.1 t a^{-1} from an area of some $20,000 \text{ m}^2$ and that of Kaminakia about 0.3 t a^{-1} from an area of approximately $30,000 \text{ m}^2$. The remaining areas would not add significant amounts of CH_4 to the entire output of the geothermal system. In fact, of the remaining area the highest hydrothermal flux areas (Micro Polyvotitis, Megalos Polyvotitis, Logothetis), with strong fumarole emissions, have characteristics that are very similar to Phlegeton and their contribution will be of the same order of magnitude and thus probably negligible. Some flux measurement made at Micro Polyvotitis confirm this hypothesis. A more substantial contribution could probably derive from the area northeast and southwest of Kaminakia along the caldera border where soil gases could be enriched in CH_4 in the same way as at Kaminakia. Previous studies on CO_2 soil degassing (Caliro et al., 2005) indicate that in these areas the fluxes tend to decrease rapidly away from the Kaminakia area especially in the southwest direction lowering their possible contribution to the total output. Consequently our best estimation of the total CH_4 output of the geothermal system of Nisyros is less than 1 t a^{-1} , which is more than one order of magnitude lower than the previous estimation (54 t a^{-1} - Etiope et al., 2007). The latter was made simply multiplying an estimated average CH_4/CO_2 ratio of the fumarolic emissions by the total CO_2 output obtained by Chiodini et al. (2005). Another source of error in the estimation of Etiope et al. (2007) derives from the great variability both in time and space of the CO_2/CH_4 ratios of the fumarole emissions at Nisyros as also evidenced by Marini and Fiebig (2005). Such great variability could introduce a great error in the CO_2/CH_4 ratio used to obtain the total CH_4 output. The CO_2/CH_4 ratio used by Etiope et al. (2007) is indeed low (167 by volume), close to the mean value of the Kaminakia crater, which is by no means representative of the whole area. Other strongly degassing areas show all considerably higher mean values accounting for a

significant part of the difference in output estimation. Moreover, as previously evidenced (D'Alessandro et al., 2009; 2011), part of the difference could be attributed to the disregarding of methanotrophic activity within the soils. Clues for methanotrophic activity in the soils of the study area are evidenced especially in the area of Kaminakia and Stefanos wher higher CO_2/CH_4 ratios with respect to the relative fumarole gases and methane consumption experiment ascertain methane microbial oxidation in soils and incubation experiments indicate methane consumption values.

**4. VULCANO ISLAND, SOUSAKI,
NEA KAMENI**

4.1.VULCANO ISLAND

Volcano island is located in the Eolic volcanic arc. Its activity started in the upper Pliocene (Frazzetta, 1984) with the first subaerial activity dated at 120 ka building up a trachybasaltic – trachyandesitic strato-cone (South Vulcano) in the southern sector of the island (Keller, 1980). This edifice was truncated by a caldera formed by several collapse events. During the last 10 ka volcanic activity produced a cone, named La Fossa Crater, 391 m high above sea level, where the last volcanic activity took place between 1888 and 1890 (Silvestri and Mercalli, 1891).



Fig. 4. 1 - Geology of Vulcano island.

Fumarolic activity is concentrated in the northern part of Fossa Grande crater and in the Porto di Levante beach. According to Chiodini and Cioni (1989), the fumaroles of Porto di Levante discharge the vapor produced by boiling of a hydrothermal system at about 200 °C. The Levante Bay area, located on the eastern side of the

isthmus of Vulcano island, is characterized by the presence of gas vents both on land and underwater. These vents are located over an elongated area that is the surface expression of an active regional fault (Frazzetta et al., 1984). After the last eruption of Vulcano island some authors reported wide fluctuations in the hydrothermal activity and consequent changes in the gas composition (Sicardi, 1940). In 1938, Sicardi reported H₂S concentrations in the dry gas of the sea shore between 8.4 and 4.7 % volume. The presence of a geothermal aquifer at shallow depth has been proved by geothermal exploration wells drilled between 1951 and 1957 in the Levante Bay area (Sommaruga, 1984). The gas emissions coming from the geothermal aquifer has been interpreted as the result of a mixing between magmatic and hydrothermal fluids feeding the crater fumaroles afterwards modified by secondary low temperature subsurface processes (Chiodini et al., 1993; 1995). Capaccioni et al. 2001 analyzed gas emissions on Vulcano and suggested the presence of three distinct groups of CO₂ rich gas emissions at different distances from the La Fossa Crater (Boatta et al., 2012). The underwater gas emissions of Levante Bay area being characterized by CO₂ contents between 97% and 98% volume, and H₂S content ranging from 2.2% close to the Faraglione to less than 0.005 % near the northern part of Levante Bay beach. Cardellini et al. (2003) measured methane fluxes in the Baia di Levante area in the range from 7 to 3900 mg m⁻² day⁻¹. In Vulcano island, fumarolic activity is concentrated in the northern part of Fossa Grande crater and in the Porto di Levante beach.

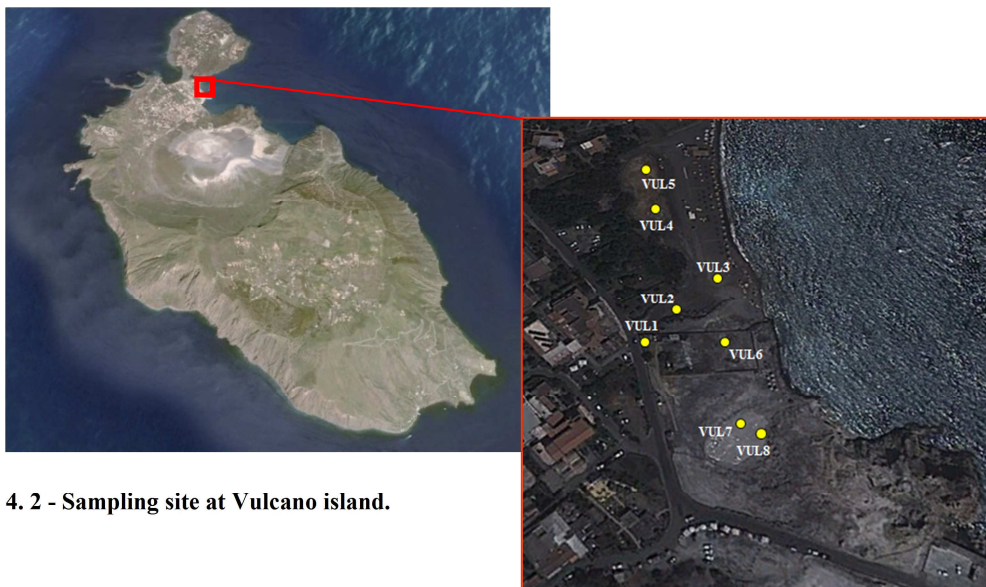


Fig. 4. 2 - Sampling site at Vulcano island.

Eight soil samples were taken from Levante bay in Vulcano island; four samples (VUL1 to VUL4) were taken from seaside and four (VUL5 – VUL8) in a geothermal bath characterize by very high hydrothermal flux (3.3.1). Ground temperature was measured in situ at 15 cm of depth in the same eight sites, pH and measure consumption were measured in laboratory. Total bacterial DNA extracted from soils were used for molecular analyses.

4.2.SOUSAKI

The Sousaki area is located about 65 km west from Athens, near the Isthmus of Corinth and is considered the NW end of the active south Aegean volcanic arc. Here, sparse outcrops of dacitic rocks are the remnants of late-Pliocene to Quaternary volcanic activity (4.0–2.3 Ma- Pe-Piper & Hatzipanagiotou 1997).

Both the vent distribution and the shape of the edifices are controlled by the E-W and the NW-SE extensional tectonic lineaments of the area, which were present since Pliocene and continue to be active up to the present (Francalanci et al. 2005). Besides volcanic rocks the following formations crop out in the area (IGME 1985):

1. Quaternary sediments: consisting of unconsolidated material with sand and rounded and angular pebbles in the torrent beds, loose sandy – clayey material and alluvial sediments.
2. Neogene sediments: composed of marly conglomerates and marly sandstones.
3. Post-upper Cretaceous ophiolitic nappe: consisting of slightly serpentinized peridotites, serpentinites and bodies of basic composition.
4. Upper Triassic–lower Cretaceous limestones.

Drilling exploration assessed the presence of a low enthalpy geothermal field, revealing two permeable formations at shallow depth (<200 m) and one at deeper levels (500–1100 m). All geothermal waters are of Na-Cl type and display temperatures in the range 50–80 °C and salinities in the range 39–49 g/l (Fytikas et al. 1995). Extended argillification-silicification of the rocks characterizes an area of about 100 × 300 m called Theochoma. The most affected rocks are those of the ophiolitic sequence and secondarily the marly Neogene sediments. Surface emanations and widespread diffuse degassing affects a smaller area estimated in

about 50×200 m (D'Alessandro et al. 2006). The main gas vents are found at the bottom of two caves on the flank of a hill. The caves called "big" and "small" have the following dimensions (height \times width \times depth) $8 \times 3 \times 10$ m and $4 \times 1.5 \times 4$ m respectively. Measured temperatures range from 37 to 44 °C (D'Alessandro et al. 2006). The emanating gases, being denser than atmospheric air, flow on the floors of the caves and eventually spill out from their mouth dispersing in the atmosphere after descending the flanks of the hill. This phenomenon can be seen when the atmospheric temperature is very low and the water vapour contained in the geothermal gases condenses creating a thin fog layer at the contact between the cold atmospheric air and the warm geothermal gases. Less defined gas vents are also found along the nearby ravine extending along the most altered area. D'Alessandro et al. (2006) identified, outside the main diffuse degassing area, other two minor degassing anomalies. The first is about 200 m south of the main gas manifestations and is probably due to the leaking of the exploratory well which was drilled there, because sign of hydrothermal alteration can be seen only on the corroded well case and on its cement base. The second is about 800 m WSW of the main gas manifestations and is characterized by alteration products covering an area of about 2000 m². As estimated from D'Alessandro et al. (2011) in Sousaki soil gas carbon dioxide is the dominant species displaying values from 926,000 to 991,000 $\mu\text{mol mol}^{-1}$. Atmospheric gases have generally low concentrations ($\text{O}_2 < 4400 \mu\text{mol mol}^{-1}$; $\text{N}_2 < 59,700 \mu\text{mol mol}^{-1}$). Hydrothermal species show variable content: CH_4 33-10,800 $\mu\text{mol mol}^{-1}$; $\text{H}_2\text{S} < 100-5000 \mu\text{mol mol}^{-1}$; $\text{H}_2 < 5-94 \mu\text{mol mol}^{-1}$. Helium concentrations range from 0.9 to 42 $\mu\text{mol mol}^{-1}$. The geothermal system of Sousaki is characterized by unusual high CH_4 fluxes (19 ta^{-1}) emitted by diffusively degassing through the soils (D'Alessandro et al., 2011).

Sousaki areas, in the Aegen Volcanic arc, represents a very active area and high methane flux was measured during previous studies. Samples were taken during a sampling campaign in autumn 2011, from four different areas located close to the main exhalative manifestation (SOUA, SOUB, SOUC and SOUD) and on the basis of previous study on methane emission (D'Alessandro et al., 2011) (Fig. 3.4.1, 3.4.2). The first three samples were strongly altered soils at short distance (tens of meters) between each other not far from the main gas manifestations (about 50 m).

These sites were chosen basing on their temperature at 20 cm depth (from 21 to 34 °C) in an attempt to sample soils with different hydrothermal upflow. At the site with the highest temperature some sulfate efflorescences were visible at the surface. The measured pH values were rather low (1.71-3.27). The fourth sample was taken along the ephemeral creek. It was composed mainly of sandy sediments and the measured temperature and pH (18.2 °C and 7.04 respectively) did not indicate hydrothermal upflow.

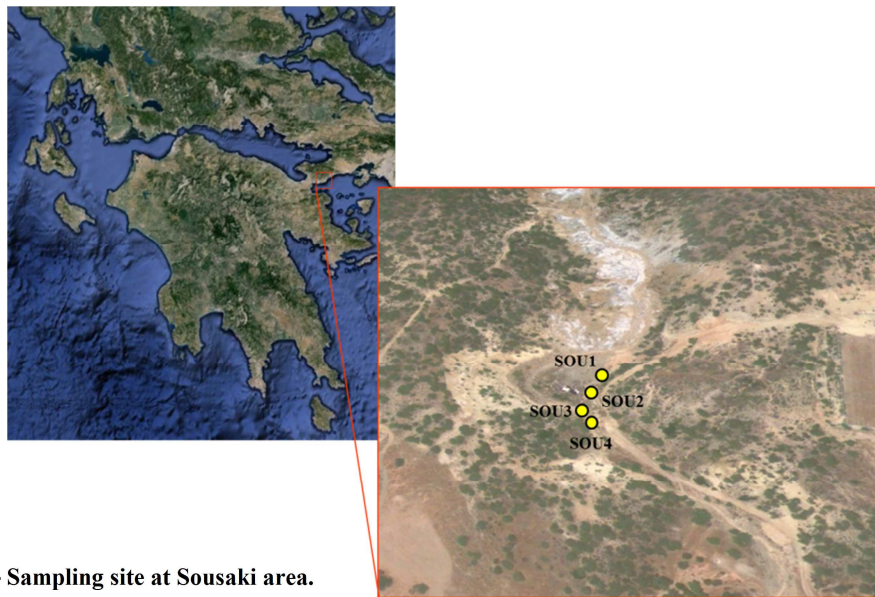


Fig. 4. 3 - Sampling site at Sousaki area.

At these site very different parameters were measured in 2009 during a previous campaign (site SOU34 - D'Alessandro et al., 2011) when temperatures of 34°C and a pH of 3.6 were measured and sulfate efflorescences were visible. Such great difference depends on the fact that this site is at the bottom of an ephemeral creek that had been dry for months before the sampling of 2009 and that was covered by water about a week before out sampling in 2011. The water flow has surely leached out of the sediment all soluble sulfate efflorescences, decreased soil temperature and increased soil pH.



Fig. 4. 4 – Sousaki Fumaroles.

4.3. NEA KAMENI (SANTORINI)

Nea Kameni is an uninhabited island in the center of the Caldera of the Santorini archipelago that also comprises the islands of Thera (Santorini) and Therasia, and the Aspronisi island and surrounds the circular depression of the Santorini caldera.

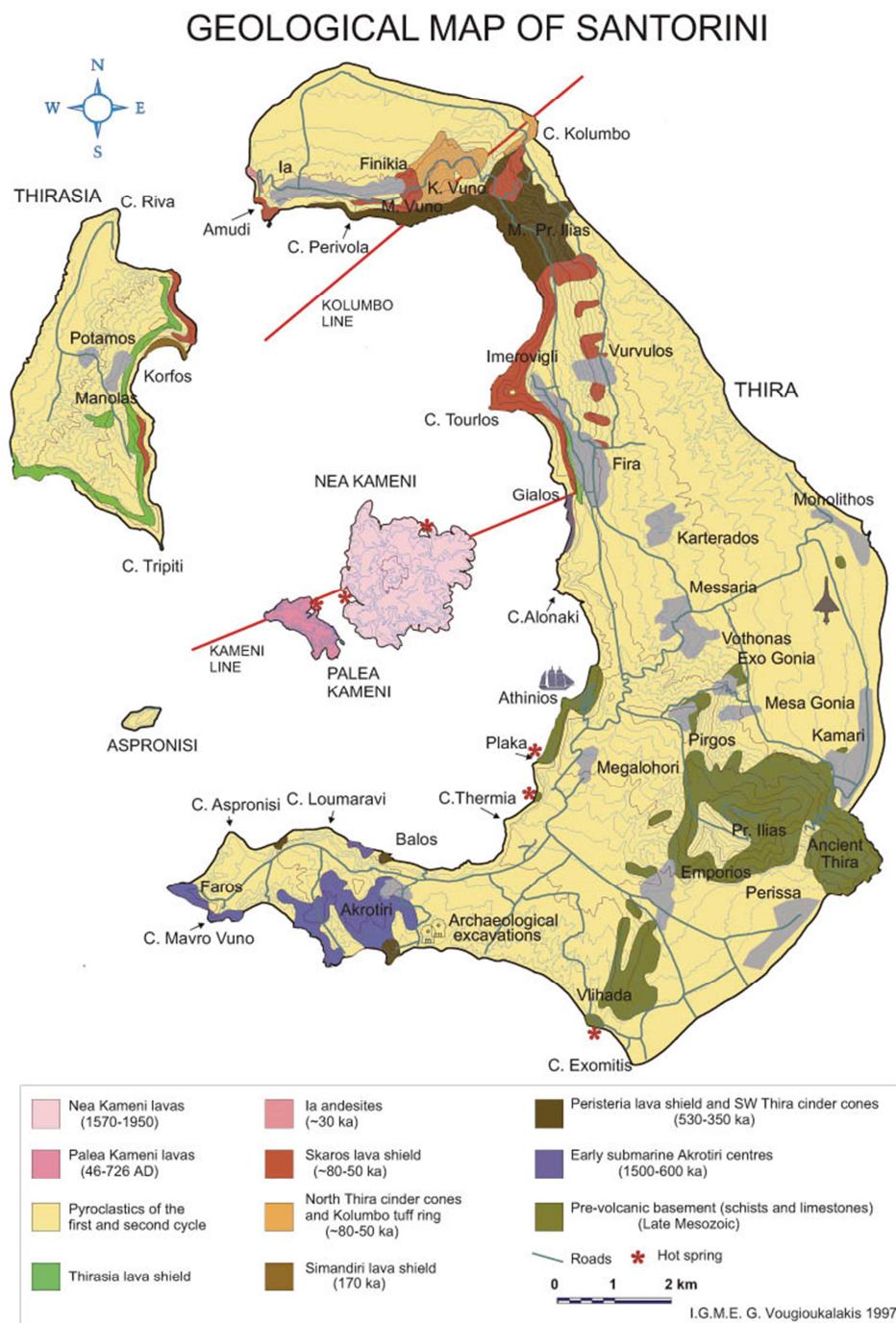


Fig. 4.5 - Geological map of Santorini island.

Santorini was formed during the Minoan eruption 3600 years ago. Post-caldera volcanic activity began close to 197 BC and formed the two small islands of Palea Kameni and Nea Kamen. Most dacitic lava flows of Nea Kameni were erupted during the last four centuries and four eruptive periods occurred between 1925 and 1950. The lava flows and pyroclastic deposits of Santorini show typical calc-alkaline compositions, from high-Al basalts to rhyodacites.

The volcanic rocks lie on top of the basement consisting of Mesozoic-Cenozoic schists and marbles. Today the thermal springs of Palea Kameni discharge steam-heated seawater, whereas the thermal springs of Thera are fed by steam-heated seawater mixed with groundwater. In addition, in Nea Kameni steaming grounds, are encountered (Marini et al., 2002).

The volcanic activity occurred on top of the metamorphic basement that outcrops at the south-eastern part of the island. This basement consists of a phyllitic epimetamorphic series of Mesozoic age. Microcrystalline thick-layered limestones with a total thickness exceeding 600 m overthrust the phyllites. The age of this formation is Upper Triassic, to Upper Cretaceous.

In the early Quaternary, the first volcanic activity occurred, depositing pyroclastics and lavas which cover the entire range of the typical calc-alkaline suite. The oldest volcanic deposits outcrop in the south-west part of the island, produced by volcanic centres located in the actual southern submarine area. The products of these centers are pyroclastics (tuffs, tuffites, hyaloclastites, scoriae, pumices and ashes), domes, lava flows and pillow lavas of andesitic-dacitic composition. A great part of these series is formed by dacitic submarine tuffs and tuffites with a thickness greater than 200 m. At the upper part of the pyroclastic series, up to 200 m above sea level, there are sedimentary levels with marine fossils which testify to the intense tectonic activity of the area in the last 2 million years. The entire series is slightly hydrothermally altered - mainly caolinized. The tectonic setting of Santorini is very intense and complicated, due also to the various subsequent caldera collapses.

The last paroxysmal eruption was the Minoan phreatoplinian explosion, which formed the pumice fall, and flow and surge deposits that cover the entire Santorini area. The post-Minoan volcanic activity was mainly restricted to the area of Palaea

and Nea Kameni island. The thermal springs of Palea Kameni discharge steam-heated seawater, whereas the thermal springs of Thera are fed by steam-heated seawater mixed with diluted groundwater (Chiodini et al., 1998). Low-pressure steaming grounds, heavily affected by air addition, are present at Nea Kameni. Furthermore, the salinity of two hot springs is higher than the one of seawater, indicating boiling seawater origin and the presence of an active high enthalpy hydrothermal system.



Fig. 4. 6 - sampling site at Nea Kameni, Santorini island.

Seven soils (NK1 to NK7) were sampled from Nea kameni island and were used for laboratory methane incubation experiment to verify methane consumption potential rate. Temperature was measured in situ by using thermal probe; pH was measured in laboratory.

4.4. RESULTS

4.4.1. METHANE CONSUMPTION

The potential methane consumption values of the sampled soils were obtained from laboratories incubation experiments. Consumption in Vulcano island soils are generally not very high (from 8.8 to 57.2) and the highest values were found at sites closer to the main gas manifestations of the area.

Site	Sample	X UTM	Y UTM	T(°C)	pH (H ₂ O)	CH ₄ consumption (ng g ⁻¹ h ⁻¹)
Vulcano Island	VUL1	496436	4252039	46.0	5.34	8.8
	VUL2	496443	4252058	38.4	3.10	25.7
	VUL3	496469	425087	32.0	2.32	17.8
	VUL4	496437	4252134	41.0	4.15	31.5
	VUL5	496428	4252171	37.5	2.69	14
	VUL6	496465	4252041	42.0	2.65	42.9
	VUL7	496471	4251991	45.0	2.08	48.5
	VUL8	496480	4251986	62.7	1.98	57.2
Santorini island	NK1	356243	4030006	55.7	4.44	35
	NK2	356239	4030014	47.3	4.58	17.5
	NK3	356002	4030056	81.1	4.70	10.2
	NK4	356227	4029975	74.7	3.51	13.1
	NK5	356152	4029939	31.0	5.70	15.7
	NK6	356119	4029948	30.8	6.26	14
	NK7	356079	4029964	27.7	6.04	23
Sousaki	SOUA	683471	4200703	20.7	3.27	2.46
	SOUB	683428	4200646	34.0	1.88	18.5
	SOUC	683398	4200608	28.8	1.71	22.2
	SOUD	683416	4200591	18.2	7.04	530

Table 4. 1 - Chemical – physical characterization and methane consumption of the sampling site in Vulcano island, Santorini island, Sousaki area.

Temperature measured at 10 cm of depth indicate value in the range of 32 to 60 °C, pH is not homogenous among samples. Higher consumption was recorded in site with higher temperature and the low pH reflecting a higher hydrothermal efflux close to the main gas manifestations of the area.

Samples from Nea Kameni were collected in a small area around the crater left by the last eruptive activity in 1950. Samples from NK1 to NK4 were collected in the area most affected by hydrothermal upflow (Tassi et al., 2013) in which most of the gas manifestations are present. The remaining samples were collected in an area less affected by hydrothermal activity. The two groups show clear differences in soil

temperature and pH. The sites in the area most affected by hydrothermal upflow show higher temperature values (47-81°C) and lower pH (3.51-4.70) with respect to the remaining sites (T 28-31°C; pH 5.70-6.26). The low concentrations of H₂S in the fumarolic gases of Nea Kameni are reflected in pH values that never reach values below 3.51 even at sites very close to the main gas manifestation (NK4).

Potential methane consumption is low but still detectable ranging from to. The two areas independently from the hydrothermal upflow show very similar values. The low measured consumption could be justified by the fact that at Nea Kameni the CH₄ fluxes are probably low. Unfortunately, until now, no measurement has been undertaken, but disregarding methanotrophic activities and considering the measured CO₂ flux values and the CO₂/CH₄ ratio of the fumarolic manifestations (Tassi et al., 2013) the highest values would be in order of 50.

Sousaki soils were sampled from different areas as indicated by temperature and pH data; this area is characterized by temperature not influenced by geothermal gradient and very low pH (1.7 – 3.3), only one site presents more basic pH close to 7 (SOUD). The higher and very significant methane consumption were recorded from SOUD soil (530 ng g⁻¹ h⁻¹) it is comparable with Pantelleria soil consumptions. Soil with higher consumption value, were sampled from the site with highest pH and the lowest temperature. Total soil DNA was extracted from sample VUL2, VUL4, VUL5, VUL7, VUL8, SOUD and PCR with specific primer for *Proteobacteria* and *Verrucomicrobia pmoA* gene were carried out with the same protocol used for Pantelleria soil. No positive results were obtained for any couple of primers utilized. Probably this first attempt failed because of low DNA quality.

4.5. DISCUSSION

Consumption values in Vulcano, Santorini and Sousaki except for one sample (SOUD) were low and in any case not comparable with consumption from Pantelleria island. Temperature, pH and methane flux are an explanation to the low consumption measured. Data from Pantelleria suggest that methanotrophic activity is influenced by pH and by methane concentration, in fact in Pantelleria soils pH is close to neutrality and experiment carried with different methane concentration

indicate that consumption increase with methane availability. Methane consumption values from Sousaki soils agreed with this and the highest consumption value was detected in a soil with neutral pH; Moreover, temperatures at Sousaki are close to the atmospheric temperature, as described in the chapter 1 vital range temperature is wide, and in this case temperature can permit methanotrophs presence, that brings us to conclude that pH is in this case the limiting variable for methanotrophic activity. Total DNA of SOUD, considering its high consumption values, was extracted to detect the presence of *pmoA* genes, but no results were obtained. Negative results in Sousaki might indicate that methanotrophs belonging to known methanotrophic *Proteobacteria* and *Verrucomicrobia* were not present in the sampled soil or that they were not much represented in total bacterial communities. In the first case, it is possible to explain high consumption with the possible presence of methanotrophic archaea (Glass et al., 2013), that were not investigated in this study; however, the detection of Archea by molecular methods is already planned. The case of investigation of Vulcano areas is quite different. Soils from Vulcano island were sampled in an area with very low pH, temperature are not very high at 15 cm, H₂S flux as reported in previous studies (Capaccioni et al., 2001) is very high, methane flux even if significant is not high in respect to other geothermal/volcanic areas; all these conditions make the absence of methanotrophs not unexpected, although some methane consumption (even if low) was recorded. Negative results from *pmoA* gene detection in samples VUL2, VUL4, VUL5, VUL7, VUL8 were probably due to low quality of the extracted DNA. In fact, the samples were used as template even to amplify the conserved region *16S* rRNA and even in this latter case no result was obtained. Soils from Vulcano island were really altered and maybe salt, humic acid did not allow to obtain pure amplifiable DNA, even if all the purification steps were performed before using it for PCR.

5. GENERAL DISCUSSION AND CONCLUSION

Geothermal and volcanic systems were selected in Italian and Greek territories because the estimated methane emissions from these areas are very high (Etiope, 2002). At the global scale, microbial oxidation in soils contributes for about 3-9% to the total removal of methane from the atmosphere. But the importance of methanotrophic organisms is even larger because they oxidize the greatest part of the methane produced in soil and in the subsoil before its emission to the atmosphere. Environmental conditions in the soils of volcanic/geothermal areas (i.e. low oxygen content, high temperature and proton activity, etc.) have long been considered inadequate for methanotrophic microorganisms and methanotrophy in geothermal areas has received so far little attention. However, recently, it has been demonstrated that methanotrophic consumption in soils occurs also under such harsh conditions (Castaldi and Tedesco 2005) due to the presence of newly discovered acidophilic and thermophilic *Verrucomicrobia*. Three closely related species were found in Italy at the Solfatara at Pozzuoli (Pol et al., 2007), at Hell's Gate in New Zealand (Dunfield et al., 2007) and in Kamchatka, Russia (Islam et al., 2008) where no other methanotrophs could be detected. We studied five geothermal system that differ for temperature, pH, CH₄ and H₂S flux. All the investigated site can be considered a natural methane sink, as demonstrate by methane consumption in all the investigated site and the identified methanotrophs in Pantelleria. The recorded methane oxidation rate were different in all the investigated areas; Principal Component Analysis were applied to compare data from different sites using temperature, pH, H₂S content as factors. Variance is in the order of 68% and according with the analyzes components, the highest consumption values were measured in soils with highest pH, low content in H₂S and low CO₂/CH₄ value. Methane oxidation potential strictly depend on the methane availability. Laboratory experiments and correlation between methane flux indicate a high methane oxidation rate when methane availability is higher.

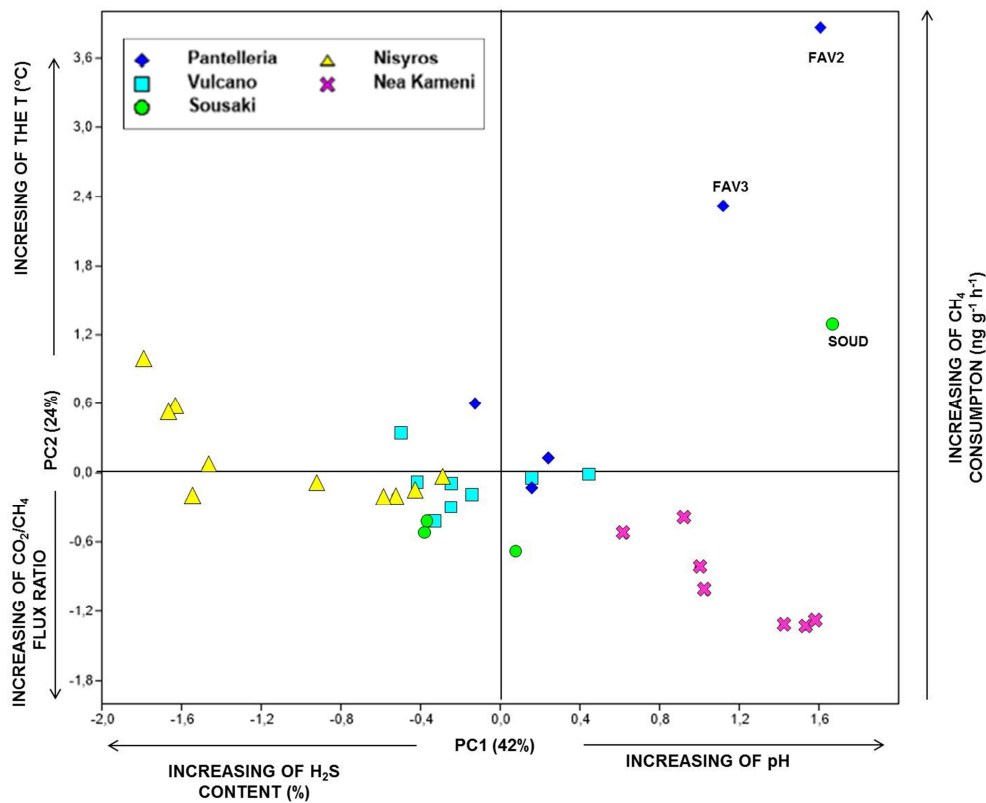


Fig. 5.1 - Principal Component Analysis to associate methane consumption recorded in incubation experiment using soils from study areas with multiple factors.

Moreover, high methane consumption were recorded in the areas with high methane flux such as Pantelleria and Sousaki, while the lowest in Nea Kameni, were methane emission are lower. Even if, Vulcano island, Kaminakia and Sousaki contribute significantly in methane emissions, methane oxidation rates are lower than in Pantelleria. The main difference between Pantelleria and the other sites is in the H₂S emission that in Pantelleria island are very low with respect to the other sites, as underlined by fumarolic gas composition. Hydrothermal conditions within the geothermal system of Pantelleria and Sousaki are such that little H₂S is produced. This means that even if the hydrothermal gas flux is huge the soil pH generally does not reach very low values. Stephanos and Phlegeton craters at Nisyros showed a different behavior with respect to Pantelleria. In fact, the CO₂/CH₄ flux ratio indicate low methane value in comparison to Pantelleria and Kaminakia (even if still very

significant), but H₂S in these craters reach really high values being a major component of the gases in Stephanos and Phlegeton.

Geothermal System	CO ₂ /CH ₄	H ₂ S ppm
Pantelleria	25 - 30	< 100 ^a
Sousaki	80 - 120	1000 – 1500 ^b
Vulcano	~50	~ 20,000 ^c
Nea Kameni	10,000	< 10 ^d
Nisyros		
Kaminakia	30 – 70	60,000 – 90,000
Stephanos	150 - 300	200,000 – 250,000
Phlegeton	900-1400	200,000 – 250,000

Table 5. 1- Comparison between studied geothermal system. a. D'Alessandro et al., 2009; b. D'Alessandro et al., 2006; c. Capaccioni et al. 2001, d. Tassi et al, 2013.

High temperature does not seem a limiting factor for methane consumption in investigate soil, at least up to 60 °C even if methanotrophs in laboratory conditions did not grow at temperature higher than 45°C.

At the end of this work, we can disregard that only Verrucomicrobial methanotrophs are living in geothermal soils because Pantelleria island soils host a wide number of Proteobacterial methanotrophs; Their presence in the soils of Pantelleria and could be explained by the fact that these soils do not have extremely low pH values (> 5). Indeed thermotollerant species belonging to *Gamma-Proteobacteria*, genetically similar to those of Pantelleria, have been previously found in the sediments of thermal springs in Kamchatka similar species could have found their niches in the shallowest part of the soils of Favara Grande where the temperatures are not so high and thrive on the abundant upraising hydrothermal methane. Moreover, Pantelleria is until now the geothermal site with higher methanotrophs diversity ever recorded. Other site showed significant consumption values and the identification of preoteobacteria in Pantelleria soils, indicate that the geothermal soils can host not only verrucomicrobial methanotrophs. Indeed thermotollerant species could found their niches in the geothermal soils where the temperatures are not so high, pH not so low and thrive on the abundant upraising hydrothermal methane.

Yearly, 22 Tg of methane were emitted globally in the atmosphere contributing to the global warming. Interest in the study of methane output in the atmosphere is increasing every day to reach a correct estimation of the geologic, and the volcanic/geothermal contribution in the increasing of methane budget in the atmosphere. The discovery of the new species of methanotrophs belong to *Verrucomicrobia* brought to reconsider the relationship between methane emission from soil and its main sink, that was considered inefficient in the case of geothermal site due to the extreme environmental conditions and this work affirming the possibilities of Proteobacterial methanotrophs even in geothermal and volcanic areas open several perspectives in terms of methane source and sink in the extreme environments and in term of extraordinary capability of methanotrophs to live and adapt in all type of environments.

6. REFERENCES

1. Ait-Benichou S., Jugnia L.B., Greer C.W., Cabral A.R., 2009: Methanotrophs and methanotrophic activity in engineered landfill biocovers, *Waste Management*, 29, 2509-2517.
2. Anthony, C. 1991: Assimilation of carbon in methylotrophs, p. 79-109. In I. Goldberg and J. S. Rokem (ed.), *Biology of methylotrophs*. Butterworth-Heinemann, Stoneham, Mass.
3. Axelson, G., and Gunnlaugsson (convenors), 2000: Long-term Monitoring of high- and low-enthalpy fields under exploitation. International Geothermal Association, World Geothermal Congress 2000 Short Courde,, Kokonoe, Kyushu District, Japan, May, 226 p.
4. Bender, M. and Conrad, R., 1995: Effect of methane concentrations and soil conditions on the induction of methane oxidation activity. *Soil Biology and Biochemistry* 27, 1517-1527.
5. Boatta F., D'Alessandro W., Gagliano A.L., Liotta M., Milazzo M., Rodolfo-Metalpac R., Hall-Spencer J.M., Parello F., 2013: Geochemical survey of Levante Bay, Vulcano Island (Italy), a natural laboratory for the study of ocean acidification, *Marine Pollution Bulletin* 73 485-494
6. Bodelier, P.L.E., Gillisen, M.J.B., Hordijk, K., Damste, J.S.S., Rijpstra, W.I.C., Geenevasen, J.A.J. and Dunfield, P.F. (2009) A reanalysis of phospholipid fatty acids as ecological biomarkers for methanotrophic bacteria. *ISME* 3: 606-617.
7. Bodrossy, L., Stralis-Pavese, N., Murrell, J. C., Radajewski, S., Weilharter, A., and Sessitsch, A., 2003: Development and validation of a diagnostic microbial microarray for methanotrophs, *Environ. Microbiol.*, 5, 566-582.
8. Bödvarsson G., 1964: Physical characteristics of natural heat sources in Iceland. Proc. UN Conf. on New Sources of Energy, Volume 2: Geothermal Energy, Rome, August 1961. United Nations, New York, 82-89.
9. Bowman, J., 2000: The methanotrophs – the families Methylococcaceae and Methylocystaceae. In *The Prokaryotes*. Dworkin, M. (ed). New York: Springer.
10. Brock, T.D. 1978. *Thermophilic Microorganisms and Life at High Temperatures*. Springer-Verlag, New York.
11. Brombach, T., Caliro, S., Chiodini, G., Fiebig, J., Hunziker, J.C., Raco, B., 2003. Geochemical evidence for mixing of magmatic fluids with seawater, Nisyros hydrothermal system, Greece, *Bull. Volcanol.*, 65, 505-516.
12. Caliro, S., Chiodini, G., Galluzzo, D., Granieri, D., La Rocca, M., Saccorotti, G., Ventura, G. 2005: Recent activity of Nisyros volcano (Greece) inferred from structural, geochemical and seismological data, *Bull. Volcanol.*, 67, 358-369.
13. Capaccioni, B., Tassi, F., Vaselli, O., 2001. Organic and inorganic geochemistry of low temperature gas discharges at the Baia di Levante beach, Vulcano Island, Italy. *J. Volcanol. Geoth. Res.* 108, 173-185.
14. Cardellini, C., Chiodini, G., Frondini, F., Granieri, D., Lewicki, J., Peruzzi, L. 2003: Accumulation chamber measurements of methane fluxes: application to volcanic-geothermal areas and landfills, *Appl. Geochem.*, 18, 45-54.
15. Castaldi, S., Tedesco, D. 2005: Methane production and consumption in an active volcanic environment of Southern Italy, *Chemosphere*, 58, 131-139.
16. Chiodini, G., Cioni, R., Marini, L., 1993. Reactions governing the chemistry of crater fumaroles from Vulcano Island, Italy, and implications for volcanic surveillance. *Appl. Geochem.* 8, 357-371.
17. Chiodini, G., Cioni, R., Marini, L., Panichi, C., 1995. Origin of the fumarolic fluids of Vulcano Island, Italy and implications for volcanic surveillance. *Progr. Oceanogr.* 57, 99-110.
18. Chiodini, G., Granieri, D., Avino, R., Caliro, S., Costa, A., 2005: Carbon dioxide diffuse degassing and estimation of heat release from volcanic and hydrothermal systems. *J. Geophys. Res.* 110, B08204. doi:10.1029/2004JB003542.
19. Cebon A, Bodrossy L, Stralis-Pavese N, Singer AC, Thompson IP, Prosser JI and Murrell JC. 2007. Nutrient amendments in soil DNA stable isotope probing experiments reduce the observed methanotroph diversity. *Appl Environ Microbiol* 73: 798-807.
20. Civetta, L., Cornette, Y., Gillot, P.Y., Orsi, G., 1988: The eruptive history of Pantelleria (Sicily channel) in the last 50 ka. *Bull. Volcanolo.* 50, 47 - 57.
21. Civetta, L., Cornette, Y., Crisci, G., Gillot, P.Y., Orsi, G., Requejo, C.S., 1984: Geology, geochronology and chemical evolution of the island of Pantelleria. *Geol. Mag.* 121, 541-562.

22. Colby, J. and Dalton, H., 1978: Resolution of the methane mono-oxygenase of *Methylococcus capsulatus* Bath into three components. Purification and properties of component C, a flavoprotein. *Biochemical Journal* 177, 903-908.
23. Conrad R., 1996: Soil Microorganisms as Controllers of Atmospheric Trace Gases (H₂, CO, CH₄, OCS, N₂O, and NO), *Microbiological Reviews*, Dec. 1996, p. 609-640.
24. Conrad, R., 2009: The global methane cycle: recent advances in understanding the microbial processes involved, *Environ. Microbiol. Rep.*, 1, 285–292.
25. Cornette, Y., Crisci, G.M., Gillot, P.Y., Orsi, G., 1983: Recent volcanic history of Pantelleria: a new interpretation. *J. Volcanol. Geotherm. Res.* 17,361 – 373.
26. Churakov, S. V., Tkachenko, S. I., Korzhinskii, M. A., Bocharnikov, R. E., and Shmulovich, K. I., 1998: Evolution of Composition of High-Temperature Fumarolic Gases from Kudryavy Volcano, Iturup, Kuril Islands: the Thermodynamic Modeling, *Geochemistry International*, Vol. 38, No. 5, 2000, pp. 436–451. Translated from *Geokhimiya*, No. 5, 2000, pp. 485–501.
27. D'Alessandro W., S. Bellomo, L. Brusca, J. Fiebig, M. Longo, M. Martelli, G. Pecoraino, F. Salerno, 2009: Hydrothermal methane fluxes from the soil at Pantelleria island (Italy), *Journal of Volcanology and Geothermal Research*, 187, 147-157.
28. D'Alessandro, W., Brusca, L., Kyriakopoulos, K., Martelli, M., Michas, G., Papadakis, G., Salerno, F. 2011: Diffuse hydrothermal methane output and evidence of methanotrophic activity within the soils at Sousaki (Greece), *Geofluids*, 11, 97–107.
29. Dalton, H. 1991: Structure and mechanism of action of the enzymes involved in methane oxidation, p. 55–68. In J. W. Kelley (ed.), *Applications of enzyme biotechnology*. Plenum Press, New York.
30. Dedysh, S. N., 2009: Exploring methanotroph diversity in acidic northern wetlands: molecular and cultivation-based studies, *Microbiology*, 78, 655–669.
31. Di Figlia M.G., Bellanca A., Neri R. and Stefansson A., 2007: Chemical weathering of volcanic rocks at the island of Pantelleria, Italy: Information from soil profile and soil solution investigations, *Chemical Geology* 246, 1–18.
32. Dlugokencky, E.J., E.G. Dutton, P.C. Novelli, P.P. Tans, K.A. Masarie, K.O. Lantz, and S. Madronich, 1996: Changes in CH₄ and CO growth rates after the eruption of Mt Pinatubo and their link with changes in tropical tropospheric UV flux. *Geophys. Res. Lett.*, 23(20), 2761-2764.
33. Dunfield P.F, Yuryev A., Senin P., Smirnova A.V., Stott M.B., Hou S., Ly B., Saw J.H., Zhou Z., Ren Y., Wang J., Mountain B.W., Crowe M.A., Weatherby T.M., Bodelier P.L.E., Liesack W., Feng L., Wang L. and Alam M., 2007: Methane oxidation by an extremely acidophilic bacterium of the phylum *Verrucomicrobia*, *nature06411*.
34. Dutaur, L., Verchot, L.V., 2007: A global inventory of the soil CH₄ sink, *Glob. Biogeochem. Cycles*, 21, GB4013.
35. Ehhalt, D., and M. Prather, 2001: Atmospheric chemistry and greenhouse gases, in *Climate Change 2001: The Scientific Basis*, edited by J. T. Houghton et al., pp. 348– 416, Cambridge Univ. Press, Cambridge, U.K.
36. Elder, J.W., 1966: heat and mass transfer in the earth, hydrothermal system. *N.Z.D.S. I.R: Bull.*, 169, 115 pp.
37. Elder, J.W., 1981, *Geothermal systems*. Acad. Press, New York, N.Y., 632 pp.
38. Etiope, G., Klusman, R.W., 2002: Geologic emissions of methane to the atmosphere. *Chemosphere* 49, 777–789.
39. Etiope, G., Fridriksson, T., Italiano, F., Winiwarer, W., Theloke, J. 2007: Natural emissions of methane from geothermal and volcanic sources in Europe, *J. Volcanol. Geotherm. Res.*, 165, 76 – 86.
40. Etiope, G., Lassey, K.R., Klusman, R.W., Boschi, E. 2008: Reappraisal of the fossil methane budget and related emission from geologic sources, *Geophys. Res. Lett.*, 35, L09307.
41. Ettwig, K.F., Alen, T., Pas-Schoonen, K.T., Jetten, M.S.M. and Strous, M., 2009: Enrichment and molecular detection of denitrifying methanotrophic bacteria of the NC10 phylum. *Appl Environ Microbiol* 75: 3656-3662.
42. Favara, R., Giammanco, S., Inguaggiato, S., Pecoraino, G., 2001: Preliminary estimate of CO₂ output from Pantelleria island volcano (Sicily, Italy): evidence of active mantle degassing. *Appl. Geochem.* 16, 883–894.
43. Fedo, C.M., Nesbitt, H.W. and Young, G.M., 1995: Unraveling the effects of potassium metasomatism in sedimentary rocks and paleosols, with implications for paleoweathering conditions and provenance. *Geology* 23, 921-924.

44. Fehn, U., Cathles, L.M. and Holland, H.D., 1978: Hydrothermal convection and uranium deposits in abnormally radioactive plutons. *Econ. geol.*, 73: 1556 - 1566.
45. Fiebig, J., Chiadini, G., Caliro, S., Rizzo, A., Spangenberg, J., Hunziker, J.C., 2004: Chemical and isotopic equilibrium between CO₂ and CH₄ in fumarolic gas discharges: generation of CH₄ in arc magmatic-hydrothermal systems. *Geochim. Cosmochim. Acta* 68, 2321–2334.
46. Fiebig J., Tassi F., D'Alessandro W., Vaselli O., Woodland A.B., 2013: Carbon-bearing gas geothermometers for volcanic-hydrothermal systems. *Chemical Geology* 351, 66–75, doi:10.1016/j.chemgeo.2013.05.006.
47. Fiebig, J., Woodland, A.B., D'Alessandro, W., Püttmann, W. 2009: Excess methane in hydrothermal emissions is abiogenic, *Geology*, 37/6, 495–498.7.
48. Frazzetta, G., La Volpe, L., Sheridan, M.F., 1984. Evolution of the Fossa cone, Vulcano. *J. Volcanol. Geoth. Res.* 17, 139–360.
49. Francalanci L, Vougioukalakis GE, Perini G, Manetti P (2005) A west-east traverse along the magmatism of the south Aegean volcanic arc in the light of volcanological, chemical and isotope data. In: The south Aegean active volcanic arc (Fytikas M, Vougioukalakis GE, *Developments in Volcanology* 7, 65-111.
50. Fytikas M, Dalambakis P, Karkoulas V, Mendrinou D (1995) Geothermal exploration and development activities in Greece during 1990–1994. *Proceedings of the World Geothermal Congress 1995, Rome.*
51. Fulignati, P., Malfitano, G., and Sbrana, A., 1997: The Pantelleria Caldera Geothermal System Data from the Hydrothermal Minerals. *J. Volcanol. Geotherm. Res.*, 75, pp. 251 – 270.
52. Giannelli, G. and Grassi, S., 2001: Water rock interaction in the active geothermal system of Pantelleria, Italy. *Chemical Geology*, 181, 133 -130.
53. Giggenbach W.F. (1980) Geothermal gas equilibria. *Geochim. Cosmochim. Acta* 44, 2021-2032.
54. Giggenbach, W.F., Goguel, R.L., 1989: Collection and Analysis of Geothermal and Volcanic Water and Gas Discharges. Report of the Dep. of Sci. and Ind. Res., Chem. Div., Petone, New Zealand. 81 pp.
55. Glass JB, Yu H, Steele JA, Dawson KS, Sun S, Chourey K, Pan C, Hettich RL, Orphan VJ. 2013 Geochemical, metagenomic and metaproteomic insights into trace metal utilization by methane-oxidizing microbial consortia in sulfidic marine sediments. *Environ Microbiol.* Oct 22. doi: 10.1111/1462-2920.12314. [Epub ahead of print] PubMed PMID: 24148160.
56. Gunter, B.D., 1978: C₁ – C₄ hydrocarbons in hydrothermal gases. *Geochim. Cosmochim. Acta* 42, 137 – 139.
57. Hanson, R.S., Hanson, T.E. 1996: Methanotrophic bacteria, *Microbiol. Rev.*, 60, 439– 471.
58. Heiri, O., Lotter A. F. and Lemcke, G., 2001: Loss-on-ignition as a method for estimating organic and carbonate content in sediments: reproducibility and comparability of results. *Journal of Paleolimnology*, 25, 101-110 p.
59. Herzberg, G., 1945: Molecular spectra and molecular structure, 2, Infrared and Raman spectra of polyatomic molecules, Lancaster Press, New York.
60. Houweling, S. 1970: Global modeling of atmospheric methane sources and sinks.
61. Keller, J., 1980. The Island of Vulcano. In: Villari, L. (Ed.), *The Aeolian Islands, an Active Volcanic Arc in the Mediterranean Sea.* Società Italiana di Mineralogia e Petrologia, Milano, pp. 29–74.
62. Keller, J. 1982: Mediterranean island arcs. In: Thorpe, R.S. (ed.) *Andesites.* Wiley, New York, pp 307–325.
63. Kip N., C. Fritz C., Langelaan E.S., Pan Y., Bodrossy L., Pancotto V., Jetten M.S.M., Smolders A.J.P., and Op den Camp H.J.M., 2012: Methanotrophic activity and diversity in different *Sphagnum magellanicum* dominated habitats in the southernmost peat bogs of Patagonia, *Biogeosciences*, 9, 47-55.
64. Kolb S and Horn MA (2012) Microbial CH₄ and N₂O consumption in acidic wetlands. *Front. Microbio.* 3:78. doi: 10.3389/fmicb.2012.00078
65. Koschorreck, M., Conrad, R. 1993: Oxidation of atmospheric methane in soil: Measurements in the field, in soil cores, and in soil samples, *Glob. Biogeochem. Cycles*, 7, 109– 121.
66. Kvenvolden K.A., Rogers B.W., 2005: Gaia's breath—global methane exhalations, *Marine and Petroleum Geology*, 22, 579-590.
67. Intergovernmental Panel on Climate Change, 2001: Climate change 2001. In: Houghton, J.T., Ding, Y., Griggs, D.J., Noguer, M., van der Linden, P.J., Dai, X., Maskell, K., Johnson, C.A. (Eds.), *The Scientific Basis.* Cambridge University press, UK.

68. Islam T, Jensen S., Reigstad L.J., Larsen Ø. and Birkeland N.K., 2008: Methane oxidation at 55°C and pH 2 by a thermoacidophilic bacterium belonging to the *Verrucomicrobia* phylum, *Microbiology*, January 8, vol. 105, no. 1, 301
69. Lacroix, A.V., 1993. Unaccounted for sources of fossil and isotopically enriched methane and their contribution to the emissions inventory: a review and synthesis. *Chemosphere* 26, 507–558.
70. Larsen, G., Gronvols, K. and Thorarinsson, S., 1979: Volcanic eruption through a geothermal borehole at Namafjall, Iceland, *Nature*, 278: 707 - 710.
71. Lelieveld, J., P. J. Crutzen, and F. J. Dentener, 1998: Changing concentration, lifetime and climate forcing of atmospheric methane, *Tellus, Ser. B*, 50, 128–150.
72. Mahood, T.M., Shock, E.L., 1998: fluid-rock interactions in the lower oceanic crust: thermodynamic models of hydrothermal alteration, *J. Geophys. Res.* 103 – B1, 547 – 575.
73. Marini, L., Fiebig, J., 2005: Fluid geochemistry of the magmatic-hydrothermal system of Nisyros (Greece), *Mém. Géol.*, 44, 192.
74. Marini, L., Principe, C., Chiodini, G., Cioni, R., Frytikas, M., Marinelli, G. 1993: Hydrothermal eruptions of Nisyros (Dodecanese, Greece). Past events and present hazard. *J. Volcanol. Geotherm. Res.*, 56, 71–95.
75. McDonald, I.R., S. Radajewski, J.C. Murrell. 2005. Stable isotope probing of nucleic acids in methanotrophs and methylotrophs: A review. *Organic Geochemistry* Vol. 36. No. 5
76. McDonald, I.R., Bodrossy, L., Chen, Y., and Murrell, J.C., 2008: Molecular Ecology Techniques for the Study of Aerobic Methanotrophs, *applied and environmental microbiology*, Mar., p. 1305–1315 Vol. 74, No. 5 0099-2240/08/\$08.000 doi:10.1128/AEM.02233-07
77. Murrell C.J. and Jetten M.S.M, 2009: The microbial methane cycle, *Environmental Microbiology Reports* 1(5), 279–284.
78. Nesbitt, H.W. and Young, G.M. 1982: Early Proterozoic climates and plate motions inferred from major element chemistry of lutites. *Nature*, 199, 715-717.
79. Op den Camp H.J.M., Islam T., Stott M.B., Harhangi H.R., Hynes A., Schouten S., Jetten M.S.M., Birkeland N.K., Pol A., Dunfield P.F., 2009: Environmental, genomic and taxonomic perspectives on methanotrophic *Verrucomicrobia*, *Environmental Microbiology Reports*, 1(5), 293-306.
80. Papadopoulos, G.A., Sachpazi, M., Panopoulou, G., Stavrakakis, G. 1998: The volcanoseismic crisis of the 1996–97 in Nisyros, SE Aegean Sea, Greece, *Terra Nova*, 10, 151–154.
81. Parello F., Allard P., D'Alessandro W., Federico C., Jean-Baptiste P., Catani O., 2000: Isotope geochemistry of Pantelleria volcanic fluids, Sicily Channel rift: a mantle volatile end-member for volcanism in southern Europe, *Earth and Planetary Science Letters*, 180, 325-339.
82. Pe-Piper G, Hatzipanagiotou K (1997) The Pliocene volcanic rocks of Crommyonia, western Greece and their implications for the early evolution of the South Aegean arc. *Geological Magazine*, 134, 55–66.
83. Pol, A., Heijmans, K., Harhangi, H.R., Tedesco, D., Jetten, M.S.M., Op den Camp, H.J.M. 2007: Methanotrophy below pH 1 by a new *Verrucomicrobia* species, *Nature*, 450, 874-878.
84. Reeburgh, W.S., 2003: Global methane biogeochemistry. In: Holland, H.D., Turekian, K.K. (Eds.), *The Atmosphere Treatise on Geochemistry*, vol. 4. Elsevier, Oxford, UK, pp. 65–89.
85. Sambrook, J., Fritsch, E.F. and Maniatis, T.A., 1989: *Molecular Cloning: A Laboratory Manual*, 2nd edn. Cold Spring Harbor, USA: Cold Spring Harbor Laboratory Press.
86. Savage K., Moore T.R., Crill P.M., 1997: Methane and carbon dioxide exchanges between the atmosphere and northern boreal forest soils. *Journal of Geophysical Research*, 102, 29279 – 29288.
87. Sicardi, L., 1940. Il recente ciclo dell'attività fumarolica dell'isola di Vulcano. *Boll. Volcanol.* 7, 85–139
88. Silvestri, O., Mercalli, G., 1891. Modo di presentarsi e cronologia delle esplosioni eruttive di Vulcano cominciate il 3–8-1888. *Ann. R. Uff. Cent. Meteor. Geodin.* 4, 120–190.
89. Sommaruga, C., 1984. Le ricerche geotermiche svolte a Vulcano negli anni '50. *Rendiconti della Soc. It. Mineral. Petrol.* 39, 355–366.
90. Tassi F., Vaselli O., Papazachos C. B., Giannini L., Chiodini G., Vougioukalakis G. E., Karagianni E., Vamvakaris D., Panagiotopoulos D., 2013: Geochemical and isotopic changes in the fumarolic and submerged gas discharges during the 2011–2012 unrest at Santorini caldera (Greece), *Bull Volcanol* 75: 711. doi:10.1007/s00445-013-0711-8.
91. Tedesco, D., Sabroux, J.C., and Pece, R., 1987, Chemical and isotopic composition and calculated equilibrium temperatures of fumarolic gases and thermal waters from Campi

-
- Flegrei and Long Valley Caldera [abs]: International Union of Geodesy and Geophysics, General Assembly, Abstracts, v. 19, p. 426.
92. Trotsenko, Y.A., and Murrell, J.C., 2008: Metabolic aspects of aerobic obligate methanotrophy. *Adv Appl Microbiol* 63: 183-229.
 93. Tsubota, J., Eshinimaev, B. Ts., Khmelenina, V. N. & Trotsenko, Y. A., 2005: *Methylothermus thermalis* gen. nov., sp. nov., a novel moderately thermophilic obligate methanotroph from a hot spring in Japan. *Int J Syst Evol Microbiol* 55, 1877–1884.
 94. Van der Werf G.R., J.T. Randerson, G.J. Collatz, L. Giglio, P.S. Kasibhatla, A.F. Arellano, Jr., S.C. Olsen, and E.S. Kasischke, 2004: Continental-scale partitioning of fire emissions during the 1997 to 2001 El Nino/La Nina period. *Science*, 303, 73-74.
 95. Vorobev, A. V., Baani, M., Doronina, N. V., Brady, A. L., Liesack, W., Dunfield, P. F., and Dedysh, S. N., 2010: *Methyloferula stellata* gen. nov., sp. nov., an acidophilic, obligately methanotrophic bacterium possessing only a soluble methane monooxygenase, *Int. J. Syst. Evol. Micr.*, 61, 2456–2463, doi:10.1099/ijs.0.028118-0.
 96. Vougioukalakis, G.E., Fytikas, M., 2005: Volcanic hazards in the Aegean area, relative risk evaluation, monitoring and present state of the active volcanic centers. In: Fytikas, M., Vougioukalakis, G.E. (Eds.), *The South Aegean Active Volcanic Arc. Developments in Volcanology*, vol. 7, pp. 161–183.
 97. Whalen S.C., Reeburgh W.S., 1996: Moisture and temperature sensitivity of CH₄ oxidation in boreal soils. *Soil Biology & Biochemistry*, 28, 1271–1281
 98. Walter, B.P., M. Heimann, and E. Matthews, 2001: Modeling modern methane emissions from natural wetlands 2. Interannual variations 1982-1993. *J. Geophys. Res.*, 106(D24), 34207-34220.
 99. Welhan, J.A., 1988: Origins of methane in hydrothermal systems. In: *origins of methane in the Earth* (Schoell Ed.). *Chem. Geol.* 71, 183–198.
 100. White, W.M., 1997: *Geochemistry*, on-line textbook, by John-Hopkins University press.
 101. Whittenburg, R., Colby, J., Dalton, H. and Reed, H.L., 1975: The different types of methaneoxidizing bacteria and some of their more unusual properties.
 102. Schlegel, H.G., Gottschalk, G., and Pfenning, N. (eds). Göttingen: Akademie der Wissenschaften: 19.
 103. Yoshino K, Nishigaki K, Husimi Y., 1991: Temperature sweep gel electrophoresis: a simple method to detect point mutations. *Nucleic Acids Res* 19: 3153.

7. MATERIALS AND METHODS

7.1. SOIL AND GAS SAMPLING

All the soil samples used for geochemical and biological analysis were taken using a sterile hand shovel and stored in sterile bags. Aliquots of soils were used for all the geochemical and biological analyses.

Soil Gases were taken from 13, 20 and 50 cm of depth in the first campaign at Pantelleria, and at 25 cm of depth in the campaign at Nisyros through Teflon tube of 5 mm ID using a plastic a tight syringe to avoid air gases contamination (Fig. 7.1).



Fig. 7. 1- Soil gases sampling from the underground.

The overpressured vials were used for CH₄ and CO₂, N₂, O₂, H₂, He analysis by using a Perkin Elmer Clarus 500 GC equipped with Carboxen 1000 columns and Flame Ionisation detector. The gas samples were injected through an automated injection valve with a 1000 µL loop. Calibration was made with certified gas mixtures. Analytical precision ($\pm 1\sigma$) was always better than $\pm 3\%$. The detection limit was about 0.1 µmol mol⁻¹

Methane output measurements were sampled by accumulation chamber method (Livingston and Hutchinson, 1995; Baciu et al., 2008). The flux chamber is made of plastic material and has cross section area of 0.07 m² and height of 10 cm. The chamber top has two fixed capillary tubes (1 mm ID and 30 cm long); one is used to collect chamber air samples and the other is used to balance the pressure between the

inside and outside. A mixing device allows the mixing of the gas inside the chamber to increase the measurement accuracy. In the inside of the chamber rotating blades permit the mixing of the accumulated gas. Three gas samples were drawn from the headspace in the chamber at fixed intervals after the deployment (5, 10 and 20 min). The 20 mL samples are collected using a 60 mL plastic syringe at a rate of 10 mL min⁻¹. The entire 20 mL sample was injected through a three-way valve and a needle into a 10 mL pre-evacuated sampling vial (Exetainer®, Labco Ltd.). The overpressured vials were sent to the laboratory for CH₄ and CO₂ analysis as described above. The flux of CO₂ and CH₄ from the soil can be calculated as the rate of concentration increases in the chamber:

$$\Phi = \frac{\delta C}{\delta t} \times \frac{V}{A}$$

where Φ is the flux of a gas, V is the volume of air in the chamber (m³), A is the area covered by the chamber (m²), C is the chamber concentration of a gas and dC/dt is the rate of concentration change in the chamber air for each gas. Volumetric concentrations are converted to mass concentrations accounting for atmospheric pressure and temperature (Fig. 7.2).

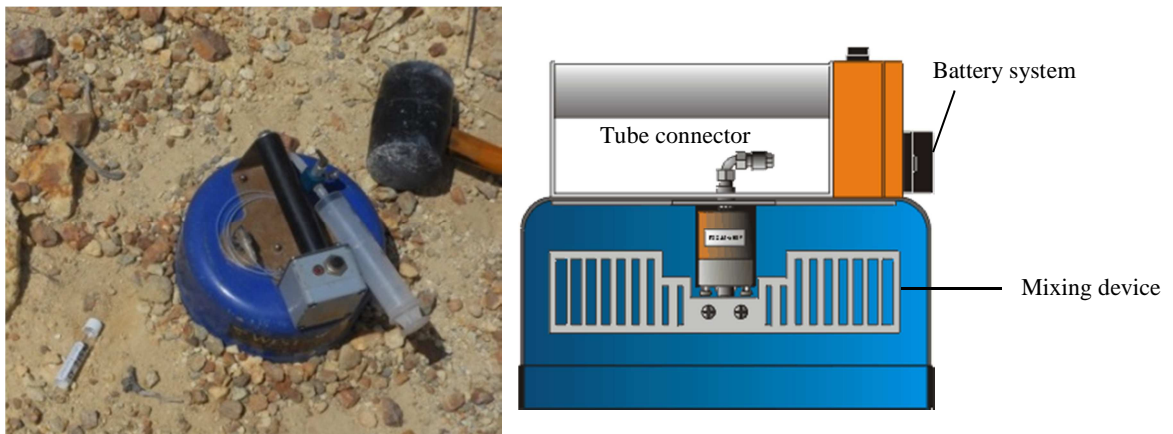


Fig. 7.2 - Accumulation chamber.

7.2. PHYSICAL-CHEMICAL SOIL CHARACTERIZATION

7.2.1. TEMPERATURE, PH, OM AND WATER CONTENT

Ground temperature measurements were made using thermal probes and a digital thermometer reading was taken 10–15 min after insertion of the thermal probe in the soil in order to achieve thermal equilibrium. Temperature value were used to create probability maps with the Inverse Distance Weight (IDW) method by using ArcMap 9.3.

Organic matter in soils was measured by loss-on-ignition analysis with heating stages of 105 °C for 4 h (for % of H₂O by mass), 400 °C for 16 h (for % organic matter by mass) (Heiri et al., 2001); NH₄⁺ was measured by spectrophotometer; soil pH was determined using a pH meter in a mixture of 1/2.5 of soil and distilled deionized water.

7.2.2. MAJOR ELEMENTS

Soil samples were used for XRF analyses, they were firstly air-dried, broken down aggregates and sieved at 2 mm. Each sieved sample was subdivided by quartering and an aliquots of the subsample ground into fine powder to yield an acceptable number of particles of each component of the heterogeneous material. To eliminate residual water, samples were placed in an oven at 110 °C for 24 h, then at 1000°C for 4 h and finally an aliquots were used to prepare powder pellets. Powder pellets were prepared by mixing soil sample with Mowiol and left 4 days until samples were completely dried. Finally, samples were manually pulverized, homogenized and pressed into pellet using boric acid as a binder.

7.2.3. ISOTOPES

Chromatographic capillary Colum Poraplot Q 25m 0.32mm i.d was used to separate and determine $\delta^{13}\text{C}$ (CH_4). Methane was oxidized to CO_2 passing through the oxidation tube at 940°C . Gas passed in the reaction tube (GC7TC) in which pyrolysis of methane with a temperature of 1450°C , during this step H_2 is formed and travelled in the spectrophotometer and the ratio D/H is measurable. Accuracy is ± 1 δ ‰ for $\delta^{13}\text{C}(\text{CH}_4)$.

7.2.4. METHANE OXIDATION POTENTIAL RATE

Methane oxidation potential of the soils was analyzed by transferring 15 gr of each air-dried soil sample in a 160-ml glass serum bottle; opened serum bottles were enriched in methane for 24 hours and at the end they were capped with a rubber stopper and sealed with aluminum crimps, after wetting with about 1 ml sterile distilled water. After sealing the bottle atmosphere was enriched in CH_4 to reach about $1000\text{-}2000\ \mu\text{mol mol}^{-1}$. Bottles were maintained at room temperature ($23\text{-}25^\circ\text{C}$) and the CH_4 concentration was measured at the beginning of the experiment and at about 24h intervals for 5 days. To better constrain the methane consumption in samples that after 24h consumed more than 30% of the initial CH_4 the experiments were repeated measuring the concentrations at about 2h interval. Samples collected in autumn from the FAV2 vertical profile were also incubated at 5, 37, 50 and 80°C . Finally, the variation of the soil CH_4 oxidation potential was analyzed on sample FAV2A with different starting CH_4 concentrations of (from about 100 to $85,000\ \mu\text{mol mol}^{-1}$). Methane concentration inside the vials was measured using CG as above. All the above incubation experiments were made in duplicate and the results expressed as average value in ng CH_4 per g of soil (dry weight) per h^{-1} .

7.2.5. GAS ANALYSES BY USING MICRO GAS CHROMATOGRAPHY

Soil gas samples from Nisyros were analyzed by using Micro Gas Chromatography. Micro GC analyses gas concentrations using small amount of sample volumes ($\times 10^{-6}$ cm³) and short analysis time (~160 s) (Kawamura Y. et al., 2001). Carrier gas used to sweep injected gas samples from the sample loop, through the gas chromatograph can operate for days on internal tanks supplied with each unit.

Module	Carrier gas	Analyze	Detector	Notes
MS	Argon	Hydrogen, Oxygene, Nitrogen, Methane, Carbon monoxide.	TCD	Optimize for low level of hydrogen (limit detection 1 ppm)
MS	Helium	Hydrogen, Oxigen, Nitrogen, Methane, Carbon monoxide	TCD	Optimize for carbon monoxide and for Hydrogen with concentration more than 350 ppm
PPU	Helium	Methane, carbon dioxide, ethylene, ethane, acetylene	TCD	C3 hydrocarbons and higher are removed by precolumn.

Table 7. 1 - Micro GC structure and functions MS = Molesieve columns; PPU = Porous Polymer column; TDC= thermal conductivity detector

Sample analyses were conducted with Micro GC MSHA CP-4900 with 3 independent modules. Each module is an independent GC complete with an inlet, pre-column and a detector. Two modules contain Molesieve (MS) columns while the third uses a Porous Polymer (PPU) column. Each module is controlled by the Varian Galaxie software; the injector uses a gas sample loop that is etched into a silicon wafer. The internal volume of the loop is 10 μ l, which permits using sample volumes of 1 to 10 μ l. Each module contains one main analytical capillary column (10 m) and one pre-column (2 m long), which is used to prevent contamination. The columns are placed in an oven at 108°C. Each module contains a dual channel thermal conductivity detector (TCD), with an internal sample volume of 200 nanoliters.

Micro GC is more advantageous than standard GC, because analyses are quicker and less amount of sample is used. Micro GC has a pre-column to prevent contamination, which after several measurement is inevitable as contaminants move from pre-column to the column and this could produce poor signal and irregular peaks in the chromatograms. Moreover, each module can detect methane, but not in concentration lower than 10 ppm. Where low methane value were measured, samples were measured again with standard GC (as above) to be have a best measures of the methane amount in the sample (Blashich et al., 2008)

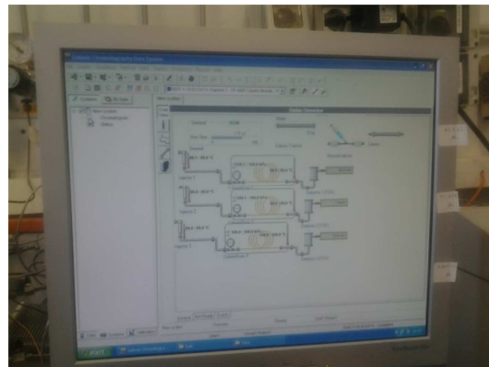
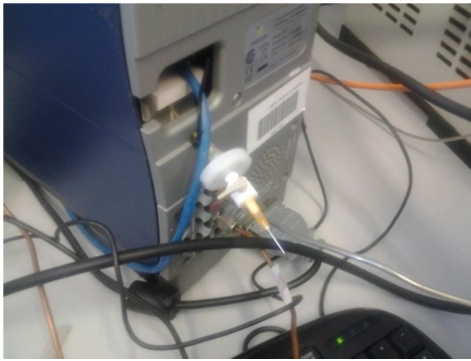


Fig. 7. 3- Micro GC.

7.3. DNA EXTRACTION METHODS

The extraction of total DNA from soil samples was performed using two different methods: the FastDNA Spin Kit for Soil (MP Biomedicals, Solon, OH, USA) and manual extraction by phenol-chloroform method.

FastDNA Spin Kit for soil: DNA was extracted from 0.5 gr of dried soil, following the manufacturer's protocol/instructions.

Phenol-chloroform method: A 0,5 gr of dried sample was added to 1.2 ml of SET buffer containing 10 mg/ml of lysozyme. Samples were incubated at 37°C for 30 min. 6 µl of proteinase K were added to each sample and the samples incubated at 37 °C for 25 min, vortexing every 5 min. this step was repeated twice. 120 µl of 10% SDS was added and samples incubated at 65°C for 45 min, inverting by hand every 5 min. Samples were centrifuged at 13000 rpm for 5 min and transferred to new collection tubes. 200 µl of K-acetate 5 M was added and samples were incubated in ice for 15 min; then centrifuged at 13000 rpm for 10 min and transferred to two new collection tube. To each sample, 1 volume of phenol-chloroform were added and mixed by vortex. Samples were centrifuged at 13000 rpm for 5 min and transferred to new collection tube. 100 µl of chloroform were added and centrifuged at 13000 for 1 min, sample was transferred to new collection tube. 1 volume of isopropanol 100% was added in each sample and incubation at room temperature follows for 1 h. samples were centrifuged for 20 min at 14000 rpm and surnatant discarded. Samples were resuspended in 20 µl of H₂O.

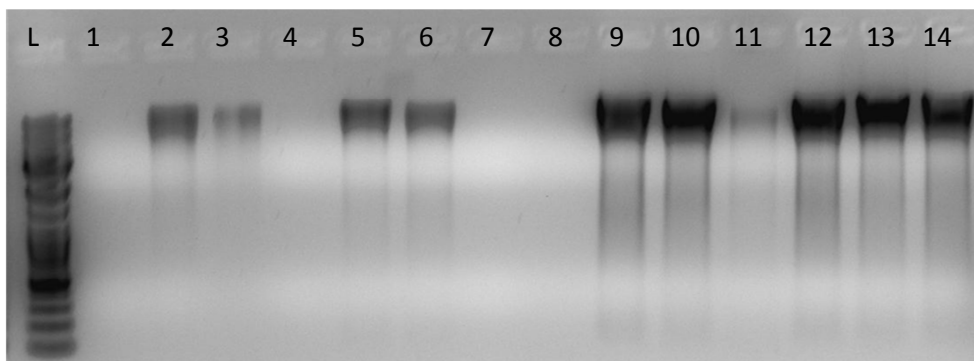


Fig. 7. 4 - Total DNA extracted from soil samples by using FastDNA Spin Kit for soil; 1. FAV1; 2. FAV2; 3. FAV1; 4. FAV2; 5. FAV3; 6. FAV3; 7. FAV4; 8. FAV5; 9. FAV6; 10. FAV7; 11. FAV8; 12. FAV9; 13. FAV9; 14. FAV10

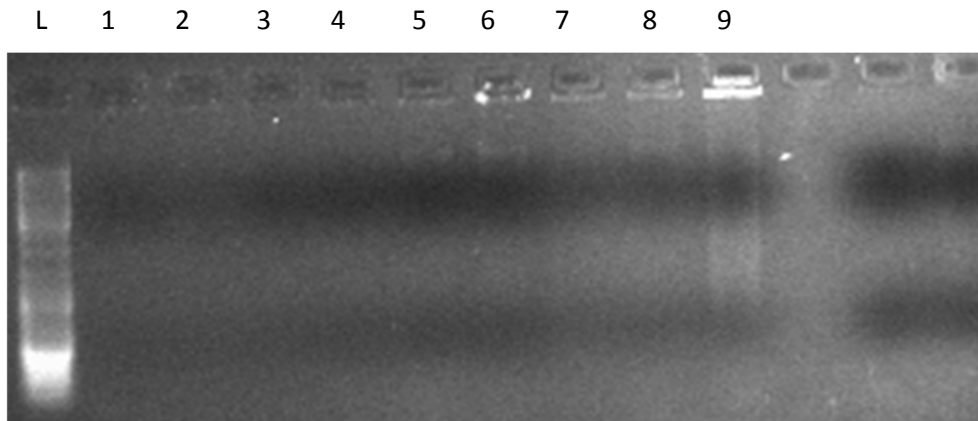


Fig. 7.5 - Total DNA extracted from soil samples by using phenol-chloroform method; 1. FAV1; 2. FAV1; 3. FAV1; 4. FAV2; 5. FAV2; 6. FAV2; 7. FAV3; 8. FAV3; 9. FAV3.

When necessary the extracted DNA was further purified using the QIAamp DNA Stool Mini Kit (QIAGEN, Germany), following the protocol from the DNA purification step and eluting in 30 μ l of DNA/RNA free water (GIBCO). The DNA quality and concentration was assessed by gel agarose (1%) electrophoresis and spectrophotometric analysis using Nanodrop. Fig. 7.4 and 7.5 show difference in DNA extraction with both protocols. Phenol-chloroform method is less expensive but it seems to be inadequate for geothermal soils. Efficiency and pureness of DNA extracted by FastDNA Spin Kit for soil guarantees the good quality of the DNA.

7.4. TEMPORAL GRADIENT GEL ELECTROPHORESIS

For TGGE (Temporal Gradient Gel Electrophoresis) analysis the hypervariable V3 region of the *16S* rRNA gene, about 200 bp long was used. V3 region was amplified by PCR and using the primer pair 341F-GC/534R (Table 2) and soil DNA as template. The PCR reaction mixture (50 μ l) contained 100 ng soil DNA, 1X PCR buffer, 0.2 mM dNTP, 10 mM of each primer and 1.5 μ l of Phire Hot Start II DNA Polymerase (Thermo Scientific). PCR was carried out with a Biometra Thermocycler using the following thermal cycling: initial denaturation at 98°C for 30 sec, followed by 35 cycles of 10 sec at 98°C, 10 sec at 72°C and final extension at 72°C for 1 min. PCR amplification products were visualized in a 1.5% agarose gel electrophoresis. For TTGE analysis 10 μ l of each PCR sample was mixed with an equal volume of loading buffer and loaded in a 8% (wt/vol) acrylamide gel (30 ml) containing 7 M

urea, 10% formamide in 1.5X Tris Acetate EDTA (TAE, 60 mM Tris-Acetate, 0.5 M Na₂ EDTA; pH 7.8). The gels were run in a DCode (Bio-Rad, Richmond, CA, USA) apparatus, at 70 V for 17 h, with a temperature ramping rate of 0.4°C/h with a starting temperature of 57°C. Gels were stained with SYBR Gold (Invitrogen) in 1X TAE for 45 min and visualized under a UV light using the ChemiDoc apparatus (BioRad).

Primer	sequence	Target gene	Reference or source
341F	5'-C CTACGGGAGGCAGCAG-3';	<i>16SrRNA</i>	Muyzer et al. 1993
534R	ATTACCGCGGCTGCTGG	<i>16SrRNA</i>	Muyzer et al. 1993
rD1	AAGGAGGTGATCCAGCC		Weisburg, et al, 1991
fD1	AGAGTTTGATCCTGGCTCAG		Weisburg, et al, 1991
A189F	GGNGACTGGGACTTCTGG	<i>pmoA (Proteobacteria)</i>	Holmes. et al.1995
A682R	GAASGCNGAGAAGAASGC	<i>pmoA(Proteobacteria)</i>	Holmes. et al.,1995
M13 F	GTAAAACGACGGCAG	TOPO-TA vector	Supplied by TOPO TA cloning kit
M13 R	CAGGAAACAGCTATGAC	TOPO-TA vector	Supplied by TOPO TA cloning kit
298f	CAGTGGATGAAYAGGTAYTGAA	<i>PmoA1-A2</i> (<i>Verrucomicrobia</i>)	This study
599r	ACCATGCGDTGTAYTCAGG	<i>PmoA1-A2</i> (<i>Verrucomicrobia</i>)	This study
156f	TGGATWGATTGGAAAGATCG	<i>PmoA3(Verrucomicrobia)</i>	This study
743r	TTCTTTACCCAACGRTTTCT	<i>PmoA3(Verrucomicrobia)</i>	This study

Table 7. 2- primer couples used for PCRs amplification.in this study.

Richness and diversity were determined by using the executable PAST version 2.17c (Hammer et al., 2001). Richness in the DNA soil samples is the simple account of the band obtained by TTGE; Diversity is the effective number of different species that are represented in the dataset (species), that in this case is the number of bands in TTGE. The effective number of species refers to the number of equally-abundant species needed to obtain the same mean proportional species abundance as that observed in the dataset of interest (where all species may not be equally abundant). A wide number of indices can be used to obtain an estimation of the diversity; the most common index is the Shannon Index (H), also knew as Shannon entropy. H is used to characterize species diversity in a community.

The proportion of species i relative to the total number of species (p_i) is calculated, and then multiplied by the natural logarithm of this proportion ($\ln p_i$). The resulting product is summed across species, and multiplied by -1.

$$H = - \sum_{i=1}^S P_i \ln p_i.$$

7.5. DETECTION OF METHANE OXIDATION GENES AND CONSTRUCTION OF A *pmoA* LIBRARY

The gene encoding the key methane oxidation enzyme pMMO was detected by amplification of metagenomic DNA extracted from soil samples using the primers A189f and A682r (table 2), targeting proteobacterial *pmoA* genes. PCR was carried out in a final volume of 50 μ l, containing 100 ng of total DNA, 10 mM solution of each oligonucleotide primer, 0.20 mM of dNTP, and 1 unit of recombinant Taq polymerase, (Invitrogen). PCR program consisted of an initial denaturation step at 98° C for 30 sec, followed by 35 cycles consisting of a denaturation step at 98 °C for 10 sec, 10 sec of annealing at 61 °C and 20 sec of extension at 72 °C.

7.6. CLONE LIBRARY CREATION

For the *pmoA* clone library, amplicons were purified using QIAquick spin columns (Qiagen, Germany) and cloned into PCRII TOPO TA (Invitrogen, USA) according to the manufacturer's instructions. The ligation mixture was used to transform One Shot TOP10 chemically competent cells. Plasmids were extracted by using GenElute Plasmid Miniprep Kit (Sigma-Aldrich, USA) and screened for the correct-size insert by PCR amplification using vector specific primers. Positive clones were sequenced using primer T7. Two novel prime couples, 298f/599r and 156f/743r (Table 7.2), targeting Verrucomicrobial *pmoA1/A2* and *pmoA3*, respectively, were designed and positively validated on *Methilacidiphilum fumarolucum* strain SoIV (kindly supplied by A. Pol). To detect Verrucomicrobial *pmoA* gene, touch-down PCR was carried out as described above with an initial denaturation at 94° C for 30 sec followed by 5

cycles consisting of denaturation of 10 sec at 94°C, annealing of 10 sec at 57°C and extension of 30 sec at 68°C; in the following 35 cycles the annealing temperature was of 52 °C for 10 sec and extension was carried out at 68°C for 30 sec. Amplicons were purified and cloned into PCR II TOPO TA (Invitrogen, USA) as described above.

7.7. ISOLATION OF METHANOTROPHIC BACTERIA

In order to enrich for methanotrophic bacteria, 15 gr of soil were placed in 125-ml sealed serum bottles; methane was added to reach an atmosphere composed in 25% of methane and incubated at 37° and 65°C for 2 weeks. Two g of enriched soil crumbles were transferred to 125-ml serum bottles containing 20 ml of low salt mineral medium M3 adjusted to pH 6 under the same conditions (Islam et al, 2008). After 2 weeks incubation at 37° and 65°C, respectively, aliquots of M3 enrichment cultures were inoculated on M3 agar-slants in 125-ml sealed serum bottles under methane enriched atmosphere and incubated as described above for 2 weeks. As soon as colonies appeared, they were transferred to obtain pure cultures that were checked for methane consumption by GC analysis as described above. Growth on alternative C sources was assessed by streaking each isolate on M3 agar plates containing methanol (0.5 %), glucose (1%), fructose (1%) and ethanol (1%), respectively, and in the absence of any other C source and incubating at 37°C. The isolates were also incubated in M3 agar in a CH₄ atmosphere at different temperatures. Each isolate was routinely grown in M3-agar slants in 120 ml serum bottle, in an atmosphere enriched in methane (25%) added every week and transferred to fresh medium every three weeks. Genomic DNA was extracted from 10 ml M3-CH₄ broth culture of each isolate grown in the conditions described above by the method described by Sambrook et al. (1989) and used as template for the amplification of the *16S* rRNA gene with universal primers (Table 7.2) and *pmoA* gene as described above. A growth curve of Pant1 was obtained by inoculating a single colony in to a 125- ml serum bottle containing 10 ml of M3 mineral medium and 10 ml of CH₄ were added in the sealed serum bottle. The culture was incubated for 10 days at 37 °C and subsequently split in five 200- ml serum bottles (2 ml each) containing 30 ml of M3 mineral

medium and 25% methane; growth was monitored as turbidity using a spectrophotometer at a wavelength of 600nm (OD_{600}). Methane concentration was measured every 12 h in parallel cultures and in uninoculated control bottles incubated under the same conditions (Fig. 7.6).

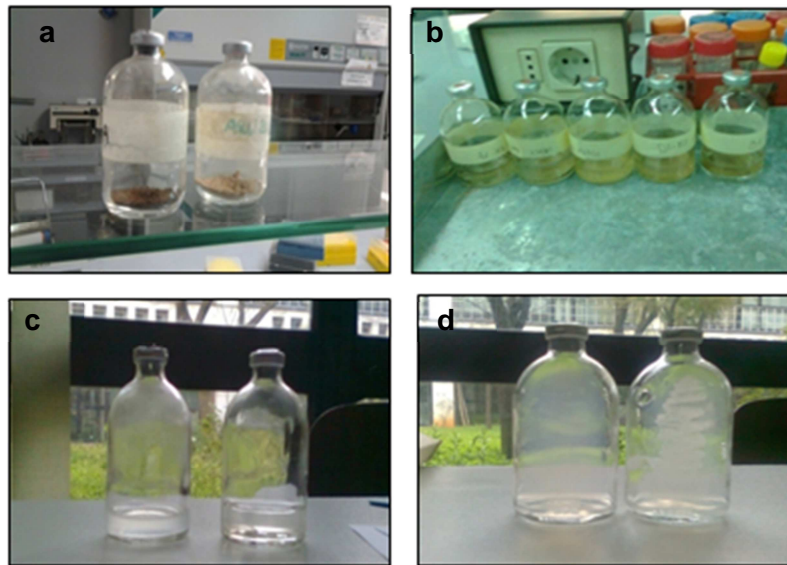


Fig. 7. 6- Isolation of methanotrophic bacteria. **a.** enrichment in methane. **b** and **c.** Enrichment cultures in M3 broth with CH_4 (25%) as sole C sources. **c.** isolate FAV2B1 in M3 agar with 25% of CH_4 (right) and negative control (left).

7.8. PRINCIPAL COMPONENTS ANALYSIS (PCA)

Principal components analysis (PCA) is a procedure for finding hypothetical variables (components) which account for as much of the variance in your multidimensional data as possible (Davis 1986, Harper 1999). PCA were applied by using the executable past. These new variables are linear combinations of the original variables. PCA has several applications, two of them are:

- Simple reduction of the data set to only two variables (the two most important components), for plotting and clustering purposes.
- More interestingly, you might try to hypothesize that the most important components are correlated with some other underlying variables.

The PCA routine finds the eigenvalues and eigenvectors of the variance-covariance matrix or the correlation matrix. Choose var-covar if all your variables are measured in the same units (e.g. centimeters). Choose correlation (normalized var-covar) if your variables are measured in different units; this implies normalizing all variables using division by their standard deviations. The eigenvalues, giving a measure of the variance accounted for by the corresponding eigenvectors (components) are given for all components. The percentages of variance accounted for by these components are also given. If most of the variance is accounted for by the first one or two components, you have scored a success, but if the variance is spread more or less evenly among the components, the PCA has in a sense not been very successful. The Jolliffe cut-off value gives an informal indication of how many principal components should be considered significant (Jolliffe, 1986). Components with eigenvalues smaller than the Jolliffe cut-off may be considered insignificant, but too much weight should not be put on this criterion. Row-wise bootstrapping is carried out if a non-zero number of bootstrap replicates (e.g. 1000) is given in the 'Boot N' box. The bootstrapped components are re-ordered and reversed according to Peres-Neto et al. (2003) to ensure correspondence with the original axes. 95% bootstrapped confidence intervals are given for the eigenvalues. The 'Scree plot' (simple plot of eigenvalues) can also be used to indicate the number of significant components. After this curve starts to flatten out, the corresponding components may be regarded as insignificant. 95% confidence intervals are shown if bootstrapping has been carried out. The eigenvalues expected under a random model (Broken Stick) are optionally plotted - eigenvalues under this curve represent non-significant components (Jackson 1993, <http://folk.uio.no/ohammer/past/multivar.html>).

7.9. REFERENCES

1. Baciú, C., Etiope, G., Cuna, S., Spulber, L. 2008: Methane seepage in an urban development area (Bacău, Romania): origin, extent, and hazard, *Geofluids*, 8, 311–320.
2. Blashich B.K Francart, W.J. Calhoun M.D, Use of automated micro gas chromatograph to monitor mine atmospheres during mine emergencies, 2008: 12th U.S./North American Mine Ventilation Symposium – Wallace (ed) ISBN 978-0-615-20009-5.
3. Davis, J.C. 1986. *Statistics and Data Analysis in Geology*. John Wiley & Sons
4. Livingston, G.P., Hutchinson, G.L. 1995: Enclosure-based measurement of trace gas exchange: applications and sources of error. In: *Biogenic Trace Gases: Measuring Emissions from Soil and Water*. Methods in Ecology (Matson, P.A. and Harriss, R.C. eds.), pp. 14–51. Blackwell Science Cambridge University Press, London.
5. Hammer, O., Harper, D.A.T and Ryan, P.D., 2001: PAST: Paleontological Statistics software package for education and data analysis. *Paleontologia Electronica* 4(1); 9 pp;
6. Holmes A.J., Costello A., Lidstrom M.E., Murrell J.C., October 1995: Evidence that particpate methane monooxygenase and ammonia monooxygenase may be evolutionarily related, *FEMS Microbiology Letters* Volume 132, Issue 3, pages 203–208.
7. Jackson, D.A. 1993. Stopping rules in principal components analysis: a comparison of heuristical and statistical approaches. *Ecology* 74:2204-2214.
8. Jolliffe, I.T. 1986. *Principal Component Analysis*. Springer-Verlag.
9. Peres-Neto, P.R., D.A. Jackson & K.M. Somers. 2003. Giving meaningful interpretation to ordination axes: assessing loading significance in principal component analysis. *Ecology* 84:2347-2363.
10. Weisburg WG, Barns SM, Pelletier DA, Lane DJ, 1991: *16S* ribosomal DNA amplification for phylogenetic study. *J Bacteriol*, 173:697–703.

8. APPENDIX I

8.1. NISYROS SOIL GASES COMPOSITON

Crater	Sample	T ₂₀ ^a	T ₅₀ ^b	He	H ₂	CH ₄	O ₂	N ₂	H ₂ S	CO ₂
		°C								
Micro Polobotes	N304	66.2	98.3	16.6	13518.7	2121.9	3.4	19.6	10.0	62.7
	N305	100	100	16.8	11576.2	2095.5	3.3	16.0	12.6	63.9
	N306	45	88.3	21.0	11042.7	2657.1	2.5	13.2	11.0	67.1
	N307	53.5	97.9	19.2	13423.3	2600.4	0.8	3.7	16.8	74.7
	N308	61.1	98.9	20.0	16036.3	2520.2	0.3	2.8	16.5	74.9
Lofos	036 A	n.d	n.d	7.8	56.3	396.4	16.6	72.2	0	9.2
	037 A	n.d	n.d	6.8	18.7	106.6	18.7	74.9	0	5.8
	212 A	n.d	n.d	6.8	8.5	2.5	19.6	74.8	0	3.3
	N313	36.7	35.1	4.9	13.8	5.2	20.5	76.8	0	0.9
	N314	33.6	37.2	6.3	39.2	0	20.0	77.1	0	2.06
	N315	38.9	46.7	6.8	12.1	6.3	17.7	75.8	0	6.1
	N316	44.4	59.5	6.3	26.1	10.1	15.8	73.7	0	10.2
	N317	54	82.8	7.8	5655.5	601.2	15.3	71.5	0.02	12.6
	N318	51.5	82	10.7	1472.5	1000.5	15.8	67.7	0.6	15.6
	N319	45.9	79.2	9.7	2771.7	443.6	15.1	74.1	0.00	10.5
	N320	43	65.8	10.5	7065.0	1343.1	13.0	65.2	1.1	20.4
	N321	58.3	0	7.8	356.4	252.0	18.2	75.0	0.00	6.3
	N322	69.8	99	20.4	8157.7	5233.9	2.2	9.8	16.7	69.0
	N323	53	99	17.6	5282.0	4634.5	4.2	22.3	11.3	59.4
	N324	48	79.2	55	14900	6694	2.45	20.2	-	75
	N325	56.4	99	7.0	1173.4	850.4	16.3	70	0.1	13.1
N326	36.7	35.1	11.5	3231.2	1684.8	13.9	62.6	1.6	21.9	
Phlegeton	023 A	n.d	n.d	15.8	5034.1	924.1	8.3	33.8	10.3	47.4
	024 A	n.d	n.d	19.4	929.9	1544.2	0.3	2.7	17.8	75.3
	025 A	n.d	n.d	18.7	1235.7	1319.6	3.6	15.9	14.9	64.3
	026 A	n.d	n.d	13.7	2060.4	830.6	8.1	38.5	7.6	45.2
	027 A	n.d	n.d	15.5	1831.4	1075.1	4.7	30.2	10.2	53.8
	028 A	n.d	n.d	12.1	3821.4	675.8	11.0	45.2	6.8	35.7
	030 A	n.d	n.d	21.3	813.1	1535.7	0.3	2.6	17.8	75.2
	031 A	n.d	n.d	14.2	4108.5	731.5	10.1	42.4	7.0	38.5
	032 A	n.d	n.d	15.2	7056.7	708.9	9.6	46.5	5.7	36.1
	033 A	n.d	n.d	22.9	7520.7	1015.0	6.6	28.8	10.1	56.1
Kaminakia	040 A	n.d	n.d	7.1	10.4	3.8	18.0	71.5	0.0	9.0
	041 A	n.d	n.d	7.9	290.7	4782.7	14.4	57.9	0.7	26.3
	042 A	n.d	n.d	5.5	24.0	2447.5	17.7	67.6	0.2	13.2
	043 A	n.d	n.d	6.3	17.8	19.0	16.3	69.1	0.0	13.5
	044 A	n.d	n.d	5.0	2.7	5.0	20.2	76.2	0.0	1.6
	045 A	n.d	n.d	6.8	2637.8	1380.9	15.9	70.2	0.0	13.1
	046 A	n.d	n.d	6.3	15.6	2.0	19.2	74.6	0.0	4.9
	047 A	n.d	n.d	6.6	8.0	4.7	18.5	72.8	0.0	7.7
	048 A	n.d	n.d	7.9	363.3	1119.5	18.7	72.9	0.0	8.4
	049 A	n.d	n.d	0.8	2615.2	4886.6	7.5	60.8	0.0	30.7
	050 A	n.d	n.d	8.9	664.8	9039.7	10.2	42.5	2.2	43.7
	051 A	n.d	n.d	6.8	192.8	2155.9	12.9	59.4	0.0	27.2
	052 A	n.d	n.d	7.9	780.0	4889.4	14.8	59.7	0.6	24.5
	053 A	n.d	n.d	6.6	523.3	2522.1	11.5	62.7	0.0	25.2
	186 A	n.d	n.d	6.8	56.0	3041.2	13.7	59.9	0.1	25.2
	189 A	n.d	n.d	6.8	26.4	15.0	19.1	74.5	0.0	5.3
	N301	27.3	29	5.3	4.9	2.1	21.0	78.0	0.0	0.4
	N302	30.5	33.4	6.0	3.8	4.6	20.8	77.6	0.0	0.9
	N303	30.5	33.6	6.6	8.5	4.2	20.5	76.7	0.0	1.6

Crater	Sample	T ₂₀ ^a	T ₅₀ ^b	He	H ₂	CH ₄	O ₂	N ₂	H ₂ S	CO ₂
	N309	32.2	46.9	6.8	103.4	766.4	14.4	63.8	0.0	21.2
	N310	31.1	34.1	6.8	38.0	18.0	14.5	64.2	0.1	20.3
	N311	30.9	35.5	5.5	9.0	14.7	18.2	73.0	0.0	8.1
	N312	34.9	38.6	6.8	46.4	62.8	12.7	60.7	0.0	26.1
	N327	59.5	96.4	26.0	6850.4	12603	2.8	14.8	8.7	69.2
	N328	28.3	42	6.0	81.9	1558.4	16.6	67.2	0.0	15.9
	N329	59.4	99.2	10.8	4.7	4.8	20.9	77.8	0.0	0.4
	N330	30.2	37.9	6.3	7.7	6.6	20.0	75.8	0.0	3.3
	N331	31.8	44.1	6.3	4.7	4.5	20.7	77.3	0.0	0.7
	N332	30	34.2	6.3	5.0	5.7	20.9	77.5	0.0	0.5
	N333	29	36.4	5.5	8.8	5.4	17.0	69.5	0.0	12.8
	N334	32.9	43.8	6.6	6.5	4.2	19.9	75.2	0.0	3.5
	N335	27.8	30.8	5.3	3.9	4.6	18.9	74.0	0.0	6.3
	N336	33.5	40.3	6.3	4.6	5.2	20.9	77.4	0.0	0.3
	N337	25.5	31.5	5.3	24.0	14.2	18.0	73.1	0.0	8.7
	N338	32	39	6.3	6.6	4.6	18.3	72.7	0.0	7.7
	N339	33.9	37	5.5	3.6	3.5	17.0	70.9	0.0	12.4
	N340	32.3	37.2	5.8	9.9	4.7	16.1	69.3	0.0	14.5
	N341	31.9	39	4.5	41.5	4.8	19.0	73.9	0.0	6.8
	N342	31.9	37	5.3	34.4	4.4	19.3	74.0	0.0	6.2
	N343	34.2	36.3	6.6	21.5	0.0	18.8	73.9	0.1	6.8
	239A	n.d	n.d	6.8	1043.4	232.2	20.2	75.8	0.2	2.8
	240 A	n.d	n.d	6.6	454.1	53.8	20.0	76.7	0.0	1.8
	240A	n.d	n.d	16.8	14781.1	4089.9	7.2	32.7	9.0	49.4
	241A	n.d	n.d	23.9	3142.4	6810.2	1.4	6.7	17.1	72.0
	242A	n.d	n.d	6.6	1360.1	289.0	16.1	75.2	0.1	7.3
	243A	n.d	n.d	6.8	51.1	12.0	18.2	76.9	0.0	3.7
	244 A	n.d	n.d	6.0	505.9	525.8	15.4	70.6	0.0	13.8
	246A	n.d	n.d	9.7	294.9	755.1	14.7	67.8	0.1	16.6
	247A	n.d	n.d	5.8	25.4	8.0	16.5	72.8	0.0	9.5
	248 A	n.d	n.d	65.1	1430.6	1587.6	14.2	62.7	1.7	20.2
Stephanos	250 A	n.d	n.d	7.6	2276.7	161.4	18.8	72.8	0.5	7.1
	251 A	n.d	n.d	6.3	70.5	4.6	18.2	71.3	0.0	9.5
	252 A	n.d	n.d	6.8	137.3	356.8	16.5	71.8	0.0	11.2
	253 A	n.d	n.d	7.1	126.7	155.7	18.6	77.1	0.0	4.2
	254 A	n.d	n.d	18.9	6390.4	5769.1	4.3	18.7	13.8	61.7
	255 A	n.d	n.d	21.8	5233.3	6988.6	2.0	10.1	15.0	68.7
	256 A	n.d	n.d	6.8	602.6	527.6	18.9	72.6	0.1	6.5
	257 A	n.d	n.d	9.5	17189.9	2562.7	10.6	55.4	1.8	29.1
	258 A	n.d	n.d	11.3	6770.9	2620.3	12.9	49.5	6.9	31.2
	259 A	n.d	n.d	12.6	2297.3	2221.0	12.1	47.4	6.9	32.8
	260 A	n.d	n.d	11.3	1875.8	2115.3	11.6	53.8	4.5	29.8
	N344	42.8	71.5	6.8	590.3	1628.2	7.6	66.3	0.0	26.4
	N345	51.3	80	8.1	63.4	769.3	16.4	71.4	0.0	12.1
	N346	56.8	94.8	8.4	3920.4	4812.9	6.7	52.1	0.3	39.6
	N347	42.9	65.2	7.9	30.1	540.9	13.7	69.6	0.0	17.2
	N348	56.9	90.4	8.7	1477.6	2792.1	12.3	59.3	0.7	27.3
Ramos	N349	43.4	55.9	6.3	13.6	94.4	18.4	73.1	0.0	8.1
	N350	58.1	85.4	8.9	965.7	2687.3	13.9	64.8	0.0	20.9
	N351	62.8	94	8.4	4898.0	6863.1	10.4	49.6	1.8	36.6
	N352	51.7	59	22.1	13335.2	19142.3	1.2	10.1	7.2	74.5
	N353	51.8	79.9	7.9	86.2	939.2	18.7	74.0	0.0	6.6

Table 8. 1 - Physical conditions and soil gases composition of the samples from Nisyros Island. a. Tempereure measured at 20 cm of depth; b. temperature measured at 50 cm of depth.

8.2. NISYROS METHANE FLUX

Name	X UTM	Y UTM	CH ₄ flux mg m ² day	Ref.
NSR1	515021	4047221	238.0	D'Alessandro et al., 2013
NSR2	515065	4047167	1062.5	D'Alessandro et al., 2013
NSR3	515014	4047051	76.5	D'Alessandro et al., 2013
NSR4	514946	4047060	238.0	D'Alessandro et al., 2013
NSR5	514966	4047167	3.4	D'Alessandro et al., 2013
NSR6	514907	4047243	663.0	D'Alessandro et al., 2013
NSR7	514871	4047306	-3.4	D'Alessandro et al., 2013
NSR8	514472	4047121	127.5	D'Alessandro et al., 2013
NSR9	514479	4047093	314.5	D'Alessandro et al., 2013
NSR10	514494	4047059	51.0	D'Alessandro et al., 2013
NSR11	514534	4047047	110.5	D'Alessandro et al., 2013
NSR12	514371	4047194	2.6	D'Alessandro et al., 2013
NSR13	514295	4047308	-0.9	D'Alessandro et al., 2013
NSR14	514233	4047380	-0.9	D'Alessandro et al., 2013
NSR15	514153	4047215	0.0	D'Alessandro et al., 2013
NSR16	514219	4046989	0.9	D'Alessandro et al., 2013
NSR17	514169	4046795	0.9	D'Alessandro et al., 2013
NSR18	514353	4046983	2.6	D'Alessandro et al., 2013
NSR19	514502	4047137	1.7	D'Alessandro et al., 2013
NSR20	514527	4047111	68.0	D'Alessandro et al., 2013
NSR21	514551	4047097	6.0	D'Alessandro et al., 2013
NSR22	514544	4047134	85.0	D'Alessandro et al., 2013
NSR23	514537	4047192	34.0	D'Alessandro et al., 2013
NSR24	514549	4047179	2.6	D'Alessandro et al., 2013
NSR25	514571	4047170	1.7	D'Alessandro et al., 2013
NSR26	514594	4047165	714.0	D'Alessandro et al., 2013
NSR27	514611	4047141	5.1	D'Alessandro et al., 2013
NSR28	514624	4047151	68.0	D'Alessandro et al., 2013
NSR29	514636	4047176	6.7	D'Alessandro et al., 2013
NSR30	514654	4047155	20.0	D'Alessandro et al., 2013
NSR31	514650	4047176	31.7	D'Alessandro et al., 2013
NSR32	514613	4047209	0.3	D'Alessandro et al., 2013
NSR33	514635	4047233	119.0	D'Alessandro et al., 2013
NSR34	514599	4047233	8.5	D'Alessandro et al., 2013
NSR35	514573	4047231	5.1	D'Alessandro et al., 2013
N1	514971	4047271	2.6	D'Alessandro et al., 2013
N2	514988	4047244	0.9	D'Alessandro et al., 2013
N3	515012	4047226	5.1	D'Alessandro et al., 2013
N4	515029	4047205	6.8	D'Alessandro et al., 2013
N5	515046	4047191	1045.5	D'Alessandro et al., 2013
N6	515068	4047174	297.5	D'Alessandro et al., 2013
N7	515059	4047143	76.5	D'Alessandro et al., 2013
N8	515052	4047120	20.4	D'Alessandro et al., 2013
N9	515037	4047084	59.5	D'Alessandro et al., 2013
N10	515043	4047061	1419.5	D'Alessandro et al., 2013
N11	515027	4047058	654.5	D'Alessandro et al., 2013
N12	515010	4047051	1419.5	D'Alessandro et al., 2013
N13	514995	4047047	127.5	D'Alessandro et al., 2013
N14	514965	4047050	8.5	D'Alessandro et al., 2013
N15	514942	4047060	170.0	D'Alessandro et al., 2013
N16	514932	4047082	178.5	D'Alessandro et al., 2013
N17	514929	4047111	238.0	D'Alessandro et al., 2013

Name	X UTM	Y UTM	CH ₄ flux mg m ² day	Ref.
N18	514925	4047138	161.5	D'Alessandro et al., 2013
N19	514219	4047572	1.7	D'Alessandro et al., 2013
N20	514206	4047584	1.7	D'Alessandro et al., 2013
N21	514199	4047572	13.6	D'Alessandro et al., 2013
N22	514177	4047590	6.8	D'Alessandro et al., 2013
N23	514188	4047586	7.7	D'Alessandro et al., 2013
N24	514183	4047571	18.7	D'Alessandro et al., 2013
N25	514175	4047566	28.1	D'Alessandro et al., 2013
N26	514165	4047573	25.5	D'Alessandro et al., 2013
N27	514155	4047570	11.9	D'Alessandro et al., 2013
N28	514157	4047552	2.6	D'Alessandro et al., 2013
N29	514148	4047551	0.9	D'Alessandro et al., 2013
N30	514134	4047552	0.0	D'Alessandro et al., 2013
N31	514724	4047872	5.1	D'Alessandro et al., 2013
N32	514723	4047809	-0.9	D'Alessandro et al., 2013
N33	514717	4047770	1.7	D'Alessandro et al., 2013
N34	514690	4047753	19.5	D'Alessandro et al., 2013
N35	514674	4047717	93.5	D'Alessandro et al., 2013
N36	514661	4047692	40.4	D'Alessandro et al., 2013
N37	514637	4047679	102.0	D'Alessandro et al., 2013
N38	514901	4047159	42.5	D'Alessandro et al., 2013
N39	514908	4047180	19.1	D'Alessandro et al., 2013
N40	514900	4047202	204.0	D'Alessandro et al., 2013
N41	514958	4047183	-0.9	D'Alessandro et al., 2013
N42	514976	4047159	0.9	D'Alessandro et al., 2013
N301A	515310	4048583	0.04	This Study
N302A	515384	4048514	-1.83	This Study
N303A	515479	4048463	0.91	This Study
N304A	514864	4048679	32.83	This Study
N305A	514856	4048673	30.63	This Study
N306A	514842	4048676	5.13	This Study
N307A	514848	4048677	-2.38	This Study
N308A	514851	4048680	18.65	This Study
N309A	515695	4048364	247.15	This Study
N310A	515688	4048334	-2.86	This Study
N311A	515663	4048292	19.17	This Study
N312A	515658	4048288	76.24	This Study
N313A	515227	4048688	8.72	This Study
N314A	515207	4048667	4.09	This Study
N315A	515190	4048650	17.22	This Study
N316A	515173	4048628	4.82	This Study
N317A	515153	4048604	14.32	This Study
N318A	515134	4048595	66.81	This Study
N319A	515109	4048583	-1.48	This Study
N320A	515095	4048585	10.3	This Study
N321A	515092	4048601	0.38	This Study
N322A	515105	4048624	13.13	This Study
N323A	515126	4048638	2.33	This Study
N324A	515139	4048658	1.99	This Study
N325A	515162	4048676	148.23	This Study
N326A	515174	4048697	77.9	This Study
N327A	515621	4048254	0.08	This Study
N328A	515640	4048269	930.57	This Study
N329A	515573	4048248	-0.47	This Study

Name	X UTM	Y UTM	CH ₄ flux mg m ² day	Ref.
N330A	515590	4048259	-1.86	This Study
N331A	515526	4048255	-4.33	This Study
N332A	515484	4048245	0.62	This Study
N333A	515517	4048143	-3.55	This Study
N334A	515452	4048158	-1.67	This Study
N335A	515486	4048116	3.09	This Study
N336A	515510	4048081	1.47	This Study
N337A	515504	4048034	126.21	This Study
N338A	515473	4048051	2.18	This Study
N339A	515476	4048008	-2.13	This Study
N340A	515442	4048027	-0.4	This Study
N341A	515444	4048067	-1.27	This Study
N342A	515431	4048111	-0.07	This Study
N343A	515418	4048135	-3.08	This Study
N344A	514870	4047612	4.31	This Study
N345A	514849	4047608	12.58	This Study
N346A	514830	4047587	3.18	This Study
N347A	514847	4047594	-4.1	This Study
N348A	514857	4047579	374.15	This Study
N349A	514866	4047588	3.48	This Study
N350A	514841	4047574	570.12	This Study
N351A	514849	4047568	-33.52	This Study
N352A	514868	4047562	123.55	This Study
N353A	514881	4047577	25.17	This Study

Table 8. 2 – methane flux measured using the accumulation chamber.

9. APPENDIX II

D'Alessandro W., Gagliano A.L., Kyriakopoulos K., and Parello F., Hydrothermal methane fluxes from the soil at lakki plain (nisyros, greece), *Bulletin of the Geological Society of Greece*, vol. XLVII 2013

Gagliano A.L., D'Alessandro W., Tagliavia M., Parello F. e Quatrini P., Methanotrophic activity and diversity of methanotrophs in a volcanic-geothermal soil, in preparation.

Boatta F., D'Alessandro W., Gagliano A.L., Liotta M., Milazzo M., Rodolfo-Metalpa R., Hall-Spencer J.M., Parello F. (2013), Geochemical survey of Levante Bay, Vulcano Island (Italy), a natural laboratory for the study of ocean acidification. *Marine Pollution Bulletin*, DOI:10.1016/j.marpolbul.2013.01.029

Communication at congress:

Gagliano A.L., Tagliavia M., D'Alessandro W., Parello F. e Quatrini P., "Greenhouse gas as a nutrient: methanotrophic activity in soils of hydrothermal systems Environmental"; - *Microbiology and Biotechnology - EMB2012*, Bologna, April 10-12 2012. *Environmental Engineering and Management Journal* March 2012 Vol.11 No. 3 Supplement ISSN 1843-3707 S147;

Gagliano A.L., D'Alessandro W., Parello F., Quatrini P. "Microbiological evidences of methanotrophic activity in the soils of the geothermal area of Pantelleria island (Italy)", 9th ISEG - International Symposium on Environmental Geochemistry, Aveiro Portugal, 15-22 July 2012.

Quatrini P., Gagliano A.L., D'Alessandro W., Monaghan D., Tagliavia M., Parello F., "Exploring methanotrophic activity in geothermal soils from Pantelleria Island (Italy)", 12th FISV congress, Rome, Italy, September 24-27, 2012.

D'Alessandro W., Gagliano A.L., Quatrini P., Parello F., The importance of methanotrophic activity in geothermal soils of Pantelleria island (Italy), *Geophysical Research Abstracts* Vol. 15, EGU2013-4530-1, 2013, EGU General Assembly 2013.

Gagliano A.L., D'Alessandro W., Parello F., Quatrini P, Methane efflux from the soil and methanotrophic activity in volcanic-geothermal areas: Examples from Italy and Greece, IAVCEI (International Association of Volcanology and Chemistry of the Earth's Interior) 2013, Kagoshima, Japan, July 20 – 24, 2013, (Oral presentation).

Gagliano A.L., D'Alessandro W., Quatrini P, Parello F., Investigation of the methanotrophic activity in the soils of a geothermal site of Pantelleria Island (Italy), *Goldschmidt 2013*, Firenze, Italia, August 25 – 30, 2013.

D'Alessandro W., Gagliano A.L., Parello F., Quatrini P., The impact of methanotrophic activity on methane emissions through the soils of geothermal areas,

ICGG12 - International Conference on Gas Geochemistry 2013, Patras, Greece, September 1-7 2013, (Oral presentation).

Gagliano A.L., D'Alessandro W., Quatrini P., Parello F.: High diversity of methanotrophic bacteria in a geothermal site: Pantelleria island, Italy, IX Forum Italiano di Scienze della Terra, Pisa, Italy, September 16-18, 2013, (Oral presentation).

Collaboration in other project:

Boatta, F., D'Alessandro, W., Gagliano, A.L., Calabrese, S., Liotta, M., Milazzo, M., et al. (2012). Another kind of "volcanic risk": the acidification of sea-water. Vulcano Island (Italy) a natural laboratory for ocean acidification studies. *Miscellanea INGV*, 15(15), 31-32.

Boatta F., D'Alessandro W., Gagliano A.L., Federico C., Calabrese S., Liotta M., Milazzo M., Parello F., Seawater Trace Metals in acidified condition: accumulation study in Blue Mussels (*Mytilus galloprovincialis*). Vulcano Island (Italy), Goldschmidt 2013, Firenze, Italia, August 25 – 30, 2013.

D'Alessandro W., Brusca L., Cinti D., Longo M., Gagliano A.L., Pecoraino G., Pizzino L., Voltattorni N., Carbon dioxide and Radon measurements in the soils of Pantelleria island (Italy), ICGG12 - International Conference on Gas Geochemistry 2013, Patras, Greece, September 1-7 2013 .

Boatta F., D'Alessandro W., Gagliano A.L., Calabrese S., Liotta M., Milazzo M., Parello F., Volcanic health hazard: the acidification of seawater and trace metals accumulation study in Blue Mussels (*Mytilus galloprovincialis*). Vulcano Island (Italy), IAVCEI (International Association of Volcanology and Chemistry of the Earth's Interior) 2013, Kagoshima, Japan, July 20 – 24, 2013.